Convergence of adaptive hybridizable discontinuous Galerkin methods for second-order elliptic equations

A DISSERTATION
SUBMITTED TO THE FACULTY OF THE GRADUATE SCHOOL
OF THE UNIVERSITY OF MINNESOTA
BY

Wujun Zhang

IN PARTIAL FULFILLMENT OF THE REQUIREMENTS
FOR THE DEGREE OF
Doctor of Philosophy

Thesis Adviser: Professor Bernardo Cockburn

August, 2012

Acknowledgements

First and foremost, I would like to thank my advisor, B. Cockburn, for guiding me through my research; his mathematical expertise and insight is very helpful and stimulating. In addition, I would like to thank him for his encouragement and personal support during the past few years.

I also would like to thank D. Schötzau for bringing to my attention a crucial result at the begining of my research; F. J. Sayas for pointing me to the red-green-blue refinement algorithm; R. H. Nochetto for inspiring me to work on the convergence and quasi-optimality of the adaptive algorithm.

Special thanks go to my parents who constantly support me during all these years.

.

Dedication

To my family

Abstract

We present several a posteriori error estimators for the so-called hybridizable discontinuous Galerkin (HDG) methods, as well as an a posteriori error estimator for variable-degree, hybridized version of the Raviart-Thomas method on nonconforming meshes, for second-order elliptic equations. We show that the error estimators provide a reliable upper and lower bound for the true error of the flux in the L^2-norm.

Moreover, we establish the convergence and quasi-optimality of adaptive hybridizable discontinuous Galerkin (AHDG) methods. We prove that the so-called quasi-error, that is, the sum of an energy-like error and a suitably scaled error estimator, is a contraction between two consecutive loops. We also show that the AHDG methods achieve optimal rates of convergence.

Contents

List of Tables

List of Figures

Chapter 1

Introduction

1.1 Background and motivation

Adaptive finite element methods (AFEMs) are finite element methods (FEMs) which utilize *a posteriori* error estimators and indicators to assess the quality of approximation and modify the mesh adaptively. These methods aim to obtain a solution with prescribed accuracy by using a minimal amount of computational work. In practice, AFEMs are known to outperform their non-adaptive counterparts, especially when the solution exhibits rapid changes and singularities. To illustrate the capability of the AFEMs, we present a simple but typical example [70]. We consider the Laplace's equation on a two-dimensional L-shaped domain Ω,

$$\Delta\, u = 0 \quad \text{in } \Omega,$$

with exact solution $u = r^{2/3} \sin(2\theta/3)$ written in polar coordinates. Note that $\boldsymbol{\nabla}\, u$ has a singularity at the reentrant corner. In Fig. 1.1.1, we see that the adaptive mesh is able to capture this singularity. Moreover, to obtain the same accuracy in the flux, AFEM requires significantly fewer degrees of freedom than the standard FEM. Indeed, FEM requires 3072 elements to bound the L^2 error of the flux around 0.025 while AFEM requires only 162 elements. This example clearly reveals the advantage of the adaptive mesh strategy.

A classic adaptive finite element method can be described by a loop as follows:

$$\text{SOLVE} \rightarrow \text{ESTIMATE} \rightarrow \text{MARK} \rightarrow \text{REFINE}.$$

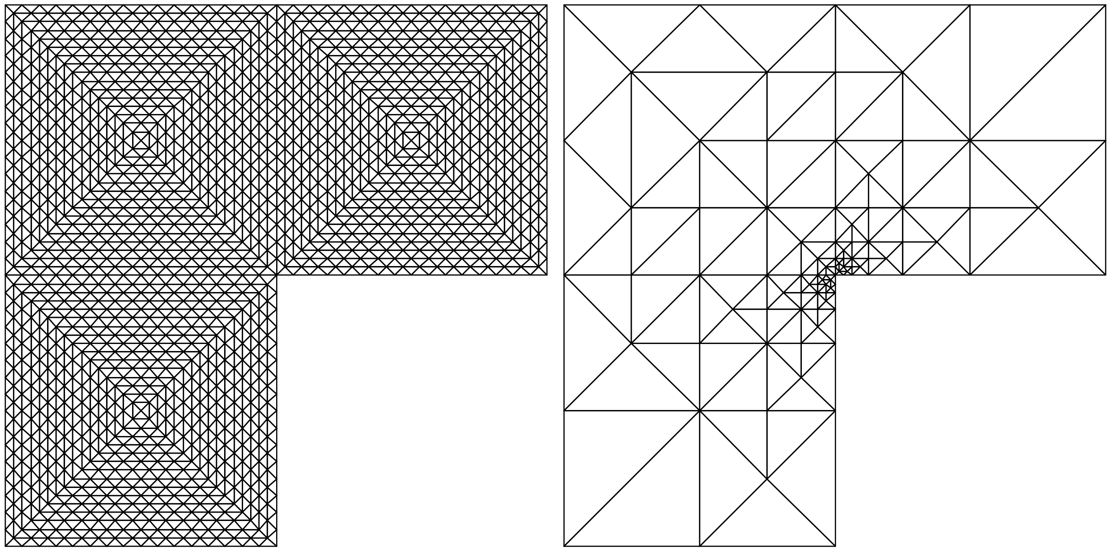

Figure 1.1.1: A comparison of uniform mesh and adaptive mesh

Let us describe each module in detail. Given a mesh $\mathcal{T}_k$, the module SOLVE yields an approximation in the finite element space V_k associated with the mesh $\mathcal{T}_k$ by using FEM. Then, we ESTIMATE the error by using an a posteriori error estimator. Using this information, we MARK the elements of the mesh $\mathcal{T}_k$ that carries the largest value of the estimator and then REFINE them to obtain the next mesh, $\mathcal{T}_{k+1}$. We repeat this loop until the error is less than a prescribed tolerance. The key ingredient of the AFEM is the a posteriori error estimator used in the ESTIMATE procedure. Next, let us discuss the module ESTIMATE in detail.

The module ESTIMATE utilizes an a posteriori error estimator to identify the region carrying the largest error. These error estimators provide reliable upper and lower bound for the true error. Note that a global upper bound ensures that the quality of approximation is below the prescribed tolerance while a local lower bound ensures that the error estimator does not overestimate the true error, thus preventing over-refining the mesh. Moreover, the estimators should be computed locally from the numerical approximation and known data of the problem, and the cost of computation should be much cheaper than solving for the numerical solution.

Starting from the pioneer work of Babuška et al. [11, 12] in the 70's, a great deal of effort has been devoted to the design of a posteriori error estimators for a variety of partial differential equations and numerical methods. We refer to [70, 3] for a review.

Although AFEMs are successfully applied in scientific and engineering computing, a complete theory ensuring the convergence and optimal convergence rate of the adaptive algorithm is still under development. It was not until 1996 that the convergence property of AFEM for multidimensional cases was established in [40] by introducing a key marking strategy, now known as Dörfler marking. Later, this result was improved in [47, 46]. On the other hand, the *optimality* of the convergence rate of AFEM was established in [16]. Later, the result was improved in [66]. All the results mentioned above established the convergence and optimality of the standard continuous Galerkin methods for second order elliptic problems. Recently, this issue was also addressed in [31, 15] for mixed finite element method and in [54, 43, 17] for discontinuous Galerkin methods.

Compared with other DG methods, the HDG methods have a significantly smaller number of globally-coupled degrees of freedom and better convergence properties. Compared with well established finite element methods, they display the typical advantages of DG methods, namely, ease in dealing with *hp*-adaptivity on conforming or nonconforming meshes, in handling boundary conditions, and in being applicable to a wide variety of problems.

However, a theory regarding the convergence property and optimal convergence rate of the AHDG methods is still lacking. In this thesis, we present the *first* convergence result for the AHDG methods for the following model problem:

$$\boldsymbol{q} + \boldsymbol{\nabla}\, u = 0 \qquad \text{in } \Omega, \tag{1.1.1a}$$

$$\nabla\cdot \boldsymbol{q} = f \qquad \text{in } \Omega, \tag{1.1.1b}$$

$$u = g \qquad \text{on } \Gamma, \tag{1.1.1c}$$

where $\Omega \in R^d$ is a polyhedral domain $(d \geq 2)$, $f \in L^2(\Omega)$ and $g \in H^{1/2}(\Omega)$.

1.2 The hybridizable discontinuous Galerkin methods

1.2.1 Notation

Throughout the thesis, unless otherwise stated, we use $\mathcal{T}_h = \{K\}$ to denote a *conforming* triangulation, made of *simplexes* K, of the domain Ω. We use h_K to denote the diameter of K and h_e the diameter of the face e of an element. We associate to this triangulation the set of interior faces $\mathcal{E}_h^i$ and the set of boundary faces $\mathcal{E}_h^\partial$. We say that $e \in \mathcal{E}_h^i$ if there are two elements K^+ and K^- in $\mathcal{T}_h$ such that $e = \partial K^+ \cap \partial K^-$, and we say that $e \in \mathcal{E}_h^\partial$ if there is an element K in $\mathcal{T}_h$ such that $e = \partial K \cap \Gamma$. We set

$$\mathcal{U}_h(e) := \begin{cases} K^+, K^- & \text{if } e \in \mathcal{E}_h^i, \\ K & \text{if } e \in \mathcal{E}_h^\partial. \end{cases}$$

and we set $\mathcal{E}_h = \mathcal{E}_h^i \cup \mathcal{E}_h^\partial$. We also set $\partial\mathcal{T}_h = \{\partial K | K \in \mathcal{T}_h\}$.

We use the conventional notation $[\![\boldsymbol{v}]\!]$ to denote the jump of vector valued function $\boldsymbol{v}$ in the normal direction across the face, $[\![\boldsymbol{v}]\!]_t$ to denote the jump of $\boldsymbol{v}$ in the tangential direction and $[\![\varphi]\!]$ to denote the jump of scalar valued function φ, that is,

$$[\![\boldsymbol{v}]\!] = \begin{cases} \boldsymbol{v}^- \cdot \boldsymbol{n}^- + \boldsymbol{v}^+ \cdot \boldsymbol{n}^+, & e \in \mathcal{E}_h^i, \\ 0, & e \in \mathcal{E}_h^\partial, \end{cases}$$

$$[\![\boldsymbol{v}]\!]_t = \begin{cases} \boldsymbol{v}^- \times \boldsymbol{n}^- + \boldsymbol{v}^+ \times \boldsymbol{n}^+, & e \in \mathcal{E}_h^i, \\ \boldsymbol{v} \times \boldsymbol{n} + \boldsymbol{\nabla_\Gamma}\, g \times \boldsymbol{n}, & e \in \mathcal{E}_h^\partial, \end{cases}$$

$$[\![\varphi]\!] = \begin{cases} \varphi^- \boldsymbol{n}^- + \varphi^+ \boldsymbol{n}^+, & e \in \mathcal{E}_h^i, \\ \varphi\boldsymbol{n} - g\boldsymbol{n}, & e \in \mathcal{E}_h^\partial. \end{cases}$$

Here, $\boldsymbol{\nabla_\Gamma}$ is the so-called surface gradient. The outward unit normal vector to ∂K is denoted by $\boldsymbol{n}$. For smooth functions η defined on Ω, we have that $\boldsymbol{\nabla_\Gamma}\,\eta := \boldsymbol{\nabla}\,\eta - (\boldsymbol{n} \cdot \boldsymbol{\nabla}\,\eta)\,\boldsymbol{n}$.

We use the standard notation $(\cdot\,,\,\cdot)_D$, $\langle\cdot\,,\cdot\,\rangle_\Gamma$ to denote the L^2 inner product on the elements D and faces Γ, respectively, that is,

$$(\boldsymbol{\sigma}, \boldsymbol{v})_D := \sum_{K \in D} \int_K \boldsymbol{\sigma}(x) \cdot \boldsymbol{v}(x)\, dx,$$

$$(\zeta, \omega)_D := \sum_{K \in D} \int_K \zeta(x) w(x) dx,$$

$$\langle \zeta, \boldsymbol{v} \cdot \boldsymbol{n} \rangle_\Gamma := \sum_{e \in \Gamma} \int_e \zeta(x) \boldsymbol{v}(x) \cdot \boldsymbol{n} dx,$$

We also use the notation $\|\cdot\|_D$ and $\|\cdot\|_\Gamma$ to denote the L^2 norm on the elements D and faces Γ, respectively.

We use the notation $'a \preceq b'$ to denote $a \le Cb$ for some generic constant C independent of mesh size. We also use the notation $'a \simeq b'$ to denote $a \preceq b \preceq a$.

Assumptions on the meshes and on the boundary condition

Finally, we make the following assumption on the meshes $\mathcal{T}_h$:

S: *The meshes $\mathcal{T}_h$ verify the shape-regularity condition, that is, there is some constant $\sigma > 0$, such that*

$$h_K/\rho_K \le \sigma \quad \forall\, K \in \mathcal{T}_h,$$

where ρ_K denotes the diameter of the largest ball inside K.

To avoid technical difficulties, we make the following assumption on the boundary condition:

B: *We assume the Dirichlet boundary data g is the trace of a continuous function included in W_h^*.*

1.2.2 The HDG methods

The HDG methods are finite element methods which seek an approximation to the exact solution $(\boldsymbol{q}|_\Omega, u|_\Omega, u|_{\partial\mathcal{E}_h})$, $(\boldsymbol{q}_h, u_h, \widehat{u}_h)$, in the space $\boldsymbol{V}_h \times W_h \times \mathsf{M}_h$ where

$$\begin{aligned}
\boldsymbol{V}_h &:= \{\boldsymbol{v} \in \boldsymbol{L}^2(\Omega) : && \boldsymbol{v}|_K \in \boldsymbol{V}(K) && \forall K \in \mathcal{T}_h\}, && \text{(1.2.1a)}\\
W_h &:= \{\omega \in L^2(\Omega) : && w|_K \in W(K) && \forall K \in \mathcal{T}_h\}, && \text{(1.2.1b)}\\
\mathsf{M}_h &:= \{m \in L^2(\mathcal{E}_h) : && m|_e \in \mathsf{M}(e) && \forall e \in \mathcal{E}_h\}, && \text{(1.2.1c)}
\end{aligned}$$

The approximation $(\boldsymbol{q}_h, u_h)$ is expressed in terms of f and $\widehat{u}_h$ by the so-called local solvers:

$$\begin{aligned}
(\boldsymbol{q}_h, \boldsymbol{v})_{\mathcal{T}_h} - (u_h, \nabla\cdot \boldsymbol{v})_{\mathcal{T}_h} &= -\langle \widehat{u}_h, \boldsymbol{v}\cdot\boldsymbol{n}\rangle_{\partial\mathcal{T}_h} && \forall\, \boldsymbol{v} \in \boldsymbol{V}_h, && \text{(1.2.2a)}\\
-(\boldsymbol{q}_h, \boldsymbol{\nabla}\,\omega)_{\mathcal{T}_h} + \langle \widehat{\boldsymbol{q}}_h\cdot\boldsymbol{n}, \omega\rangle_{\partial\mathcal{T}_h} &= (f, \omega)_{\mathcal{T}_h} && \forall\, \omega \in W_h, && \text{(1.2.2b)}
\end{aligned}$$

and $\widehat{u}_h \in \mathsf{M}_h$ is determined by the boundary condition

$$\langle \widehat{u}_h, \mu\rangle_\Gamma = \langle g, \mu\rangle_\Gamma, \quad \forall \mu \in \mathsf{M}_h, \qquad \text{(1.2.3a)}$$

and by the transmission condition

$$\langle [\![\widehat{\boldsymbol{q}}_h]\!], \mu \rangle_{\mathcal{E}_h^i} = 0, \qquad \forall \mu \in \mathsf{M}_h. \tag{1.2.3b}$$

In this general framework, to define a particular method, we only have to specify (1) the numerical trace $\widehat{\boldsymbol{q}}_h$, (2) the local spaces $\boldsymbol{V}(K) \times W(K)$, and (3) the space of approximate traces $\mathsf{M}(e)$. See the main examples in the table below.

Table 1.2.1: Main examples of HDG methods

Method	$\widehat{\boldsymbol{q}}_h$	$\boldsymbol{V}(K)$	$W(K)$	$\mathsf{M}(e)$
RT-H	$\boldsymbol{q}_h$	$\boldsymbol{\mathcal{P}}_p(K) + \boldsymbol{x}\,\mathcal{P}_p(K)$	$\mathcal{P}_p(K)$	$\mathcal{P}_p(e)$
BDM-H	$\boldsymbol{q}_h$	$\boldsymbol{\mathcal{P}}_p(K)$	$\mathcal{P}_{p-1}(K)$	$\mathcal{P}_p(e)$
LDG-H	$\boldsymbol{q}_h + \tau\,(u_h - \widehat{u}_h)\,\boldsymbol{n}$	$\boldsymbol{\mathcal{P}}_p(K)$	$\mathcal{P}_p(K)$	$\mathcal{P}_p(e)$
IP-H	$-\boldsymbol{\nabla}\,u_h + \tau\,(u_h - \widehat{u}_h)\,\boldsymbol{n}$	$\boldsymbol{\mathcal{P}}_p(K)$	$\mathcal{P}_p(K)$	$\mathcal{P}_p(e)$
CG-H	new unknown	$\boldsymbol{\mathcal{P}}_{p-1}(K)$	$\mathcal{P}_p(K)$	$\mathcal{P}_p(e)$

Here, $\mathcal{P}_p(K)$ and $\mathcal{P}_p(e)$ denote the space of polynomials with degree no great than p on a simplex K or a face e, respectively. And $\boldsymbol{\mathcal{P}}_p(K)$ denotes the space of vector valued function with each of its components in $\mathcal{P}_p(K)$.

For the CG-H method, which as shown in [34], is nothing but a rewriting of the original CG method, some minor modifications are in order. First, we force the space of traces to be a space of continuous functions, that is, we take

$$\mathsf{M}_h := \mathsf{M}_{k,h}^c := \{\mu \in \mathcal{C}^0(\mathcal{E}_h) \ : \ \mu|_e \in \mathcal{P}_p(e)\}.$$

Then, we define the local solver as follows. On the element K, the local solver $(\boldsymbol{q}_h, u_h, \widehat{\boldsymbol{q}}_h) \in \boldsymbol{V}(K) \times W(K) \times \boldsymbol{T}(\partial K)$, where

$$\boldsymbol{T}(\partial K) := \{\boldsymbol{n}_K\, w|_{\partial K} : \ w \in W(K)\},$$

is the solution of the problem

$$(\boldsymbol{q}_h, \boldsymbol{v})_K - (u_h, \nabla\cdot \boldsymbol{v})_K = -\langle \widehat{u}_h, \boldsymbol{v}\cdot\boldsymbol{n}\rangle_{\partial K} \quad \forall \boldsymbol{v} \in \boldsymbol{V}(K), \tag{1.2.4a}$$

$$-(\boldsymbol{q}_h, \boldsymbol{\nabla}\, w)_K + \langle \widehat{\boldsymbol{q}}_h \cdot \boldsymbol{n}, w\rangle_{\partial K} = (f, w) \qquad \forall w \in W(K), \tag{1.2.4b}$$

$$u_h = \widehat{u}_h \qquad \text{on } \partial K, \tag{1.2.4c}$$

We refer the reader to [34] for more examples of hybridizable methods. For an a priori error analysis of these methods, we refer the reader to [35, 38]; see also the previous work in [33, 36].

1.3 Organization of the thesis

The goal of the thesis is to develop a posteriori error estimates for the hybridizable discontinuous Galerkin (HDG) method and to understand the convergence and optimality of the adaptive HDG methods. In order to achieve this goal, we carried out the research in four steps.

In Chapter 2, we propose the *first* a posteriori error estimator for the HDG method. We show that the error estimator η_h provides upper and lower bound for the error

$$\mathsf{e}_h^2 := \| \boldsymbol{q} - \boldsymbol{q}_h \|_\Omega^2 + \Phi_h,$$

where $\| \cdot \|_\Omega$ denotes the $L^2(\Omega)$-norm, and where Φ_h is expressed in terms of the divergence of $\boldsymbol{q}-\boldsymbol{q}_h$ inside the elements, of the normal component of $\boldsymbol{q}-\widehat{\boldsymbol{q}}_h$ on the boundary of the elements, of the gradient of $u-u_h^*$ inside the elements, and of the jump of $u-u_h^*$ across inter-element boundaries. Here, u_h^* denotes a local post-processing of the approximation provided by the HDG method. Numerical experiments in two-space dimensions are presented.

The result above is not completely satisfactory. Although we show that the estimator is equivalent to the error e_h, the term of primary interest is the L^2-error in the flux only. In order to tackle this problem, we start with the hybridized Raviart Thomas (RT) method, which is similar to, yet much simpler than, the HDG methods. In Chapter 3, we show that

$$C_2\eta_h^2 \leq \| \boldsymbol{q} - \boldsymbol{q}_h \|_\Omega^2 \leq C_1\eta_h^2,$$

for two positive constants C_1 and C_2. Moreover, we show that the estimate above holds for variable-degree hybridized Raviart-Thomas method on nonconforming meshes.

Using the technique developed for the RT method, we then establish a unified a posteriori error estimation for a large class of HDG methods in Chapter 4. In particular, we derive a reliable and efficient error estimator for the error in an energy norm.

This result is crucial to establish the convergence and optimality of the adaptive HDG methods.

Finally, in Chapter 5, building upon the knowledge gathered in the previous chapters, we show that the total error, that is, the sum of the error in the energy norm and scaled error estimator and data oscillation, is a contraction between two consecutive iterations. Moreover, we also show that the error in the energy norm converges with the optimal rate.

Chapter 2

A posteriori error estimation for the LDG-H method

2.1 Introduction

In this chapter, we use the idea of employing the postprocessing [58] and the approach used in [55] to obtain the first reliable and efficient error estimator for HDG methods with optimal order of convergence in all space dimensions.

We show that the error is controlled only by the data oscillation and the difference between the trace of the scalar variable and the corresponding numerical trace. Here we assume that g is a continuous function which is piecewise polynomial of degree p on the polyhedral boundary Γ.

In section 2.2, we introduce the a posteriori error estimator and present the main result of the chapter. In section 2.3, we present the analysis of its reliability and efficiency and in section 2.4 , we provide numerical results showing the performance of the estimator.

2.2 Main Result

2.2.1 Local postprocessing

Just as the accuracy of the approximate scalar variable of mixed methods can be improved by an element-by-element computation of a new approximation [7, 19, 24, 22, 65], for HDG methods, several postprocessings have been proposed in [33, 36, 35] which achieve a similar goal.

Here, we take the postprocessing u_h^* in the space

$$W_h^* = \{w \in L^2(K), w|_K \in \mathcal{P}_{p+1}(K), \quad \forall K \in \mathcal{T}_h\}, \tag{2.2.1}$$

and define it as follows. When $p \geq 1$, the solution u_h^* satisfies the following equations

$$(u_h^* - u_h, w)_K = 0, \qquad \forall w \in \mathcal{P}_{p-1}(K), \tag{2.2.2a}$$

$$(\boldsymbol{\nabla}\, u_h^*, \boldsymbol{\nabla}\, w)_K = -(\boldsymbol{q}_h, \boldsymbol{\nabla}\, w)_K, \qquad \forall w \in W_{p+1}(K), \tag{2.2.2b}$$

for each simplex K, where

$$W_{p+1}(K) = \{w \in \mathcal{P}_{p+1}(K) : \quad (w, v) = 0 \quad \forall\, v \in \mathcal{P}_{p-1}(K)\}.$$

When $p = 0$, we define u_h^* on the simplex $K \in \mathcal{T}_h$ by requiring that

$$\int_F u_h^* = \int_F \widehat{u}_h, \quad \forall F \in \partial K,$$

for each face F of K. Note that in this case we have that $\boldsymbol{q}_h = -\boldsymbol{\nabla}\, u_h^*$. The postprocessed solution u_h^* is well defined and converges with order $p+2$ for $p \geq 1$, and with order 1 for $p = 0$ for conforming meshes; see [35].

Note that $(u_h^* - u_h)$ depends on $(\widehat{u}_h - u_h)$ only. Indeed, from the HDG formulation (1.2.2), when $p \geq 1$,

$$\begin{aligned}(\boldsymbol{\nabla}(u_h^* - u_h), \boldsymbol{\nabla}\, w)_K &= -(\boldsymbol{q}_h + \boldsymbol{\nabla}\, u_h, \boldsymbol{\nabla}\, w)_K, \\ &= \langle \widehat{u}_h - u_h, \boldsymbol{\nabla}\, w \cdot \boldsymbol{n}\rangle_{\partial K}, \quad \forall w \in W_{p+1}(K)\end{aligned}$$

and when $p = 0$,

$$\int_F u_h^* - u_h = \int_F \widehat{u}_h - u_h, \quad \forall F \in \partial K,$$

We can define the following lifting operator Φ. When $p \geq 1$, $\Phi(\widehat{u}_h - u_h)$ is a polynomial in the space $W_{p+1}(K)$ satisfying

$$(\boldsymbol{\nabla}\, \Phi(\widehat{u}_h - u_h), \boldsymbol{\nabla}\, w)_K = -\langle \widehat{u}_h - u_h, \boldsymbol{\nabla}\, w \cdot \boldsymbol{n} \rangle_{\partial K}, \quad \forall w \in W_{p+1}(K),$$

for each simplex K. When $p = 0$, we require $\Phi(\widehat{u}_h - u_h) \in \mathcal{P}_1(K)$ satisfying

$$\int_F \Phi(\widehat{u}_h - u_h) = \int_F (\widehat{u}_h - u_h), \quad \forall F \in \partial K,$$

for each face F of K. And we have

$$u_h^* = u_h + \Phi(\widehat{u}_h - u_h). \tag{2.2.3}$$

2.2.2 The a posteriori error estimate

To state our main result, we need to introduce some notation. We denote by $\| \zeta \|_{0,D}$ the L^2-norm of the function ζ over the domain D. We then set, for each simplex $K \in \mathcal{T}_h$,

$$\| w \|_{H^1(K)} := (\| w \|_{0,K}^2 + h_K^2 \| \nabla w \|_{0,K}^2)^{1/2}, \tag{2.2.4a}$$

$$\| w \|_{1/2,\partial K} := \inf_{\phi \in H^1(K), T\phi = w} h_K^{-1} \| \phi \|_{H^1(K)}, \tag{2.2.4b}$$

where $T\phi$ denotes the trace of $\phi \in H^1(K)$ on the boundary of the triangle K. We also set

$$\| w \|_{-1/2,\partial K} := \sup_{\mathsf{w} \in H^1(K)} \frac{\langle w, \mathsf{w} \rangle_{\partial K}}{\| \mathsf{w} \|_{1/2,\partial K}}, \tag{2.2.4c}$$

$$\| \boldsymbol{v} \|_{div,K} := (\| \boldsymbol{v} \|_K^2 + h_K^2 \| \nabla \cdot \boldsymbol{v} \|_{0,K}^2)^{1/2}. \tag{2.2.4d}$$

Our main result provides upper and lower bounds of the error

$$\begin{aligned} \mathsf{e}_h := (&\| \boldsymbol{q} - \boldsymbol{q}_h \|_{div,\mathcal{T}_h}^2 + \| \, [\![u - u_h^*]\!] \, \|_{1/2,\mathcal{E}_h}^2 \\ &+ \| \nabla(u - u_h^*) \|_{0,\mathcal{T}_h}^2 + \| (\boldsymbol{q} - \widehat{\boldsymbol{q}}_h) \cdot \boldsymbol{n} \|_{-1/2,\partial\mathcal{T}_h})^{1/2}, \end{aligned} \tag{2.2.5}$$

where

$$
\begin{aligned}
\| \boldsymbol{q} - \boldsymbol{q}_h \|_{div,\mathcal{T}_h} &:= (\sum_{K\in\mathcal{T}_h} \| \boldsymbol{q} - \boldsymbol{q}_h \|^2_{div,K})^{1/2}, && (2.2.6a)\\
\| [\![u - u_h^*]\!] \|_{1/2,\mathcal{E}_h} &:= (\sum_{E\in\partial\mathcal{T}_h} h_E^{-1} \| [\![u - u_h^*]\!] \|^2_{0,E})^{1/2}, && (2.2.6b)\\
\| \nabla(u - u_h^*) \|_{0,\mathcal{T}_h} &:= (\sum_{K\in\mathcal{T}_h} \| \nabla u - \nabla u_h^* \|^2_{0,K})^{1/2}, && (2.2.6c)\\
\| (\boldsymbol{q} - \widehat{\boldsymbol{q}}_h)\cdot\boldsymbol{n} \|_{-1/2,\partial\mathcal{T}_h} &:= (\sum_{K\in\mathcal{T}_h} \| (\boldsymbol{q} - \widehat{\boldsymbol{q}}_h)\cdot\boldsymbol{n} \|^2_{-1/2,\partial K})^{1/2}, && (2.2.6d)
\end{aligned}
$$

in terms of the error estimator

$$\eta_h := (\eta_{1,h}^2 + \eta_{2,h}^2)^{1/2}, \tag{2.2.7}$$

where

$$
\begin{aligned}
\eta_{1,h} := \| f - \mathsf{P}_W f \|_{-1,\mathcal{T}_h} &:= (\sum_{K\in\mathcal{T}_h} h_K^2 \| f - \mathsf{P}_W f \|^2_{0,K})^{1/2}, && (2.2.8a)\\
\eta_{2,h} := \| \mathcal{L}(\widehat{u}_h - u_h) \|_{0,\mathcal{T}_h} &:= (\sum_{K\in\mathcal{T}_h} h_K^{-1} \| \mathsf{P}_M(\mathsf{Id} - \Phi)(\widehat{u}_h - u_h) \|^2_{0,\partial K} && (2.2.8b)\\
&\quad + \sum_{e\in\mathcal{E}_h} h_e^{-1} \| [\![(\mathsf{Id} - \mathsf{P}_M)\Phi(\widehat{u}_h - u_h)]\!] \|^2_{0,e}\\
&\quad + \sum_{K\in\mathcal{T}_h} h_K \| \tau(\widehat{u}_h - u_h) \|^2_{0,\partial K})^{1/2},
\end{aligned}
$$

where P_W is the L_2-orthogonal projection into W_h and P_M is the L_2-orthogonal projection into $\mathcal{P}_p(e)$, for each face $e \in \mathcal{E}_h$. Here, we point out that to numerically evaluate the negative-order norm used to define the fourth term of the error (2.2.5), we approximate it by solving a corresponding dual problem locally in some large finite element space. We refer the reader to Lemma 2.4.1 for details.

We can now state our main result.

Theorem 2.2.1 (Reliability and Efficiency of the error estimator)**.** *Assume that the meshes satisfy the shape-regularity assumption* **A**. *Then there are two constants C_1 and C_2 depending only on the constant σ, and p such that*

$$C_1 \eta_h^2 \le \mathsf{e}_h^2 \le C_2\, \eta_h^2.$$

The proof is based on a key observation stated in Lemma 2.3.5 and on the idea of constructing an error estimator by using a post-processed solution. Thanks to these two ideas, we avoid the conventional technique based on Helmholtz decompositions and the saturation assumption, and establish the result for any space dimensions. This result provides a reliable and efficient a posteriori error estimator which holds for all dimensions under standard assumptions on the mesh. Note that the error is bounded by the data oscillation and quantities depending solely on the jump $\widehat{u}_h - u_h$ on $\partial\mathcal{T}_h$.

2.3 Proof

In this section, we provide a proof of our main result, Theorem 2.2.1. We proceed in three steps. We begin by gathering a few, simple auxiliary results that we are going to use in the analysis. We then establish a key estimate of the error in the approximate flux. Finally, we prove the efficiency and reliability of the estimator.

2.3.1 Step 1: Some auxiliary results

We begin by proving several auxiliary lemmas which will be useful in the proof of main theorem.

Some relations between norms

We have the following well known trace inequality in terms of the norm defined in the last section. The proof can be found in [55].

Lemma 2.3.1. *It holds for any simplex $K \in \mathcal{T}_h$,*

$$\| \boldsymbol{v} \cdot \boldsymbol{n} \|_{-1/2,\partial K} \leq \| \boldsymbol{v} \|_{div,K}.$$

Next, we show that the L_2-norm $\| \cdot \|_{0,\partial K}$ and negative-order norm $\| \cdot \|_{-1/2,\partial K}$ are equivalent on the space

$$\mathsf{M}_h(\partial K) := \{ w|_e \in \mathcal{P}_p(e) \ \text{ for all faces } e \text{ of } K \}.$$

Lemma 2.3.2. *For all $w \in \mathsf{M}_h(\partial K)$, we have*

$$C_{s1}^{-1} \| w \|_{-1/2,\partial K} \leq h_K^{1/2} \| w \|_{0,\partial K} \leq C_{s1} \| w \|_{-1/2,\partial K},$$

where C_{s1} depends on the shape regularity constant σ and on the polynomial degree p of the space $\mathsf{M}_h(\partial K)$.

Proof. To prove the inequality, we begin by associating to every simplex $K \in \mathcal{T}_h$ the set $\widehat{K}$ defined as follow. It is a set of unit diameter, such that the transformation F from $\widehat{K}$ to K is given by

$$x = F(\widehat{x}) = h_K \widehat{x} + b.$$

It follows immediately that, if we set $\widehat{w}(\widehat{x}) := w(x)$,

$$\begin{aligned} \| w \|_{1,K}^2 &:= \| w \|_K^2 + h_K^2 \| \nabla w \|_K^2 \\ &= h_K^d (\| \widehat{w} \|_{\widehat{K}}^2 + \| \widehat{\nabla} \widehat{w} \|_{\widehat{K}}^2) \\ &= h_K^d \| \widehat{w} \|_{1,\widehat{K}}^2, \end{aligned}$$

and that $\langle w, \mathsf{w} \rangle_{\partial K} = h_K^{d-1} \langle \widehat{w}, \widehat{\mathsf{w}} \rangle_{\partial \widehat{K}}$, where d denotes the dimension of the element K.

Next, we note that, by the definition of half-order norm (2.2.4b) and the negative-order norm $\| \cdot \|_{-1/2,\partial K}$ (2.2.4c)

$$\begin{aligned} \| \mathsf{w} \|_{1/2,\partial K} &:= \inf_{\phi \in H^1(K), T\phi = \mathsf{w}} h_K^{-1} \| \phi \|_{H^1(\Omega)}, \\ \| w \|_{-1/2,\partial K} &:= \sup_{\mathsf{w} \in H^1(K)} \frac{\langle w, \mathsf{w} \rangle_{\partial K}}{\| \mathsf{w} \|_{1/2,\partial K}} \end{aligned}$$

we have

$$\begin{aligned} \| w \|_{-1/2,\partial K} &= \sup_{\mathsf{w} \in H^1(K)} \frac{\langle w, \mathsf{w} \rangle_{\partial K}}{h_K^{-1} \| \mathsf{w} \|_{H^1(\Omega)}} \\ &= \sup_{\widehat{\mathsf{w}} \in H^1(\widehat{K})} \frac{h_K^{d-1} \langle \widehat{w}, \widehat{\mathsf{w}} \rangle_{\partial \widehat{K}}}{h_K^{d/2-1} \| \widehat{\mathsf{w}} \|_{1,\widehat{K}}} \\ &= h_K^{d/2} \| \widehat{w} \|_{-1/2,\partial \widehat{K}}. \end{aligned}$$

On the other hand, we have

$$\| w \|_{0,\partial K} = h_K^{\frac{d-1}{2}} \| \widehat{w} \|_{0,\partial \widehat{K}}.$$

Using the fact that all norms on the finite dimensional space are equivalent, we get

$$\begin{aligned} \| w \|_{0,\partial K} &\leq h_K^{\frac{d-1}{2}} C_{s1}(\widehat{K}, p) \| \widehat{w} \|_{-1/2,\partial \widehat{K}} \\ &= C_{s1}(\widehat{K}, p) h_K^{-1/2} \| w \|_{-1/2,\partial K}, \end{aligned} \tag{2.3.1}$$

and,

$$\| w \|_{0,\partial K} \geq h_K^{\frac{d-1}{2}} C_{s1}^{-1}(\widehat{K}, p) \| \widehat{w} \|_{-1/2,\partial \widehat{K}} \quad (2.3.2)$$
$$= C_{s1}^{-1}(\widehat{K}, p) h_K^{-1/2} \| w \|_{-1/2,\partial K}.$$

where $C_{s1}(\widehat{K}, p)$ depends continuously on the shape of $\widehat{K}$.

Considering the family $\widehat{K}(\sigma)$ of all the simplexes $\widehat{K}$ with unit diameter, one vertex in the origin and satisfying the shape regularity condition, we get, by compactness ([25] subsection III.2.4), that

$$C_{s1}(\sigma, p) := \sup_{\widehat{K} \in \widehat{K}(\sigma)} C_{s1}(\widehat{K}, p) < \infty.$$

Hence, from (2.3.1) and (2.3.2), one has

$$C_{s1}^{-1}(\sigma, p) \| w \|_{-1/2,\partial K} \leq h_K^{1/2} \| w \|_{\partial K} \leq C_{s1}(\sigma, p) \| w \|_{-1/2,\partial K}.$$

This completes the proof. □

Some relations between residuals

Finally, we need to show that residuals coming from the equations defining the HDG method (1.2.2), are strongly connected.

Lemma 2.3.3. *It holds*

$$\Big(\sum_{K \in \mathcal{T}_h} h_K^2 \| \mathsf{P}_W f - \nabla \cdot \boldsymbol{q}_h \|_{0,K}^2\Big)^{1/2} \leq C_{s2} \| (\widehat{\boldsymbol{q}}_h - \boldsymbol{q}_h) \cdot \boldsymbol{n} \|_{-1/2,\partial \mathcal{T}_h}.$$

Moreover,

$$\| \boldsymbol{q}_h + \nabla u_h^* \|_{0,\mathcal{T}_h} \leq C_{s2} \Big(\sum_{K \in \mathcal{T}_h} h_K^{-1} \| \mathsf{P}_M (\widehat{u}_h - u_h^*) \|_{0,\partial K}^2\Big)^{1/2},$$
$$\Big(\sum_{K \in \mathcal{T}_h} h_K^{-1} \| \mathsf{P}_M (\widehat{u}_h - u_h^*) \|_{0,\partial K}^2\Big)^{1/2} \leq C_{s2} \| \boldsymbol{q}_h + \nabla u_h^* \|_{0,\mathcal{T}_h},$$

where C_{s2} is some constant depending on shape regularity σ and polynomial degree p only.

Proof. It suffices to show that, for each simplex K,

$$h_K^{-1}\| \mathsf{P}_M(\widehat{u}_h - u_h^*) \|_{0,\partial K}^2 \leq C_{s2}^2 \| \boldsymbol{q}_h + \nabla u_h^* \|_{0,K}^2,$$
$$\| \mathsf{P}_W f - \nabla\cdot \boldsymbol{q}_h \|_{0,K}^2 \leq C_{s2}^2 h_K^{-1} \| (\widehat{\boldsymbol{q}}_h - \boldsymbol{q}_h)\cdot \boldsymbol{n} \|_{0,\partial K}^2.$$

From the equations defining the HDG method (1.2.2) and the definition of the postprocessing u_h^*, (2.2.3), we have that

$$(\boldsymbol{q}_h + \nabla u_h^*, \boldsymbol{v})_K = \langle \mathsf{P}_M(\widehat{u}_h - u_h^*), \boldsymbol{v}\cdot\boldsymbol{n}\rangle_{\partial K}, \qquad \forall \boldsymbol{v} \in \mathcal{P}_p(K)^d, \tag{2.3.3a}$$
$$(\mathsf{P}_W f - \nabla\cdot \boldsymbol{q}_h, \omega) = \langle (\widehat{\boldsymbol{q}}_h - \boldsymbol{q}_h)\cdot\boldsymbol{n}, \omega\rangle_{\partial K}. \qquad \forall w \in \mathcal{P}_p(K). \tag{2.3.3b}$$

Taking $\omega = \mathsf{P}_W f - \nabla\cdot \boldsymbol{q}_h$ in the above equation (2.3.3b), and using the fact that

$$\| \omega \|_{0,\partial K} \leq C_{s2} h_K^{-1/2} \| \omega \|_{0,K},$$

where $C_{s2} = C_{s2}(\sigma, p)$ is some constant depending on shape regularity σ and polynomial degree p, we immediately obtain

$$\| \mathsf{P}_W f - \nabla\cdot \boldsymbol{q}_h \|_{0,K} \leq C_{s2} h_K^{-1/2} \| (\widehat{\boldsymbol{q}}_h - \boldsymbol{q}_h)\cdot\boldsymbol{n} \|_{0,\partial K}.$$

Thus, the first inequality follows from lemma 2.3.2.

To prove the remaining inequalities, we denote

$$V_0 = \{\boldsymbol{v} \in \mathcal{P}_p(K)^d, \boldsymbol{v}\cdot\boldsymbol{n} = 0 \text{ on each edge } e \in \partial K\},$$

and $V_0^\perp$ as the L_2-orthogonal complement of V_0 in $\mathcal{P}_p(K)^d$. Note from equation (2.3.3a) that

$$(\boldsymbol{q}_h + \nabla u_h^*, \boldsymbol{v}) = 0, \qquad \forall \boldsymbol{v} \in V_0,$$

which implies that $\boldsymbol{q}_h + \nabla u_h^* \in V_0^\perp$. Choosing $\boldsymbol{v} = \boldsymbol{q}_h + \nabla u_h^*$ in (2.3.3a), and using the fact that

$$h_K^{-1/2} \| \boldsymbol{v} \|_{0,K} \leq C_{s2} \| \boldsymbol{v}\cdot\boldsymbol{n} \|_{0,\partial K}, \qquad \forall \boldsymbol{v} \in V_0^\perp,$$

we have the second inequality.

Similarly, for $p \geq 1$, we can take $\boldsymbol{v}\cdot\boldsymbol{n} = \mathsf{P}_M(\widehat{u}_h - u_h^*)$ in equation (2.3.3a). The last inequality follows from the fact that

$$\| \boldsymbol{v}\cdot\boldsymbol{n} \|_{0,\partial K} \leq C_{s2} h_K^{-1/2} \| \boldsymbol{v} \|_{0,K}.$$

For $p = 0$, by the definition of the postprocessing u_h^*, the inequalities are trivially true since all the involved quantities are equal to zero. This completes the proof. $\square$

By using the triangle inequality and the fact that $\widehat{u}_h$ is single valued across the interior faces, we can easily obtain the following consequence of the last result.

Corollary 2.3.1.

$$\begin{aligned}&\sum_{e\in\mathcal{E}_h^i} h_e^{-1}\| [\![u_h^*]\!] \|_{0,e}^2 + \sum_{e\in\mathcal{E}_h^\partial} h_e^{-1}\| g - u_h^* \|_{0,e}^2 \\ &\le C_{s2}(\sum_{e\in\mathcal{E}_h} h_e^{-1}\| (\mathsf{Id} - \mathsf{P}_M)\, [\![u_h^*]\!] \|_{0,e}^2 + \sum_{K\in\mathcal{T}_h} \| \boldsymbol{q}_h + \nabla u_h^* \|_{0,K}^2).\end{aligned}$$

Approximation by continuous functions

We are also going to make use of the fact that the approximate solution u_h^* can be approximated by a continuous, piecewise polynomial function $\tilde{u}_h^*$ in the post processing space W_h^* (2.2.1). This will allow us to show that the quality of the approximation can be controlled by the jump of u_h^*. The following result can be found in [41], Theorem 2.2.

Lemma 2.3.4. *For any $w_h \in W_h^*$ and multi-index α with $|\alpha| = 0, 1$ the following approximation results holds: Let g be the restriction to Γ of a function in $W_h^* \cap H^1(\Omega)$. Then there exits a function $\tilde{w}_h \in W_h^* \cap H^1(\Omega)$ satisfying $\tilde{w}_h|_\Gamma = g$ and*

$$\begin{aligned}\sum_{K\in\mathcal{T}_h} \| D^\alpha(w_h - \tilde{w}_h) \|_K^2 \le & C_j \sum_{e\in\mathcal{E}_h^i} h_e^{1-2|\alpha|}\| [\![w_h]\!] \|_e^2 \\ & + C_j \sum_{e\in\mathcal{E}_h^\partial} h_e^{1-2|\alpha|}\| g - w_h \|_e^2\end{aligned}$$

where the constant $C_j = C_j(\sigma, p+1)$ depends on the shape regularity constant σ and on the polynomial degree $p+1$ of the finite element space W_h^*.

2.3.2 Step 2: A crucial estimate

Here we establish what we consider to be the crucial estimate of the analysis. It is a small modification of a similar result obtained in [55].

Lemma 2.3.5. *For any function ϕ in $\mathcal{C}^1(\mathcal{T}_h) \cap \mathcal{C}^0(\Omega)$, there exists a constant C_σ depending only on the shape regularity constant of the mesh, σ, such that*

$$\| \boldsymbol{q} - \boldsymbol{q}_h \|_{0,\mathcal{T}_h}^2 \le C_\sigma(\eta_q^2 + \eta_\phi^2) - \langle (\boldsymbol{q} - \widehat{\boldsymbol{q}}_h) \cdot \boldsymbol{n}, g - \phi \rangle_\Gamma,$$

where

$$\eta_q^2 = \sum_{K\in\mathcal{T}_h} h_K^2 \| f - \mathsf{P}_W f \|_{0,K}^2 + \sum_{K\in\mathcal{T}_h} h_K \| (\widehat{\boldsymbol{q}}_h - \boldsymbol{q}_h)\cdot \boldsymbol{n} \|_{0,\partial K}^2,$$
$$\eta_\phi^2 = \sum_{K\in\mathcal{T}_h} \| \boldsymbol{q}_h + \nabla\phi \|_{0,K}^2,$$

Proof. Let K be an arbitrary simplex of the triangulation $\mathcal{T}_h$, then, we have

$$\| \boldsymbol{q} - \boldsymbol{q}_h \|_{0,K}^2 = (\boldsymbol{q} - \boldsymbol{q}_h, \boldsymbol{q} + \nabla\phi - \boldsymbol{q}_h - \nabla\phi)_K,$$

and, since $\boldsymbol{q} = -\nabla u$, after a simple integration by parts, we get

$$\begin{aligned} \| \boldsymbol{q} - \boldsymbol{q}_h \|_{0,K}^2 =& (\nabla\cdot(\boldsymbol{q} - \boldsymbol{q}_h), u - \phi)_K - \langle u - \phi, (\boldsymbol{q} - \boldsymbol{q}_h)\cdot\boldsymbol{n}\rangle_{\partial K} \\ & - (\boldsymbol{q} - \boldsymbol{q}_h, \boldsymbol{q}_h + \nabla\phi)_K. \end{aligned}$$

The estimate of the last term follows immediately by applying Cauchy-Schwarz and Young inequalities:

$$(\boldsymbol{q} - \boldsymbol{q}_h, \boldsymbol{q}_h + \nabla\phi)_K \le \frac{1}{4\epsilon}\| \boldsymbol{q}_h + \nabla\phi \|_{0,K}^2 + \epsilon \| \boldsymbol{q} - \boldsymbol{q}_h \|_{0,K}^2 \tag{2.3.2}$$

The harder part is to estimate the first two terms, namely,

$$T_K := (\nabla\cdot(\boldsymbol{q} - \boldsymbol{q}_h), u - \phi)_K - \langle u - \phi, (\boldsymbol{q} - \boldsymbol{q}_h)\cdot\boldsymbol{n}\rangle_{\partial K}.$$

To do so, we add and subtract $\mathsf{P}_K f$ in the first term and $\widehat{\boldsymbol{q}}_h \cdot \boldsymbol{n}$ in the second term, and obtain

$$T_K := T_{1,K} + T_{2,K} + T_{3,K}, \tag{2.3.3}$$

where

$$\begin{aligned} T_{1,K} :=& (f - \mathsf{P}_K f, u - \phi)_K, \\ T_{2,K} :=& -\langle u - \phi, (\boldsymbol{q} - \widehat{\boldsymbol{q}}_h)\cdot\boldsymbol{n}\rangle_{\partial K}, \\ T_{3,K} :=& (\mathsf{P}_K f - \nabla\cdot\boldsymbol{q}_h, u - \phi)_K - \langle u - \phi, (\widehat{\boldsymbol{q}}_h - \boldsymbol{q}_h)\cdot\boldsymbol{n}\rangle_{\partial K}. \end{aligned}$$

To estimate $T_{1,K}$, we only need to note that for any constant μ,

$$\begin{aligned} (f - \mathsf{P}_K f, u - \phi)_K &= (f - \mathsf{P}_K f, u - \phi - \mu)_K \\ &\le \frac{1}{4\epsilon} h_K^2 \| f - \mathsf{P}_K f \|_{0,K}^2 + \epsilon h_K^{-2} \| u - \phi - \mu \|_{0,K}^2. \end{aligned}$$

By the Bramble-Hilbert Lemma,

$$h_K^{-2}\| (u-\phi-\mu) \|_{0,K}^2 \le C_p \| \nabla(u-\phi) \|_{0,K}^2,$$

where the Poincaré constant C_p depends on the shape regularity constant σ. Thus,

$$T_{1,K} \le \frac{1}{4\epsilon} h_K^2 \| f - \mathsf{P}_K f \|_{0,K}^2 + \epsilon C_p \| \boldsymbol{q} + \nabla\phi \|_{0,K}^2. \tag{2.3.4}$$

For the second term $T_{2,K}$, note that, since ϕ is continuous across the edges, we have that

$$\sum_K T_{2,K} = -\sum_{K\in\mathcal{T}_h} \langle (\boldsymbol{q}-\widehat{\boldsymbol{q}}_h)\cdot\boldsymbol{n}, u-\phi\rangle_{\partial K} = -\langle (\boldsymbol{q}-\widehat{\boldsymbol{q}}_h)\cdot\boldsymbol{n}, u-\phi\rangle_{\Gamma}.$$

It remains to estimate $T_{3,K}$. By the second equation defining the HDG method (1.2.2), for each simplex $K\in\mathcal{T}_h$, we have that

$$\langle (\boldsymbol{q}_h-\widehat{\boldsymbol{q}}_h)\cdot\boldsymbol{n}, \omega\rangle_{\partial K} = (\mathsf{P}_K f - \nabla\cdot\boldsymbol{q}_h, \omega)_K, \quad \forall\omega\in W_h(K),$$

which implies that

$$\begin{aligned} T_{3,K} &= \langle \mathsf{P}_K(u-\phi)-(u-\phi), (\widehat{\boldsymbol{q}}_h-\boldsymbol{q}_h)\cdot\boldsymbol{n}\rangle_{\partial K}. \\ &\le \frac{1}{4\epsilon} h_K \| (\widehat{\boldsymbol{q}}_h-\boldsymbol{q}_h)\cdot\boldsymbol{n} \|_{0,\partial K}^2 + \epsilon h_K^{-1} \| \mathsf{P}_K(u-\phi)-(u-\phi) \|_{0,\partial K}^2. \end{aligned}$$

By the trace inequality and the Bramble-Hilbert lemma, we get

$$\begin{aligned} h_K^{-1}\| \mathsf{P}_K(u-\phi)-u+\phi \|_{0,\partial K}^2 &\le C_t h_K^{-2} \| \mathsf{P}_K(u-\phi)-u+\phi \|_{0,K}^2 \\ &\le C_{t2} \| \nabla u - \nabla\phi \|_{0,K}^2, \end{aligned}$$

where C_{t2} depends on the shape regularity constant σ. Thus, we have

$$T_{3,K} \le \frac{1}{4\epsilon} h_K \| (\widehat{\boldsymbol{q}}_h-\boldsymbol{q}_h)\cdot\boldsymbol{n} \|_{0,\partial K}^2 + \epsilon C_{t2} \| \boldsymbol{q}+\nabla\phi \|_{0,K}^2. \tag{2.3.5}$$

Using the estimates obtained in (2.3.2) to (2.3.5), we conclude that

$$\begin{aligned} \| \boldsymbol{q}-\boldsymbol{q}_h \|_{0,\mathcal{T}_h}^2 \le &\sum_{K\in\mathcal{T}_h} \frac{1}{4\epsilon} \| \boldsymbol{q}_h + \nabla\phi \|_{0,K}^2 + \sum_{K\in\mathcal{T}_h} \epsilon \| \boldsymbol{q}-\boldsymbol{q}_h \|_{0,K}^2 \\ &+ \sum_{K\in\mathcal{T}_h} \frac{1}{4\epsilon} h_K^2 \| f - \mathsf{P}_K f \|_{0,K}^2 + \sum_{K\in\mathcal{T}_h} \epsilon C_p \| (\boldsymbol{q}+\nabla\phi) \|_{0,K}^2 \\ &+ \sum_{K\in\mathcal{T}_h} \frac{1}{4\epsilon} h_K \| (\widehat{\boldsymbol{q}}_h-\boldsymbol{q}_h)\cdot\boldsymbol{n} \|_{0,\partial K}^2 + \sum_{K\in\mathcal{T}_h} \epsilon C_{t2} \| \boldsymbol{q}+\nabla\phi \|_{0,K}^2 \\ &- \langle (\boldsymbol{q}-\widehat{\boldsymbol{q}}_h)\cdot\boldsymbol{n}, u-\phi\rangle_{\Gamma}, \end{aligned} \tag{2.3.6}$$

and, after simple algebraic manipulations, that

$$\| \boldsymbol{q} - \boldsymbol{q}_h \|_{0,\mathcal{T}_h}^2 \leq \frac{1}{4\epsilon}\eta_q^2 + (\frac{1}{4\epsilon} + \epsilon C_p + \epsilon C_{t2})\eta_\phi^2 \\ + \epsilon(1 + C_p + C_{t2})\| \boldsymbol{q} - \boldsymbol{q}_h \|_{0,\mathcal{T}_h}^2 - \langle(\boldsymbol{q} - \widehat{\boldsymbol{q}}_h) \cdot \boldsymbol{n}, u - \phi\rangle_\Gamma.$$

The result follows by choosing ϵ small enough. This completes the proof of Lemma 2.3.5. □

Note that only the second equation in the HDG formulation (1.2.2) was used in the proof, and that the function ϕ is an arbitrary, continuous and piecewise differentiable function.

2.3.3 Step 3: Proof of the efficiency and reliability of the estimator

Theorem 2.2.1 will immediately from Lemma 2.3.6, which establishes the efficiency of the estimator, and from Lemma 2.3.7, which establishes its reliability.

The efficiency of the estimator

We are ready now to obtain a lower bound for the error e_h.

Lemma 2.3.6 (Efficiency of the error estimator)**.** *We have that*

$$C_1 \eta_h^2 \leq \mathsf{e}_h^2,$$

where C_1 is some constant depending only on the shape regularity constant σ and the degree of the polynomial p.

Proof. Let us begin by estimating $\eta_{1,h}$. By definition, (2.2.8a),

$$\eta_{1,h}^2 := \sum_{K \in \mathcal{T}_h} h_K^2 \| f - \mathsf{P}_W f \|_{0,K}^2 \leq \sum_{K \in \mathcal{T}_h} h_K^2 \| f - \nabla\cdot \boldsymbol{q}_h \|_{0,K}^2 \leq \mathsf{e}_h^2,$$

since $\mathsf{P}_W f$ is the L^2-projection into the space W_h and $\nabla\cdot \boldsymbol{q}_h \in W_h$.

Next, let us estimate $\eta_{2,h}$. By definition (2.2.8b),

$$\eta_{2,h} := (T_1^2 + T_2^2 + T_3^2)^{1/2},$$

where

$$T_1^2 := \sum_{K\in\mathcal{T}_h} h_K^{-1} \| \, \mathsf{P}_M(\mathsf{Id}-\Phi)(\widehat{u}_h - u_h) \, \|_{0,\partial K}^2,$$
$$T_2^2 := \sum_{e\in\mathcal{E}_h} h_e^{-1} \| \, [\![(\mathsf{Id}-\mathsf{P}_M)\Phi(\widehat{u}_h - u_h)]\!] \, \|_{0,e}^2,$$
$$T_3^2 := \sum_{K\in\mathcal{T}_h} h_K \| \, \tau(\widehat{u}_h - u_h) \, \|_{0,\partial K}^2.$$

We shall proceed in three steps and estimate each component of the estimator. Our first goal is to establish an upper bound for T_1^2. Note from the definition of postprocessing (2.2.3), we have

$$T_1^2 = \sum_{K\in\mathcal{T}_h} h_K^{-1} \| \, \mathsf{P}_M(\widehat{u}_h - u_h^*) \, \|_{0,\partial K}^2,$$

and by Lemma (2.3.3), we have

$$\begin{aligned} T_1^2 &\le C_{s2}^2 \sum_{K\in\mathcal{T}_h} \| \, \boldsymbol{q}_h + \nabla u_h^* \, \|_{0,K}^2 \\ &\le 2C_{s2}^2 \sum_{K\in\mathcal{T}_h} (\| \, \boldsymbol{q} + \nabla u_h^* \, \|_{0,K}^2 + \| \, \boldsymbol{q} - \boldsymbol{q}_h \, \|_{0,K}^2) \\ &\le 2C_{s2}^2 \mathsf{e}_h^2. \end{aligned}$$

Next, our task is to estimate T_2^2. Again, by definition of post-processing (2.2.3), we have

$$T_2^2 = h_e^{-1} \| \, (\mathsf{Id} - \mathsf{P}_M) \, [\![u_h^* - u_h]\!] \, \|_{0,e}^2.$$

Since $\mathsf{P}_M \, [\![u_h]\!] = [\![u_h]\!]$, we get

$$T_2^2 = h_e^{-1} \| \, (\mathsf{Id} - \mathsf{P}_M) \, [\![u_h^*]\!] \, \|_{0,e}^2 \le \mathsf{e}_h^2.$$

We now only have to estimate T_3^2. From the definition of numerical flux $\widehat{\boldsymbol{q}}_h \cdot \boldsymbol{n}$ for LDG-H method (Table 1.2.2), we get

$$T_3^2 := \sum_{K\in\mathcal{T}_h} h_K \| \, \tau(\widehat{u}_h - u_h) \, \|_{0,\partial K}^2 = \sum_{K\in\mathcal{T}_h} h_K \| \, (\widehat{\boldsymbol{q}}_h - \boldsymbol{q}_h) \cdot \boldsymbol{n} \, \|_{0,\partial K}^2.$$

If suffices to show that

$$T_3^2 \leq C_4 \sum_{K\in\mathcal{T}_h} (\|\,(\boldsymbol{q}-\widehat{\boldsymbol{q}}_h)\cdot\boldsymbol{n}\,\|_{-1/2,\partial K}^2 + \|\,\boldsymbol{q}-\boldsymbol{q}_h\,\|_{div,K}^2).$$

We see, by Lemma 2.3.2, that we have

$$\begin{aligned} h_K\|\,(\widehat{\boldsymbol{q}}_h-\boldsymbol{q}_h)\cdot\boldsymbol{n}\,\|_{0,\partial K}^2 &\leq C_{s1}^2\|\,(\widehat{\boldsymbol{q}}_h-\boldsymbol{q}_h)\cdot\boldsymbol{n}\,\|_{-1/2,\partial K}^2. \\ &\leq 2C_{s1}^2\|\,(\boldsymbol{q}-\boldsymbol{q}_h)\cdot\boldsymbol{n}\,\|_{-1/2,\partial K}^2 + 2C_{s1}^2\|\,(\boldsymbol{q}-\widehat{\boldsymbol{q}}_h)\cdot\boldsymbol{n}\,\|_{-1/2,\partial K}^2, \\ &\leq 2C_{s1}^2\|\,(\boldsymbol{q}-\widehat{\boldsymbol{q}}_h)\cdot\boldsymbol{n}\,\|_{-1/2,\partial K}^2 + 2C_{s1}^2C_{t1}^2\|\,\boldsymbol{q}-\boldsymbol{q}_h\,\|_{div,K}^2. \end{aligned}$$

by Lemma 2.3.1. Thus, we can take $C_4 := 2C_{s1}^2 \max\{1, C_{t1}^2\}$.

This completes the proof.

□

The reliability of the estimator

To complete the proof of Theorem 2.2.1 it only remains to prove an upper bound for the error e_h. It is contained in the following result.

Lemma 2.3.7 (Reliability of the error estimator)**.** *We have that*

$$\mathsf{e}_h^2 \leq C_2\eta_h^2.$$

where C_2 is a constant depending only on the shape regularity constant σ and the degree of the polynomial p.

Proof. Since by definition of postprocessing, (2.2.3), we have

$$\begin{aligned} \mathsf{P}_M(\mathsf{Id}-\Phi)(\widehat{u}_h-u_h) &= \mathsf{P}_M(\widehat{u}_h-u_h^*), \\ [\![(\mathsf{Id}-\mathsf{P}_M)\Phi(\widehat{u}_h-u_h)]\!] &= [\![(\mathsf{Id}-\mathsf{P}_M)(u_h^*-u_h)]\!] = (\mathsf{Id}-\mathsf{P}_M)\,[\![u_h^*]\!], \end{aligned}$$

and, since by definition of the numerical flux $\widehat{\boldsymbol{q}}_h$, we have that

$$\tau(u_h-\widehat{u}_h) = (\widehat{\boldsymbol{q}}_h-\boldsymbol{q}_h)\cdot\boldsymbol{n},$$

it is enough to show that

$$\mathsf{e}_h^2 \leq C_2(\sum_{K\in\mathcal{T}_h} h_K^2 \| f - \mathsf{P}_W f \|_{0,K}^2 + \sum_{K\in\mathcal{T}_h} \| \boldsymbol{q}_h + \nabla u_h^* \|_{0,K}^2 \\ + h_e^{-1} \| (\mathsf{Id} - \mathsf{P}_M) [\![u_h^*]\!] \|_{0,e}^2 + \sum_{K\in\mathcal{T}_h} h_K \| (\widehat{\boldsymbol{q}}_h - \boldsymbol{q}_h)\cdot \boldsymbol{n} \|_{0,\partial K}^2).$$

By definition of the error (2.2.5), we have that

$$\mathsf{e}_h := (\| \boldsymbol{q} - \boldsymbol{q}_h \|_{div,\mathcal{T}_h}^2 + \| \, [\![u - u_h^*]\!] \|_{1/2,\mathcal{E}_h}^2 \\ + \| \nabla (u - u_h^*) \|_{0,\mathcal{T}_h}^2 + \| (\boldsymbol{q} - \widehat{\boldsymbol{q}}_h)\cdot \boldsymbol{n} \|_{-1/2,\partial\mathcal{T}_h}^2)^{1/2},$$

and so, we shall show that each of the four terms inside the square root can be bounded by a constant times η_h^2.

Let us begin by estimating $\| \boldsymbol{q} - \boldsymbol{q}_h \|_{div,\mathcal{T}_h}^2$. By definition (2.2.6), and also by (2.2.4d),

$$\begin{aligned} \| \boldsymbol{q} - \boldsymbol{q}_h \|_{div,\mathcal{T}_h}^2 &= \| \boldsymbol{q} - \boldsymbol{q}_h \|_{0,\mathcal{T}_h}^2 + \sum_{K\in\mathcal{T}_h} h_K^2 \, \| f - \nabla\cdot \boldsymbol{q}_h \|_{0,K}^2 \\ &= \| \boldsymbol{q} - \boldsymbol{q}_h \|_{0,\mathcal{T}_h}^2 + \sum_{K\in\mathcal{T}_h} h_K^2 (\| f - \mathsf{P}_W f \|_{0,K}^2 + \| \mathsf{P}_W f - \nabla\cdot \boldsymbol{q}_h \|_{0,K}^2) \\ &\leq \| \boldsymbol{q} - \boldsymbol{q}_h \|_{0,\mathcal{T}_h}^2 + \eta_{1,h}^2 + C_{s2}^2 \, h_K \| (\widehat{\boldsymbol{q}}_h - \boldsymbol{q}_h)\cdot \boldsymbol{n} \|_{0,K}^2, \end{aligned}$$

by definition of $\eta_{1,h}$, (2.2.8a), and by Lemma 2.3.3.

It remains to estimate $\| \boldsymbol{q} - \boldsymbol{q}_h \|_{0,\mathcal{T}_h}^2$. To do that, we note that, by Lemma 2.3.5, for any function ϕ in $\mathcal{C}^1(\mathcal{T}_h) \cap \mathcal{C}^0(\Omega)$, we have

$$\| \boldsymbol{q} - \boldsymbol{q}_h \|_{0,\mathcal{T}_h}^2 \leq \; C_\sigma (\eta_q^2 + \eta_\phi^2) - \langle (\boldsymbol{q} - \widehat{\boldsymbol{q}}_h)\cdot \boldsymbol{n}, g - \phi \rangle_\Gamma$$

where

$$\eta_q^2 = (\sum_{K\in\mathcal{T}_h} h_K^2 \| f - \mathsf{P}_W f \|_{0,K}^2 + \sum_{K\in\mathcal{T}_h} h_K \| (\widehat{\boldsymbol{q}}_h - \boldsymbol{q}_h)\cdot \boldsymbol{n} \|_{0,\partial K}^2)$$

We now take $\phi := \tilde{u}_h^* \in W_h^* \cap \mathcal{C}^0(\Omega)$, where, by the result of Lemma 2.3.4, the function $\tilde{u}_h^*$ satisfies

$$\tilde{u}_h^* = g \qquad \text{on } \Gamma, \tag{2.3.7a}$$

$$\sum_{K\in\mathcal{T}_h} \| \nabla (u_h^* - \tilde{u}_h^*) \|_{0,K}^2 \leq C_j \sum_{e\in\mathcal{E}_h^i} h_e^{-1} \| \, [\![u_h^*]\!] \|_{0,e}^2. \tag{2.3.7b}$$

We immediately obtain that $\langle(\boldsymbol{q}-\widehat{\boldsymbol{q}}_h)\cdot\boldsymbol{n}, g-\phi\rangle_\Gamma = 0$, by property (2.3.7a), and that

$$\begin{aligned}\eta_\phi^2 &= \sum_{K\in\mathcal{T}_h} \|\,\boldsymbol{q}_h + \nabla\tilde{u}_h^*\,\|_{0,K}^2 \\ &\le \sum_{K\in\mathcal{T}_h} \|\,\boldsymbol{q}_h + \nabla u_h^*\,\|_{0,K}^2 + \sum_{K\in\mathcal{T}_h} \|\,\nabla(u_h^* - \tilde{u}_h^*)\,\|_{0,K}^2, \\ &\le \sum_{K\in\mathcal{T}_h} \|\,\boldsymbol{q}_h + \nabla u_h^*\,\|_{0,K}^2 + C_j \sum_{e\in\mathcal{E}_h^i} h_E^{-1}\|\,[\![u_h^*]\!]\,\|_{0,e}^2,\end{aligned}$$

by property (2.3.7b). This proves that $\|\,\boldsymbol{q}-\boldsymbol{q}_h\,\|_{div,\mathcal{T}_h}$ is bounded by a constant times η_h.

To bound the second term in the definition of the error e_h, we simply invoke Corollary 2.3.1 to get

$$\|\,[\![u-u_h^*]\!]\,\|_{1/2,\mathcal{E}_h}^2 \le C_{s2}\Big(\sum_{e\in\mathcal{E}_h} h_e^{-1}\|\,(\mathsf{Id}-\mathsf{P}_M)\,[\![u_h^*]\!]\,\|_{0,e}^2 + \sum_{K\in\mathcal{T}_h}\|\,\boldsymbol{q}_h+\nabla u_h^*\,\|_{0,K}^2\Big).$$

Let us now bound the third term $\|\,\nabla(u-u_h^*)\,\|_{0,\mathcal{T}_h}$. We have

$$\|\,\nabla(u-u_h^*)\,\|_{0,\mathcal{T}_h}^2 \le 2\sum_{K\in\mathcal{T}_h}\|\,\boldsymbol{q}_h+\nabla u_h^*\,\|_{0,K}^2 + 2\sum_{K\in\mathcal{T}_h}\|\,\boldsymbol{q}-\boldsymbol{q}_h\,\|_{0,K}^2.$$

The estimate now follows from the estimate of the term $\|\boldsymbol{q}-\boldsymbol{q}_h\|_{0,\mathcal{T}_h}^2$ obtained above.

Finally, to estimate $\Theta := \|\,(\boldsymbol{q}-\widehat{\boldsymbol{q}}_h)\cdot\boldsymbol{n}\,\|_{-1/2,\partial\mathcal{T}_h}$, we proceed as follows. By the triangle inequality,

$$\begin{aligned}\Theta^2 &:= \sum_{K\in\mathcal{T}_h}\|\,(\boldsymbol{q}-\widehat{\boldsymbol{q}}_h)\cdot\boldsymbol{n}\,\|_{-1/2,\partial K}^2 \\ &\le\; 2\sum_{K\in\mathcal{T}_h}\|\,(\boldsymbol{q}-\boldsymbol{q}_h)\cdot\boldsymbol{n}\,\|_{-1/2,\partial K}^2 +\; 2\sum_{K\in\mathcal{T}_h}\|\,(\boldsymbol{q}_h-\widehat{\boldsymbol{q}}_h)\cdot\boldsymbol{n}\,\|_{-1/2,\partial K}^2,\end{aligned}$$

and, by Lemma 2.3.1 and by Lemma 2.3.2,

$$\Theta^2 \le\; 2\sum_{K\in\mathcal{T}_h}\|\,(\boldsymbol{q}-\boldsymbol{q}_h)\,\|_{div,K}^2 +\; 2\,C_{s1}^2\sum_{K\in\mathcal{T}_h} h_K\|\,(\boldsymbol{q}_h-\widehat{\boldsymbol{q}}_h)\cdot\boldsymbol{n}\,\|_{0,\partial K}^2,$$

The estimate of $\|\,(\boldsymbol{q}-\widehat{\boldsymbol{q}}_h)\cdot\boldsymbol{n}\,\|_{-1/2,\partial\mathcal{T}_h}$ now follows from the previously obtained estimate for $\|\boldsymbol{q}-\boldsymbol{q}_h\|_{div,\mathcal{T}_h}$. This completes the proof. $\square$

2.4 Numerical Results

In this section, we present numerical experiments devised to verify the reliability and efficiency properties of the a posteriori estimate predicted by our theoretical result, Theorem 2.2.1, in the two dimensional case. Moreover, we explore how the estimates behave as we change the polynomial degree of the HDG method, p, and its stabilization function, τ. We do not always take the boundary value g to be piecewise polynomial. In this case, g is approximated by some piecewise polynomial g_h and the quality of this approximation is controlled by a boundary oscillation term $osc^2(g, \mathcal{E}_h^\partial)$. We refer the reader to [73] for details. However, in this chapter, for simplicity, we neglect the boundary oscillation term.

2.4.1 Preliminaries

We do this by using a test problem with a smooth solution and one with a solution presenting a singularity. The exact solutions are:

$$\begin{aligned} u &= \sin(\pi x)\sin(\pi y), && \Omega := (0,1)^2, \\ u &= r^{2/3}\sin(2\theta/3), && \Omega := (-1,1)^2 \setminus (0,1)\times(-1,0). \end{aligned}$$

In both test problems, we set the Dirichlet boundary data g equal to the exact solution u. Note that for the first problem we have $f = \pi^2 \sin(\pi x)\sin(\pi y), g = 0$ and that for the second we have $f = 0$ and g is not piecewise polynomial on the boundary Γ.

We present two sets of experiments. In the first, we test the behavior of the a posteriori estimate with uniform mesh refinement. For both test problems, we take the stabilization function τ to be equal to 1 and let the polynomial degree p take the values 0, 1 and 2. In addition, for the test problem with a nonsmooth solution, we take the polynomial degree p to be 1 and take the stabilization function τ to be $10^{-3}, 10$ and 10^2.

In the second set of experiments, we test the behavior of the a posteriori estimate with adaptive mesh refinement. We only consider the more difficult of the test problems, namely, the one with the nonsmooth solution, and take the polynomial degree p to be 1 and 2, and the stabilization function τ to be $10^{-3}, 1$ and 10^2.

In each of our experiments, we monitor the four terms of the error e_h given by (2.2.6) as well as the four terms of the estimator η_h given by (2.2.8). The *computational order of convergence* of each of these quantities is calculated as follows. Suppose that $e(N)$ and $e(\tilde{N})$ is any of the above quantities for two consecutive triangulations with N and $\tilde{N}$ number of triangles, respectively. Then, the computational rate of convergence is given by

$$-2\frac{\log(e(N)/e(\tilde{N}))}{\log(N/\tilde{N})}.$$

Let us point out that, in order to evaluate the last component of the error, namely,

$$\Big(\sum_{K\in\mathcal{T}_h} \| (\boldsymbol{q}-\widehat{\boldsymbol{q}}_h)\cdot\boldsymbol{n} \|^2_{-1/2,\partial K}\Big)^{1/2},$$

see (2.2.6d), we are going to use the following lemma; see [25].

Lemma 2.4.1.

$$\| v^* \|_{-1/2,\partial K} = h_K^{-1} \| \bar{v}^* \|_{1,K},$$

where $\bar{v}^*$ is the solution of the variational Neumann problem,

$$h_K^2 \int_K \nabla\bar{v}^*\cdot\nabla v dx + \int_K \bar{v}^* v dx = h_K^2\langle v^*, v\rangle_{\partial K}, \qquad \forall v\in H^1(K).$$

In practice, we use a discrete version of of this result and take $\bar{v}^*\in W_{p+1}(K)$ as the solution of

$$h_K^2 \int_K \nabla\bar{v}^*\cdot\nabla v dx + \int_K \bar{v}^* v dx = h_K^2\langle v^*, v\rangle_{\partial K}, \qquad \forall v\in W_{p+1}(K).$$

Note that, from the definition of post-processing, (2.2.3), we have

$$\begin{aligned}
\sum_{K\in\mathcal{T}_h} h_K^{-1}\| \mathsf{P}_M(\mathsf{Id}-\Phi)(\widehat{u}_h-u_h) \|^2_{0,\partial K} &= \sum_{K\in\mathcal{T}_h} h_K^{-1}\| \mathsf{P}_M(\widehat{u}_h-u_h^*) \|^2_{0,\partial K}\\
\sum_{e\in\mathcal{E}_h} h_e^{-1}\| [\![(\mathsf{Id}-\mathsf{P}_M)\Phi(\widehat{u}_h-u_h)]\!] \|^2_{0,e} &= \sum_{e\in\mathcal{E}_h} h_e^{-1}\| (\mathsf{Id}-\mathsf{P}_M)\, [\![u_h^*]\!] \|^2_{0,e},\\
\sum_{K\in\mathcal{T}_h} h_K\| \tau(\widehat{u}_h-u_h) \|^2_{0,\partial K} &= \sum_{K\in\mathcal{T}_h} h_K\| (\widehat{\boldsymbol{q}}_h-\boldsymbol{q}_h)\cdot\boldsymbol{n} \|^2_{0,\partial K}
\end{aligned}$$

Hence, we use the above notation to denote the three components of the estimator $\eta_{2,h}$ hereafter.

2.4.2 Uniform refinement

The numerical results for the smooth solution test problem are shown in Table 2.4.1; we take $\tau = 1$ and $p \in \{0, 1, 2\}$. We see that *each* of the components of the error as well as those of the estimator converge at an *optimal* order of $p+1$; the term $\| f - \mathsf{P}_W f \|_{-1,\mathcal{T}_h}$ converges even faster, namely, at the order of $p+2$. These numerical results agree with the a priori error estimates obtained in [35] and, more importantly, they verify that the error estimate is reliable and efficient.

The numerical results for the non-smooth solution test problem are shown in Table 2.4.2; we also take $\tau = 1$ and $p \in \{0, 1, 2\}$. In this case, not all the components of the error or those of the estimator converge at the same rate. Note that, all the individual error components of and the estimators $\| \boldsymbol{q}_h + \nabla u_h^* \|_{0,\mathcal{T}_h}$ and $\| (\mathsf{Id} - \mathsf{P}_M) [\![u_h^*]\!] \|_{1/2,\mathcal{E}_h}$ converge with order $N^{-2/3}$ approximately, but that the estimator $\| (\boldsymbol{q}_h - \widehat{\boldsymbol{q}}_h) \cdot \boldsymbol{n} \|_{-1/2,\partial\mathcal{T}_h}$ converges with order $N^{-5/3}$, that is, much faster. Furthermore, for $p = 0$, since $\nabla u_h^* = -\boldsymbol{q}_h$, the second estimator $\| \boldsymbol{q}_h + \nabla u_h^* \|_{0,\mathcal{T}_h}$ is identically equal to zero. This seems to suggest that the estimator η_h could be dominated by $\| (\mathsf{Id} - \mathsf{P}_M) [\![u_h^*]\!] \|_{1/2,\mathcal{E}_h}$ and the residual $\| f - \mathsf{P}_K f \|_{-1,\mathcal{T}_h}$.

In order to explore the effect of τ, we continue our experiment on the L-shaped domain using $p = 1$ and vary τ from 10^{-3} to 10^2. The history of convergence of each individual error and estimator is displayed in Table 2.4.3. We see that the effect of τ is negligible when τ tends to zero. On the other hand, as τ grows, we observe that each individual error becomes larger, and that the estimators $\| \boldsymbol{q}_h + \nabla u_h^* \|_{0,\mathcal{T}_h}$ and $\| (\mathsf{Id} - \mathsf{P}_M) [\![u_h^*]\!] \|_{1/2,\mathcal{E}_h}$ take longer to reach the asymptotic regime and converge at with order $N^{-2/3}$. The last estimator $\| (\boldsymbol{q}_h - \widehat{\boldsymbol{q}}_h) \cdot \boldsymbol{n} \|_{-1/2,\partial\mathcal{T}_h}$ becomes larger as τ grows, but decreases much faster as the mesh gets finer. Thus, we conclude that the quality of our estimator is not apparently affected by either small or large values of the stabilization function τ as the mesh gets finer and finer.

2.4.3 Adaptive refinement

Next, we present the numerical result obtained from an adaptive algorithm. The adaptive algorithm used in this work is the following:

1. Start with a mesh $\mathcal{T}_h$.

2. Solve the discrete problem (1.2.2).

3. Compute the estimator.

4. Decide to stop or go to the next step.

5. Mark the elements to be refined.

6. Modify the mesh with the so-called *red-green-blue* procedure.

7. Denote the new mesh by $\mathcal{T}_h$ and return to step 2.

The marking strategy, based on η_K, is originally due to Dörfler [40] and consists in selecting a subset M of $\mathcal{T}_h$ such that $\alpha^2 \sum_{K\in\mathcal{T}_h} \eta_K^2 \leq \sum_{K\in M} \eta_K^2$, where the parameter α is taken in $(0,1)$. Here, we take $\alpha = 1/2$.

In Fig 2.4.1, we display meshes obtained with the above adaptive procedure. Note that the algorithm is able to properly locate the singularity of the exact solution at the point $(0,0)$. Note also that, for about the same accuracy $\mathsf{e}_h \simeq 0.040$, the use of polynomials of degree 2 requires 88 elements while using polynomials of degree 1 requires 240 elements. Since the manipulation of the mesh takes up a significant amount of computational effort, working with high-order polynomials might be advantageous.

In the legend of Fig. 2.4.2, we use the following notation $\eta^1_{2,h} = \|\, \mathsf{P}_M(\widehat{u}_h - u_h^*) \,\|_{0,\partial\mathcal{T}_h}$, $\eta^2_{2,h} = \|\, (\mathsf{Id} - \mathsf{P}_M) \, [\![u_h^*]\!] \,\|_{1/2,\mathcal{E}_h}$, $\eta^3_{2,h} = \|\, (\widehat{\boldsymbol{q}}_h - \boldsymbol{q}_h) \cdot \boldsymbol{n} \,\|_{-1/2,\partial\mathcal{T}_h}$. We see that the last three components of the estimator, namely, $\eta_{2,h}$ $\eta_{3,h}$ and $\eta_{4,h}$, and the error decrease at the same rate. In order to judge the quality of our error estimator, we compute an effective index, which is defined as the ratio e_h/η_h. In Fig. 2.4.3, we see that the effective index is bounded from above and below, this verifies the reliability and efficiency of our a posteriori error estimator. We also observe that the effectivity index does not show any significant change of behavior when τ varies from 0.001 to 1 while the index changes drastically as τ grows from 1 to 100. This phenomenon seems to suggests that, rouglhy speaking, the effectivity index of adaptive HDG methods with a small stabilization function τ is more *robust* than with a large τ.

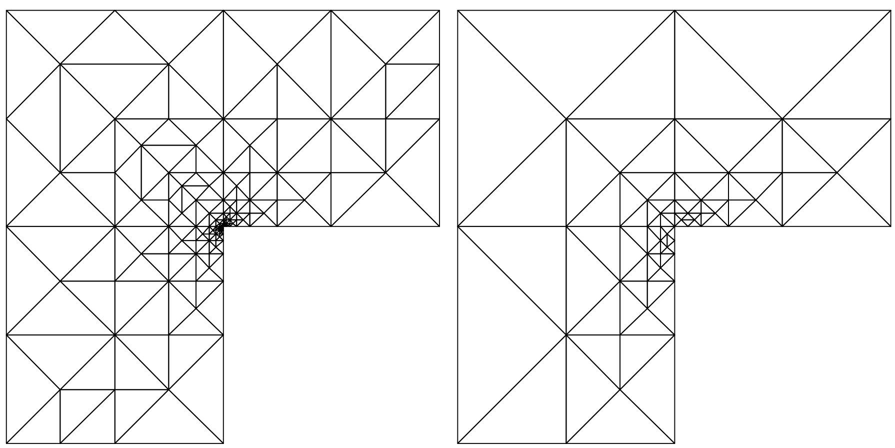

Figure 2.4.1: Example of adaptive meshes

Table 2.4.1: The effect of the polynomial degree p for smooth solution

$p = 0$

Mesh	$\\| \boldsymbol{q} - \boldsymbol{q}_h \\|_{div,\mathcal{T}_h}$		$\\| [\![u_h^*]\!] \\|_{1/2,\mathcal{E}_h}$		$\\| \nabla(u - u_h^*) \\|_{0,\mathcal{T}_h}$		$\\| (\boldsymbol{q} - \widehat{\boldsymbol{q}}_h) \cdot \boldsymbol{n} \\|_{-1/2,\partial\mathcal{T}_h}$	
N	error	order	error	order	error	order	error	order
16.	0.27E+01	-	0.56E+00	-	0.11E+01	-	0.84E+00	-
64.	0.14E+01	0.99	0.50E+00	0.14	0.58E+00	0.94	0.41E+00	1.05
256.	0.68E+00	0.99	0.31E+00	0.72	0.30E+00	0.97	0.21E+00	0.98
1024.	0.34E+00	1.00	0.17E+00	0.88	0.15E+00	0.99	0.10E+00	0.98
4096.	0.17E+00	1.00	0.86E-01	0.95	0.75E-01	0.99	0.53E-01	0.99
Mesh	$\\| f - \mathsf{P}_W f \\|_{-1,\mathcal{T}_h}$		$\\| \mathsf{P}_M(\widehat{u}_h - u_h^*) \\|_{0,\mathcal{T}_h}$		$\\| (\mathsf{Id} - \mathsf{P}_M) [\![u_h^*]\!] \\|_{1/2,\mathcal{E}_h}$		$\\| (\widehat{\boldsymbol{q}}_h - \boldsymbol{q}_h) \cdot \boldsymbol{n} \\|_{-1/2,\partial\mathcal{T}_h}$	
N	estimator	order	estimator	order	estimator	order	estimator	order
16.	0.89E+00	-	0.11E-14	-	0.56E+00	-	0.87E+00	-
64.	0.23E+00	1.97	0.16E-14	-	0.50E+00	0.14	0.46E+00	0.92
256.	0.57E-01	1.99	0.32E-14	-	0.31E+00	0.72	0.23E+00	0.98
1024.	0.14E-01	2.00	0.59E-14	-	0.17E+00	0.88	0.12E+00	0.99
4096.	0.36E-02	2.00	0.11E-13	-	0.86E-01	0.95	0.59E-01	1.00

$p = 1$

Mesh	$\\| \boldsymbol{q} - \boldsymbol{q}_h \\|_{div,\mathcal{T}_h}$		$\\| [\![u_h^*]\!] \\|_{1/2,\mathcal{E}_h}$		$\\| \nabla(u - u_h^*) \\|_{0,\mathcal{T}_h}$		$\\| (\boldsymbol{q} - \widehat{\boldsymbol{q}}_h) \cdot \boldsymbol{n} \\|_{-1/2,\partial\mathcal{T}_h}$	
N	error	order	error	order	error	order	error	order
16.	0.91E+00	-	0.77E-01	-	0.19E+00	-	0.14E+00	-
64.	0.23E+00	1.97	0.28E-01	1.45	0.50E-01	1.93	0.31E-01	2.13
256.	0.59E-01	1.99	0.81E-02	1.79	0.13E-01	1.98	0.78E-02	2.01
1024.	0.15E-01	2.00	0.22E-02	1.91	0.32E-02	1.99	0.20E-02	2.00
4096.	0.37E-02	2.00	0.55E-03	1.96	0.79E-03	2.00	0.49E-03	1.99
Mesh	$\\| f - \mathsf{P}_W f \\|_{-1,\mathcal{T}_h}$		$\\| \mathsf{P}_M(\widehat{u}_h - u_h^*) \\|_{0,\mathcal{T}_h}$		$\\| (\mathsf{Id} - \mathsf{P}_M) [\![u_h^*]\!] \\|_{1/2,\mathcal{E}_h}$		$\\| (\widehat{\boldsymbol{q}}_h - \boldsymbol{q}_h) \cdot \boldsymbol{n} \\|_{-1/2,\partial\mathcal{T}_h}$	
N	estimator	order	estimator	order	estimator	order	estimator	order
16.	0.27E+00	-	0.37E-01	-	0.57E-01	-	0.24E+00	-
64.	0.34E-01	2.97	0.88E-02	2.06	0.25E-01	1.18	0.61E-01	1.96
256.	0.43E-02	2.99	0.22E-02	2.02	0.75E-02	1.74	0.15E-01	1.99
1024.	0.54E-03	3.00	0.54E-03	2.01	0.20E-02	1.89	0.38E-02	2.00
4096.	0.68E-04	3.00	0.13E-03	2.00	0.52E-03	1.95	0.96E-03	2.00

$p = 2$

Mesh	$\\| \boldsymbol{q} - \boldsymbol{q}_h \\|_{div,\mathcal{T}_h}$		$\\| [\![u_h^*]\!] \\|_{1/2,\mathcal{E}_h}$		$\\| \nabla(u - u_h^*) \\|_{0,\mathcal{T}_h}$		$\\| (\boldsymbol{q} - \widehat{\boldsymbol{q}}_h) \cdot \boldsymbol{n} \\|_{-1/2,\partial\mathcal{T}_h}$	
N	error	order	error	order	error	order	error	order
16.	0.19E+00	-	0.56E-02	-	0.25E-01	-	0.14E-01	-
64.	0.24E-01	2.97	0.12E-02	2.27	0.32E-02	2.97	0.18E-02	2.98
256.	0.30E-02	2.99	0.17E-03	2.78	0.40E-03	2.99	0.23E-03	2.99
1024.	0.37E-03	3.00	0.22E-04	2.91	0.50E-04	3.00	0.28E-04	2.99
4096.	0.47E-04	3.00	0.29E-05	2.96	0.62E-05	3.00	0.36E-05	2.99
Mesh	$\\| f - \mathsf{P}_W f \\|_{-1,\mathcal{T}_h}$		$\\| \mathsf{P}_M(\widehat{u}_h - u_h^*) \\|_{0,\mathcal{T}_h}$		$\\| (\mathsf{Id} - \mathsf{P}_M) [\![u_h^*]\!] \\|_{1/2,\mathcal{E}_h}$		$\\| (\widehat{\boldsymbol{q}}_h - \boldsymbol{q}_h) \cdot \boldsymbol{n} \\|_{-1/2,\partial\mathcal{T}_h}$	
N	estimator	order	estimator	order	estimator	order	estimator	order
16.	0.22E-01	-	0.35E-02	-	0.55E-02	-	0.37E-01	-
64.	0.14E-02	3.98	0.45E-03	2.93	0.12E-02	2.25	0.48E-02	2.96
256.	0.89E-04	3.99	0.58E-04	2.97	0.17E-03	2.78	0.60E-03	2.99
1024.	0.56E-05	4.00	0.73E-05	2.99	0.22E-04	2.91	0.76E-04	3.00
4096.	0.35E-06	4.00	0.92E-06	2.99	0.29E-05	2.96	0.95E-05	3.00

Table 2.4.2: The effect of the polynomial degree p for non-smooth solution

$p = 0$

Mesh	$\Vert \boldsymbol{q} - \boldsymbol{q}_h \Vert_{div,\mathcal{T}_h}$		$\Vert [\![u_h^*]\!] \Vert_{1/2,\mathcal{E}_h}$		$\Vert \nabla(u - u_h^*) \Vert_{0,\mathcal{T}_h}$		$\Vert (\boldsymbol{q} - \widehat{\boldsymbol{q}}_h) \cdot \boldsymbol{n} \Vert_{-1/2,\partial\mathcal{T}_h}$	
N	error	order	error	order	error	order	error	order
12.	0.35E+00	-	0.45E+00	-	0.32E+00	-	0.36E+00	-
48.	0.23E+00	0.58	0.32E+00	0.49	0.22E+00	0.56	0.21E+00	0.80
192.	0.15E+00	0.63	0.22E+00	0.53	0.14E+00	0.62	0.12E+00	0.76
768.	0.96E-01	0.65	0.15E+00	0.55	0.91E-01	0.64	0.77E-01	0.68
3072.	0.61E-01	0.66	0.10E+00	0.56	0.58E-01	0.65	0.47E-01	0.71
12288.	0.39E-01	0.66	0.70E-01	0.56	0.36E-01	0.66	0.29E-01	0.69

Mesh	$\Vert f - \mathsf{P}_W f \Vert_{-1,\mathcal{T}_h}$		$\Vert \mathsf{P}_M(\widehat{u}_h - u_h^*) \Vert_{0,\mathcal{T}_h}$		$\Vert (\mathsf{Id} - \mathsf{P}_M) [\![u_h^*]\!] \Vert_{1/2,\mathcal{E}_h}$		$\Vert (\widehat{\boldsymbol{q}}_h - \boldsymbol{q}_h) \cdot \boldsymbol{n} \Vert_{-1/2,\partial\mathcal{T}_h}$	
N	estimator	order	estimator	order	estimator	order	estimator	order
12.	0.00E+00	-	0.91E-15	-	0.45E+00	-	0.36E+00	-
48.	0.00E+00	-	0.18E-14	-	0.32E+00	0.49	0.19E+00	0.94
192.	0.00E+00	-	0.34E-14	-	0.22E+00	0.53	0.96E-01	0.97
768.	0.00E+00	-	0.65E-14	-	0.15E+00	0.55	0.49E-01	0.98
3072.	0.00E+00	-	0.13E-13	-	0.10E+00	0.56	0.24E-01	0.99
12288.	0.00E+00	-	0.26E-13	-	0.70E-01	0.56	0.12E-01	1.00

$p = 1$

Mesh	$\Vert \boldsymbol{q} - \boldsymbol{q}_h \Vert_{div,\mathcal{T}_h}$		$\Vert [\![u_h^*]\!] \Vert_{1/2,\mathcal{E}_h}$		$\Vert \nabla(u - u_h^*) \Vert_{0,\mathcal{T}_h}$		$\Vert (\boldsymbol{q} - \widehat{\boldsymbol{q}}_h) \cdot \boldsymbol{n} \Vert_{-1/2,\partial\mathcal{T}_h}$	
N	error	order	error	order	error	order	error	order
12.	0.16E+00	-	0.92E-01	-	0.13E+00	-	0.11E+00	-
48.	0.10E+00	0.63	0.59E-01	0.65	0.85E-01	0.62	0.70E-01	0.69
192.	0.64E-01	0.65	0.38E-01	0.65	0.54E-01	0.65	0.44E-01	0.67
768.	0.41E-01	0.66	0.24E-01	0.66	0.34E-01	0.66	0.28E-01	0.67
3072.	0.26E-01	0.66	0.15E-01	0.66	0.22E-01	0.66	0.17E-01	0.67
12288.	0.16E-01	0.66	0.94E-02	0.67	0.14E-01	0.66	0.11E-01	0.67

Mesh	$\Vert f - \mathsf{P}_W f \Vert_{-1,\mathcal{T}_h}$		$\Vert \mathsf{P}_M(\widehat{u}_h - u_h^*) \Vert_{0,\mathcal{T}_h}$		$\Vert (\mathsf{Id} - \mathsf{P}_M) [\![u_h^*]\!] \Vert_{1/2,\mathcal{E}_h}$		$\Vert (\widehat{\boldsymbol{q}}_h - \boldsymbol{q}_h) \cdot \boldsymbol{n} \Vert_{-1/2,\partial\mathcal{T}_h}$	
N	estimator	order	estimator	order	estimator	order	estimator	order
12.	0.00E+00	-	0.38E-01	-	0.68E-01	-	0.41E-01	-
48.	0.00E+00	-	0.24E-01	0.66	0.44E-01	0.64	0.14E-01	1.53
192.	0.00E+00	-	0.15E-01	0.66	0.28E-01	0.65	0.47E-02	1.59
768.	0.00E+00	-	0.96E-02	0.67	0.18E-01	0.66	0.15E-02	1.62
3072.	0.00E+00	-	0.60E-02	0.67	0.11E-01	0.66	0.49E-03	1.64
12288.	0.00E+00	-	0.38E-02	0.67	0.71E-02	0.66	0.16E-03	1.65

$p = 2$

Mesh	$\Vert \boldsymbol{q} - \boldsymbol{q}_h \Vert_{div,\mathcal{T}_h}$		$\Vert [\![u_h^*]\!] \Vert_{1/2,\mathcal{E}_h}$		$\Vert \nabla(u - u_h^*) \Vert_{0,\mathcal{T}_h}$		$\Vert (\boldsymbol{q} - \widehat{\boldsymbol{q}}_h) \cdot \boldsymbol{n} \Vert_{-1/2,\partial\mathcal{T}_h}$	
N	error	order	error	order	error	order	error	order
12.	0.81E-01	-	0.44E-01	-	0.81E-01	-	0.69E-01	-
48.	0.51E-01	0.66	0.28E-01	0.65	0.52E-01	0.64	0.43E-01	0.68
192.	0.32E-01	0.66	0.18E-01	0.66	0.33E-01	0.65	0.27E-01	0.66
768.	0.20E-01	0.66	0.11E-01	0.66	0.21E-01	0.66	0.17E-01	0.66
3072.	0.13E-01	0.66	0.71E-02	0.67	0.13E-01	0.66	0.11E-01	0.67
12288.	0.81E-02	0.66	0.44E-02	0.67	0.84E-02	0.67	0.68E-02	0.67

Mesh	$\Vert f - \mathsf{P}_W f \Vert_{-1,\mathcal{T}_h}$		$\Vert \mathsf{P}_M(\widehat{u}_h - u_h^*) \Vert_{0,\mathcal{T}_h}$		$\Vert (\mathsf{Id} - \mathsf{P}_M) [\![u_h^*]\!] \Vert_{1/2,\mathcal{E}_h}$		$\Vert (\widehat{\boldsymbol{q}}_h - \boldsymbol{q}_h) \cdot \boldsymbol{n} \Vert_{-1/2,\partial\mathcal{T}_h}$	
N	estimator	order	estimator	order	estimator	order	estimator	order
12.	0.00E+00	-	0.21E-01	-	0.26E-01	-	0.16E-01	-
48.	0.00E+00	-	0.13E-01	0.66	0.16E-01	0.64	0.50E-02	1.64
192.	0.00E+00	-	0.83E-02	0.66	0.10E-01	0.65	0.16E-02	1.65
768.	0.00E+00	-	0.53E-02	0.66	0.66E-02	0.66	0.51E-03	1.66
3072.	0.00E+00	-	0.33E-02	0.67	0.41E-02	0.66	0.16E-03	1.66
12288.	0.00E+00	-	0.21E-02	0.67	0.26E-02	0.67	0.51E-04	1.67

Table 2.4.3: The effect of the stabilization function τ

$\tau = 10^{-3}$

Mesh	$\Vert \boldsymbol{q} - \boldsymbol{q}_h \Vert_{div,\mathcal{T}_h}$		$\Vert [\![u_h^*]\!] \Vert_{1/2,\mathcal{E}_h}$		$\Vert \nabla(u - u_h^*) \Vert_{0,\mathcal{T}_h}$		$\Vert (\boldsymbol{q} - \widehat{\boldsymbol{q}}_h) \cdot \boldsymbol{n} \Vert_{-1/2,\partial\mathcal{T}_h}$	
N	error	order	error	order	error	order	error	order
12.	0.16E+00	-	0.95E-01	-	0.14E+00	-	0.11E+00	-
48.	0.10E+00	0.64	0.60E-01	0.67	0.87E-01	0.65	0.70E-01	0.68
192.	0.65E-01	0.66	0.38E-01	0.67	0.55E-01	0.66	0.44E-01	0.67
768.	0.41E-01	0.66	0.24E-01	0.67	0.35E-01	0.67	0.28E-01	0.67
3072.	0.26E-01	0.67	0.15E-01	0.67	0.22E-01	0.67	0.18E-01	0.67
Mesh	$\Vert f - \mathsf{P}_W f \Vert_{-1,\mathcal{T}_h}$		$\Vert \mathsf{P}_M(\widehat{u}_h - u_h^*) \Vert_{0,\mathcal{T}_h}$		$\Vert (\mathsf{Id} - \mathsf{P}_M) [\![u_h^*]\!] \Vert_{1/2,\mathcal{E}_h}$		$\Vert (\widehat{\boldsymbol{q}}_h - \boldsymbol{q}_h) \cdot \boldsymbol{n} \Vert_{-1/2,\partial\mathcal{T}_h}$	
N	estimator	order	estimator	order	estimator	order	estimator	order
12.	0.00E+00	-	0.38E-01	-	0.71E-01	-	0.43E-04	-
48.	0.00E+00	-	0.24E-01	0.67	0.45E-01	0.66	0.15E-04	1.56
192.	0.00E+00	-	0.15E-01	0.66	0.28E-01	0.67	0.48E-05	1.61
768.	0.00E+00	-	0.96E-02	0.67	0.18E-01	0.67	0.16E-05	1.63
3072.	0.00E+00	-	0.60E-02	0.67	0.11E-01	0.67	0.50E-06	1.65

$\tau = 10^{1}$

Mesh	$\Vert \boldsymbol{q} - \boldsymbol{q}_h \Vert_{div,\mathcal{T}_h}$		$\Vert [\![u_h^*]\!] \Vert_{1/2,\mathcal{E}_h}$		$\Vert \nabla(u - u_h^*) \Vert_{0,\mathcal{T}_h}$		$\Vert (\boldsymbol{q} - \widehat{\boldsymbol{q}}_h) \cdot \boldsymbol{n} \Vert_{-1/2,\partial\mathcal{T}_h}$	
N	error	order	error	order	error	order	error	order
12.	0.18E+00	-	0.74E-01	-	0.13E+00	-	0.16E+00	-
48.	0.11E+00	0.74	0.53E-01	0.49	0.78E-01	0.68	0.81E-01	1.01
192.	0.65E-01	0.74	0.35E-01	0.57	0.50E-01	0.64	0.46E-01	0.81
768.	0.40E-01	0.69	0.23E-01	0.62	0.33E-01	0.62	0.28E-01	0.72
3072.	0.25E-01	0.66	0.15E-01	0.64	0.21E-01	0.63	0.17E-01	0.68
Mesh	$\Vert f - \mathsf{P}_W f \Vert_{-1,\mathcal{T}_h}$		$\Vert \mathsf{P}_M(\widehat{u}_h - u_h^*) \Vert_{0,\mathcal{T}_h}$		$\Vert (\mathsf{Id} - \mathsf{P}_M) [\![u_h^*]\!] \Vert_{1/2,\mathcal{E}_h}$		$\Vert (\widehat{\boldsymbol{q}}_h - \boldsymbol{q}_h) \cdot \boldsymbol{n} \Vert_{-1/2,\partial\mathcal{T}_h}$	
N	estimator	order	estimator	order	estimator	order	estimator	order
12.	0.00E+00	-	0.32E-01	-	0.53E-01	-	0.31E+00	-
48.	0.00E+00	-	0.23E-01	0.48	0.38E-01	0.49	0.12E+00	1.39
192.	0.00E+00	-	0.15E-01	0.61	0.26E-01	0.55	0.42E-01	1.48
768.	0.00E+00	-	0.95E-02	0.65	0.17E-01	0.60	0.14E-01	1.55
3072.	0.00E+00	-	0.60E-02	0.66	0.11E-01	0.63	0.48E-02	1.60

$\tau = 10^{2}$

Mesh	$\Vert \boldsymbol{q} - \boldsymbol{q}_h \Vert_{div,\mathcal{T}_h}$		$\Vert [\![u_h^*]\!] \Vert_{1/2,\mathcal{E}_h}$		$\Vert \nabla(u - u_h^*) \Vert_{0,\mathcal{T}_h}$		$\Vert (\boldsymbol{q} - \widehat{\boldsymbol{q}}_h) \cdot \boldsymbol{n} \Vert_{-1/2,\partial\mathcal{T}_h}$	
N	error	order	error	order	error	order	error	order
12.	0.25E+00	-	0.25E-01	-	0.26E+00	-	0.45E+00	-
48.	0.15E+00	0.77	0.25E-01	0.01	0.14E+00	0.85	0.19E+00	1.23
192.	0.88E-01	0.76	0.22E-01	0.17	0.74E-01	0.97	0.95E-01	1.01
768.	0.51E-01	0.77	0.18E-01	0.33	0.37E-01	0.98	0.45E-01	1.08
3072.	0.29E-01	0.81	0.13E-01	0.46	0.21E-01	0.86	0.22E-01	1.03
12288.	0.17E-01	0.80	0.87E-02	0.55	0.13E-01	0.70	0.12E-01	0.89
Mesh	$\Vert f - \mathsf{P}_W f \Vert_{-1,\mathcal{T}_h}$		$\Vert \mathsf{P}_M(\widehat{u}_h - u_h^*) \Vert_{0,\mathcal{T}_h}$		$\Vert (\mathsf{Id} - \mathsf{P}_M) [\![u_h^*]\!] \Vert_{1/2,\mathcal{E}_h}$		$\Vert (\widehat{\boldsymbol{q}}_h - \boldsymbol{q}_h) \cdot \boldsymbol{n} \Vert_{-1/2,\partial\mathcal{T}_h}$	
N	estimator	order	estimator	order	estimator	order	estimator	order
12.	0.00E+00	-	0.91E-02	-	0.19E-01	-	0.11E+01	-
48.	0.00E+00	-	0.12E-01	-0.36	0.17E-01	0.17	0.50E+00	1.12
192.	0.00E+00	-	0.10E-01	0.18	0.15E-01	0.17	0.23E+00	1.10
768.	0.00E+00	-	0.80E-02	0.36	0.12E-01	0.32	0.98E-01	1.25
3072.	0.00E+00	-	0.57E-02	0.50	0.91E-02	0.45	0.38E-01	1.38
12288.	0.00E+00	-	0.37E-02	0.60	0.63E-02	0.53	0.13E-01	1.48

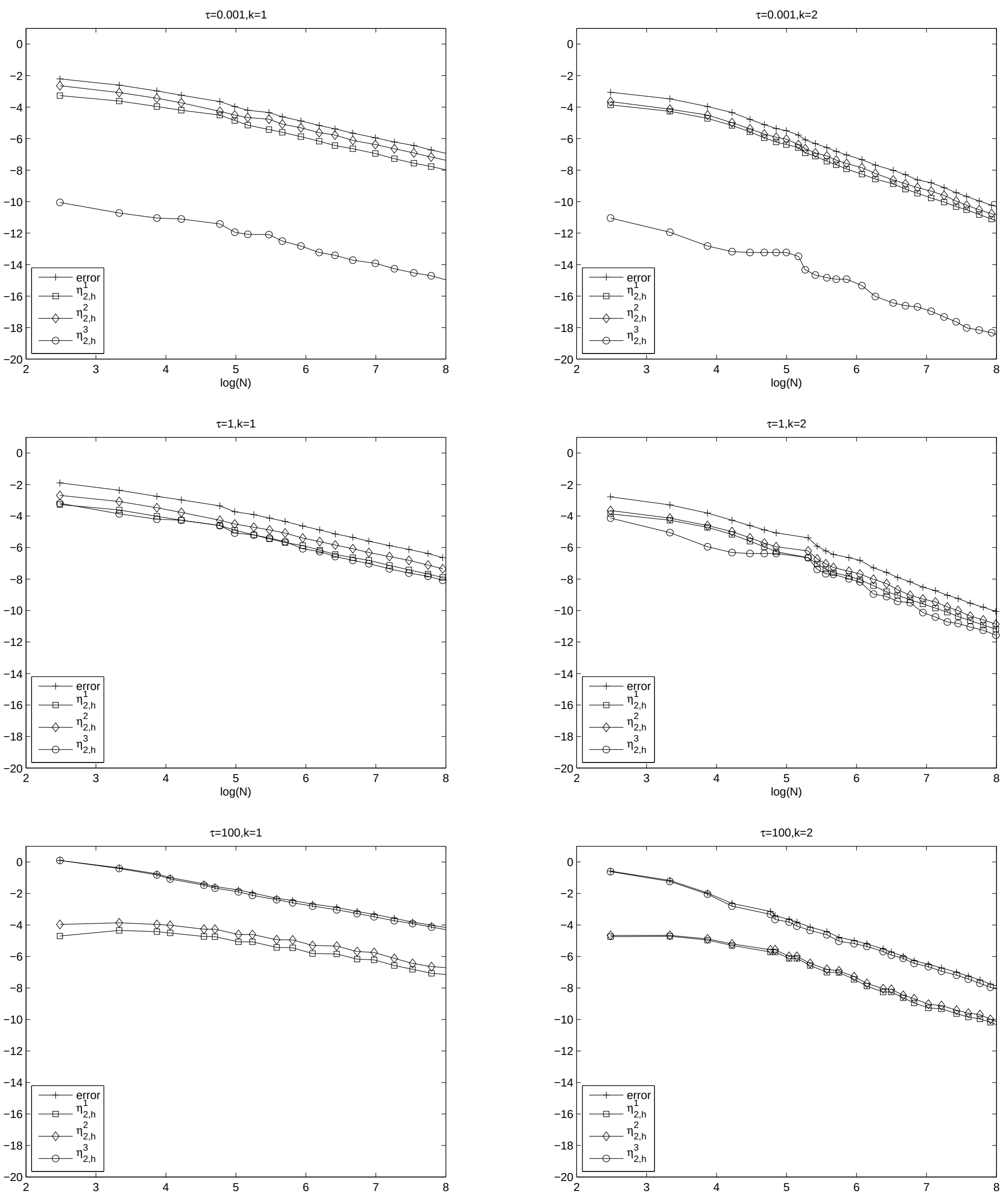

Figure 2.4.2: History of convergence for adaptive refinement.

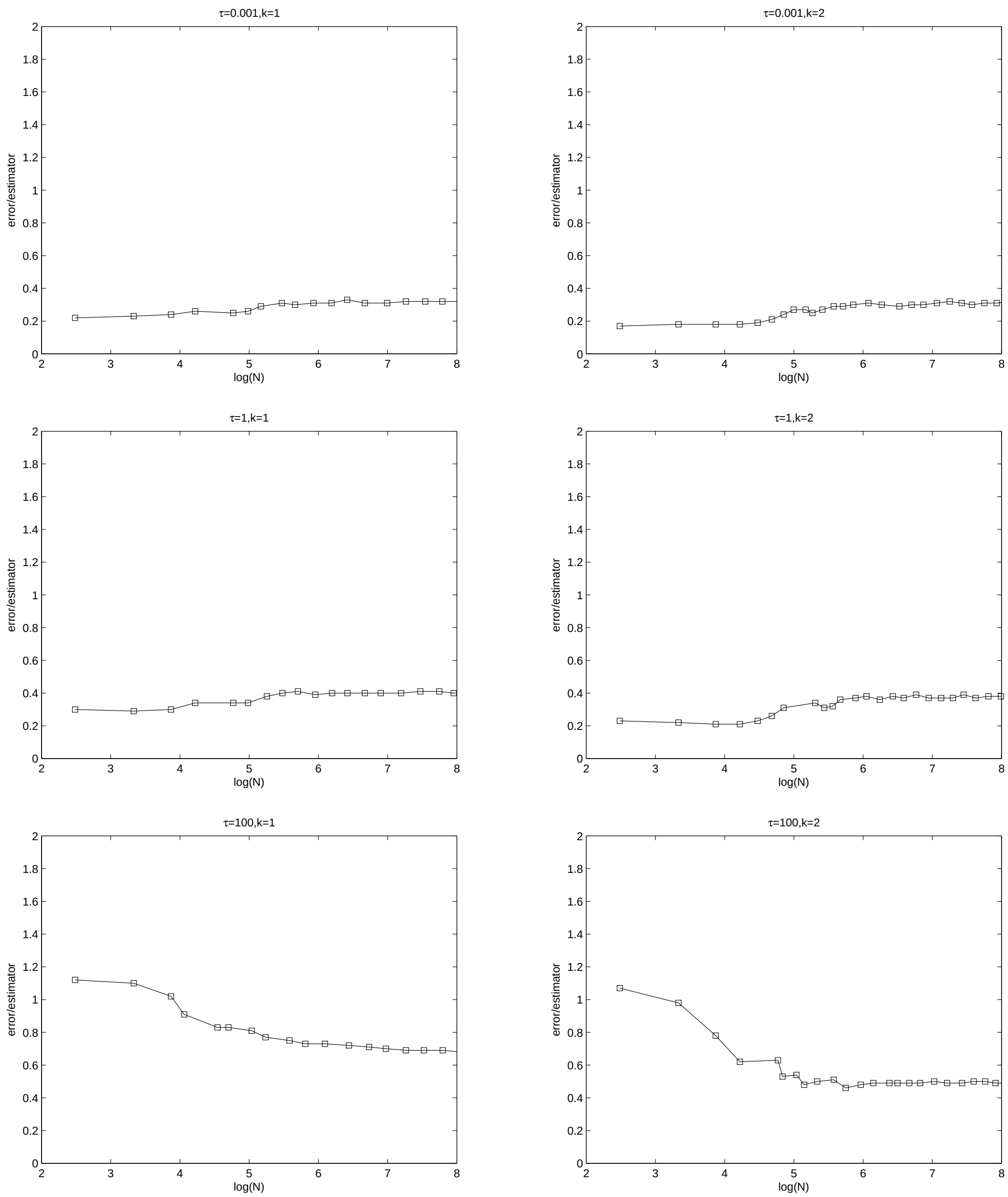

Figure 2.4.3: Adaptive refinement, nonsmooth solution: Effectivity index.

Chapter 3

A posteriori error analysis for the RT method

3.1 Introduction

In the implementation of adaptive finite element methods, hanging nodes are frequently employed in order to accelerate the convergence rate, efficiently allocate degree of freedom and facilitate the local refinement. However, only a few a posteriori error analyzes for the mixed methods [61, 59, 22, 24] have been carried out on nonconforming meshes most probably because the mixed methods were originally formulated on conforming meshes only.

In fact, it was not until a decade ago that the first Raviart-Thomas (RT) element and the Brezzi-Douglas-Fortin-Marini (BDFM) element [23] on nonconforming quadrilateral meshes were analyzed by Ainsworth and Pinchedez in their study in the *hp*-approximation theory of mixed methods [4] in two space dimensions. In the case of nonconforming meshes made of simplexes in arbitrary dimensions, a hybridized version of RT method was presented by Cockburn, Gopalakrishnan and Lazarov in [34]. In this paper, we derive an a posteriori error estimate for variable-degree hybridized Raviart-Thomas (RT-H) method on nonconforming meshes based on the framework of [34]. We aim to establish the reliability and efficiency of the estimator for the model problem (1.1.1a).

This chapter is organized as follows. In section 3.2, we introduce the hybridized RT methods, the a posteriori error estimator and the main result. In section 3.3, we present the analysis of its reliability and efficiency. In section 3.4, we end the chapter with a concluding remark.

3.2 Main Result

3.2.1 Notation

Let $\mathcal{T}_h = \{K\}$ be a triangulation of the domain Ω made of triangles or squares K in two space dimensions or tetrahedra or cubes K in three space dimensions.

Given two meshes $\mathcal{T}_1$ and $\mathcal{T}_2$, we say $\mathcal{T}_1 \leq \mathcal{T}_2$ if $\mathcal{T}_2$ can be obtained from $\mathcal{T}_1$ via a finite number of refinement steps. In this work, we consider the following refinement step. Given a mesh $\mathcal{T}_H$, we take a subset of $\mathcal{T}_H$ and, in two space dimensions, we divide each of its triangles or quadrilaterals into four congruent triangles or four quadrilaterals; in three space dimensions, we divide each of its tetrahedra or cubes into eight elements [68, 60]. Thus, starting from a given initial conforming mesh $\mathcal{T}_0$, a uniform refinement gives us the following sequence of conforming meshes,

$$\mathcal{T}_0 \leq \mathcal{T}_1 \leq \mathcal{T}_2 \leq \ldots \leq \mathcal{T}_{k-1} \leq \mathcal{T}_k \leq \mathcal{T}_{k+1} \leq \ldots \tag{3.2.1}$$

3.2.2 Assumptions on the meshes and boundary condition

In this work, nonconforming meshes are allowed provided that they satisfy the following assumptions:

A0. *The meshes $\mathcal{T}_h$ are obtained from an initial conforming mesh $\mathcal{T}_0$ via a finite number of refinement steps.*

A simple fact following from this assumption is that for each element $K \in \mathcal{T}_h$, K is also an element of some conforming meshes $\mathcal{T}_l$ in the sequence (3.2.1). Here, we follow the definition introduced in [17]. We define the level of $K \in \mathcal{T}_h$ as $L(K) = l$, if $K \in \mathcal{T}_l$.

Let $\mathcal{T}_H$ be the "largest" conforming mesh such that $\mathcal{T}_H \leq \mathcal{T}_h$, that is,

$$\mathcal{T}_n \leq \mathcal{T}_H, \quad \text{for any conforming mesh } \mathcal{T}_n \text{ satisfying } \mathcal{T}_n \leq \mathcal{T}_h.$$

We say an element $T \in \mathcal{T}_H$ is the conforming parent of an element $K \in \mathcal{T}_h$ if $K \subset T$.

We also define the level of nonconformity as

$$L_n(K) = L(K) - L(T).$$

Our second assumption is the following.

A1. *The level of nonconformity is bounded, that is,*

$$L_n(K) \leq L, \quad \textit{for each element } K \in \mathcal{T}_h, \tag{3.2.2}$$

for some positive integer L.

It follows immediately from this assumption that

$$C_e^{-1} h_{K_1} \leq h_{K_2} \leq C_e h_{K_1}, \quad \forall K_1, K_2 \text{ such that } m_{d-1}(K_1 \cap K_2) > 0.$$

where m_{d-1} is the $(d-1)$-Lebesgue measure.

We also introduce the following notation. Set $\partial\mathcal{T}_h = \{e : e \text{ is a face of } K \in \mathcal{T}_h\}$. For each face e in $\partial\mathcal{T}_h$, set

$$w(e) := \{K \in \mathcal{T}_h,\, m_{d-1}(e \cap \partial K) > 0\,\}.$$

We view $\partial\mathcal{T}_h$ as the union of four disjoint classes:

$$\begin{aligned}
\mathcal{E}^{\partial} &= \{\, e \in \partial\mathcal{T}_h \, : |w(e)| = 1, \text{ that is, } e \text{ is a boundary face}\,\},\\
\mathcal{E}^{f1} &= \{\, e \in \partial\mathcal{T}_h \, : |w(e)| = 2, \; e \text{ is a face of one element } K \text{ only } \}.\\
\mathcal{E}^{f2} &= \{\, e \in \partial\mathcal{T}_h \, : |w(e)| = 2, \; e \text{ is a shared face of two elements } K_1, K_2\,\},\\
\mathcal{E}^{hn} &= \{\, e \in \partial\mathcal{T}_h \, : |w(e)| > 2, \text{ that is, there is at least one hanging node on } e\,\},
\end{aligned}$$

where $|w(e)|$ denotes the cardinality of the set $w(e)$. Figure 3.2.1 illustrates the last three different types of faces. We set

$$\mathcal{F}_h := \{\, e \in \partial\mathcal{T}_h \, : e \notin \mathcal{E}^{f1}\,\}. \tag{3.2.3}$$

For every face $e \in \mathcal{F}_h$, set $n := \min\{L(K) \, : K \in w(e)\,\}$ and $m := \max\{L(K) \, : K \in w(e)\,\}$. We denote

$$\begin{aligned}
\tilde{w}(e) &:= \{K_1, K_2 \in \mathcal{T}_n \, : e \text{ is a shared face of } K_1 \text{ and } K_2 \;\},\\
w^*(e) &:= \{K \in \mathcal{T}_m \, : K \subset \tilde{w}(e)\},\\
v^*(e) &:= \{K \in w^*(e) \, : m_{d-1}(e \cap \partial K) > 0\},
\end{aligned}$$

We also denote F_e be the face of an element $K \in v^*(e)$ such that $F_e \subset e$.

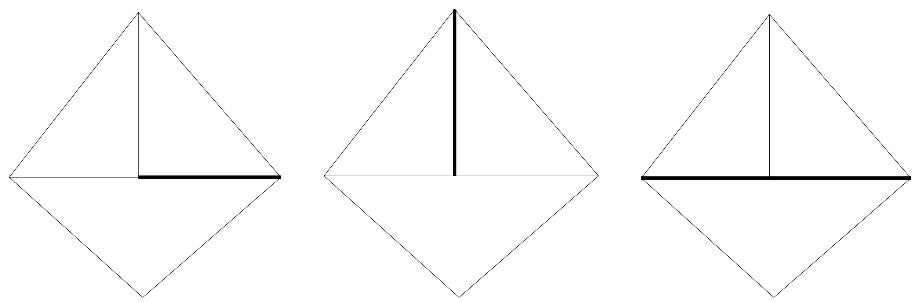

Figure 3.2.1: Example of nonconforming meshes I.

3.2.3 The hybridized Raviart-Thomas method on meshes with hanging nodes

Under the framework of the HDG method in section 1.2.2, to define the hybridized Raviart-Thomas method, we only need to specify (1) the numerical trace $\widehat{\boldsymbol{q}}_h$, (2) the local spaces $\boldsymbol{V}(K) \times W(K)$, and (3) the space of approximate traces $\mathsf{M}(e)$.

For the case of the variable-degree hybridized Raviart-Thomas (RT-H) method on nonconforming meshes made of simplexes, we take $\boldsymbol{V}(K) \times W(K)$ as the Raviart-Thomas space of degree $p(K)$:

$$\boldsymbol{V}(K) = \mathcal{P}_{p(K)}(K)^d + \boldsymbol{x}\,\mathcal{P}_{p(K)}(K), \quad W(K) = \mathcal{P}_{p(K)}(K), \quad p(K) \geq 0,$$

where $\mathcal{P}_{p(K)}(K)$ denotes the space of polynomial with degree less than or equal to $p(K)$ on the element K and $\mathcal{P}_{p(K)}(K)^d$ denotes the set of vector functions whose components are in $\mathcal{P}_{p(K)}(K)$. We define the space of approximate traces as:

$$\mathsf{M}(e) = \mathcal{P}_{p(e)}(e),$$

where the polynomial degree $p(e)$ has to be suitably related to $p(K)$, as we show below.

For the square and cube elements, we take $\boldsymbol{V}(K) \times W(K)$ as the Raviart-Thomas space of degree $p(K)$:

$$\boldsymbol{V}(K) = \mathrm{RT}_{p(K)}(K), \quad W(K) = \mathcal{Q}_{p(K)}(K), \quad p(K) \geq 0,$$

where

$$\mathrm{RT}_k(K) = \begin{cases} \mathcal{P}_{p+1,p}(K) \times \mathcal{P}_{p,p+1}(K) & \text{for square,} \\ \mathcal{P}_{p+1,p,p}(K) \times \mathcal{P}_{p,p+1,p}(K) \times \mathcal{P}_{p,p,p+1}(K) & \text{for cube,} \end{cases}$$

and $\mathcal{P}_{p+1,p,p}(K)$ denotes the space of polynomial with degree less than or equal to $p+1$ in x variable and with degree less than or equal to p in the other two variables on the element K and $\mathcal{Q}_p(K)$ denotes the space of polynomial with degree less than or equal to p in all variables. We define the space of approximate traces as:

$$\mathsf{M}(e) = \mathcal{Q}_{p(e)}(e).$$

Finally, for $e \in \mathcal{E}_h$ we take $p(e) := \max\{p(K^+), p(K^-)\}$ and require that

$$\text{if } e \text{ is not a face of } K^-, \text{ then } p(K^+) \geq p(K^-).$$

The variable-degree RT-H method described above is uniquely solvable [34] on nonconforming meshes satisfying condition $\mathbf{A_0}, \mathbf{A_1}, \mathbf{A_2}$. For the error analysis purpose, we shall impose a bound for the polynomial degree $p(K)$ and require $p(K) \leq \mathsf{p}$ for all $K \in \mathcal{T}_h$ for some positive integer p, hereafter.

3.2.4 Local post-processing

Here, for simplexes, we take a *crucial* post-processing u_h^* in the space

$$W_h^* = \{w \in L^2(K), w|_K \in \mathcal{P}_{p(K)+2}(K), \quad \forall K \in \mathcal{T}_h\}, \tag{3.2.4}$$

and for square and cube elements, we take the post-processing u_h^* in the space

$$W_h^* = \{w \in L^2(K), w|_K \in \mathcal{Q}_{p(K)+2}(K), \quad \forall K \in \mathcal{T}_h\}, \tag{3.2.5}$$

and define it as follows. The solution u_h^* satisfies the following equations

$$(u_h^* - u_h, w)_{\mathcal{T}_h} = 0, \qquad \text{for all piecewise constant } w, \tag{3.2.6a}$$

$$(\boldsymbol{\nabla}\, u_h^*, \boldsymbol{\nabla}\, w)_{\mathcal{T}_h} = -(\boldsymbol{q}_h, \boldsymbol{\nabla}\, w)_{\mathcal{T}_h}, \qquad \text{for all } w \in W_h^*. \tag{3.2.6b}$$

The post-processed solution u_h^* is well defined and converges with order $p+2$ for $p \geq 1$, and with order 1 for $p = 0$ for uniform meshes; see [7].

3.2.5 The a posteriori error estimate

Our main result provides upper and local lower bounds of the error

$$\mathsf{e}_h := \|\, \boldsymbol{q} - \boldsymbol{q}_h \,\|_{0,\mathcal{T}_h},$$

in terms of the data oscillation

$$ocs_h(f, \mathcal{T}_h) := (\sum_{K \in \mathcal{T}_h} h_K^2 \| f - \mathsf{P}_W f \|_{0,K}^2)^{1/2}, \tag{3.2.7}$$

and the error estimator

$$\eta_h := (\sum_{e \in \mathcal{F}_h} (\eta_{1,h}^2(e) + \eta_{2,h}^2(e) + \eta_{3,h}^2(e)))^{1/2}, \tag{3.2.8}$$

where

$$\eta_{1,h}(e) := \sum_{K \in w(e)} \| \boldsymbol{q}_h + \nabla u_h^* \|_{0,K}, \tag{3.2.9a}$$

$$\eta_{2,h}(e) := h_e^{-1/2} \| (\mathsf{Id} - \mathsf{P}_{M_0}) [\![u_h^*]\!] \|_{0,e}, \tag{3.2.9b}$$

$$\eta_{3,h}(e) := h_e^{-1/2} \| (\mathsf{P}_{M_0} - \mathsf{P}_{\mathcal{M}_0}) [\![u_h^*]\!] \|_{0,e}. \tag{3.2.9c}$$

Here, P_W is the L_2-orthogonal projection into the space W_h, P_{M_0} the L_2-orthogonal projection into the space

$$\mathsf{M}_{0,h} := \{\mu \in L_2(\partial \mathcal{T}_h),\, \mu|_e \in \mathcal{P}_0(e),\ \text{for each face } e \in \mathcal{E}_h\},$$

and $\mathsf{P}_{\mathcal{M}_0}$ the L_2-orthogonal projection into the space

$$\mathcal{M}_{0,h} := \{\mu \in L_2(\partial \mathcal{T}_h),\, \mu|_e \in \mathcal{P}_0(e),\ \text{for each face } e \in \mathcal{F}_h\ \}.$$

We emphasize that, because of the nonconformity of the meshes, a face $e \in \mathcal{E}_h$ is not necessarily a face in $\mathcal{F}_h$, see definition (3.2.3). Note that $\mathsf{P}_{M_0} = \mathsf{P}_{\mathcal{M}_0}$ if and only if the mesh $\mathcal{T}_h$ is conforming. The last estimator $\eta_{3,h}$ explicitly captures the nonconformity on the meshes.

3.2.6 The main property of the error estimator

We are now ready to state the result.

Theorem 3.2.1 (Reliability and Efficiency of the error estimator)**.** *Assume that the mesh assumptions* $\mathbf{A_0}, \mathbf{A_1}, \mathbf{A_2}$ *and the boundary condition assumption* $\mathbf{B}$ *are satisfied.*

Then there are two constants C_1 and C_2 depending only on the constants L, σ, and p *such that*

$$\| \boldsymbol{q} - \boldsymbol{q}_h \|_{0,\mathcal{T}_h}^2 \leq C_2(\eta_h^2 + osc_h^2(f, \mathcal{T}_h)).$$

Moreover, for each face $e \in \mathcal{F}_h$,

$$C_1 \eta_h^2(e) \leq \sum_{K \in \tilde{w}(e)} \| \boldsymbol{q} - \boldsymbol{q}_h \|_{0,K}^2,$$

where

$$\eta_h^2(e) = \eta_{1,h}^2(e) + \eta_{2,h}^2(e) + \eta_{3,h}^2(e).$$

The main result establishes the reliability and efficiency of the error estimator in terms of the L_2 error of the flux only. Moreover, the analysis is not restricted to quadrisection and octasection refinement. These two refinement are introduced in order to ensure the RT-H method is well defined. The result still holds for other refinements as long as the hybridized mixed methods are well defined. For other refinements, we refer the interested reader to [9, 16].

3.3 Proof

We begin by gathering a few, simple auxiliary results that we are going to use in the analysis. We then establish a key connection between the residuals. Finally, we prove the efficiency and reliability of the estimator.

3.3.1 Auxiliary Results

We are going to make use of the fact that the approximate solution u_h^* can be approximated by a continuous, piecewise polynomial function $\tilde{u}_h^*$ in the post-processing space W_h^* (3.2.4), (3.2.5). This will allow us to show that the quality of the approximation can be controlled by the size of the interelement jumps of u_h^*. The following result is proved in [41, 54] for nonconforming meshes with uniform polynomial degree.

Lemma 3.3.1. *For any $w_h \in W_h^*$ and multi-index α with $|\alpha| = 0, 1$ the following approximation results holds: Let g be the restriction to Γ of a function in $W_h^* \cap H^1(\Omega)$.*

Then there exists a function $\tilde{w}_h \in W_h^* \cap H^1(\Omega)$ satisfying $\tilde{w}_h|_\Gamma = g$ and

$$\begin{aligned}\sum_{K\in\mathcal{T}_h} \| D^\alpha(w_h - \tilde{w}_h) \|_K^2 \leq & C_j \sum_{e\in\mathcal{E}_h^i} h_e^{1-2|\alpha|} \| [\![w_h]\!] \|_e^2 \\ & + C_j \sum_{e\in\mathcal{E}_h^\partial} h_e^{1-2|\alpha|} \| g - w_h \|_e^2\end{aligned}$$

where the constant $C_j = C_j(\sigma, \mathsf{p}, L)$.

We shall also use the following estimate for the error in the flux. The proof can be found in Chapter 2.

Lemma 3.3.2. *For any function ϕ in $H^1(\Omega)$, there exists a constant $C_{\sigma,L} = C_{\sigma,L}(\sigma,\, L)$, such that*

$$\| \boldsymbol{q} - \boldsymbol{q}_h \|_{0,\mathcal{T}_h}^2 \leq C_{\sigma,L}(ocs_h^2(f, \mathcal{T}_h) + \eta_\phi^2) - \langle (\boldsymbol{q} - \boldsymbol{q}_h) \cdot \boldsymbol{n}, g - \phi \rangle_\Gamma,$$

where

$$\eta_\phi^2 := \sum_{K\in\mathcal{T}_h} \| \boldsymbol{q}_h + \nabla\phi \|_{0,K}^2,$$

We also observe from the equations defining the hybridized mixed method (1.2.2) that the residual in the element are strongly connected with the residual across the faces.

Lemma 3.3.3. *It holds for any face $e \in \mathcal{F}_h$ that*

$$h_e^{-1} \| \mathsf{P}_{\mathcal{M}_0} [\![u_h^*]\!] \|_{0,e}^2 \leq C_s \sum_{K\in w(e)} \| \boldsymbol{q}_h + \boldsymbol{\nabla}\, u_h^* \|_{0,K},$$

where $C_s = C_s(\sigma, \mathsf{p}, L)$.

Proof. From the equation defining the hybridized mixed methods (1.2.2a) and that defining the post-processing (3.2.6), we obtain for each element K,

$$(\boldsymbol{q}_h, \boldsymbol{v})_K - (u_h^*, \nabla\cdot \boldsymbol{v})_K = -\langle \widehat{u}_h, \boldsymbol{v}\cdot\boldsymbol{n} \rangle_{\partial K},$$

for all $\boldsymbol{v}$ in the lowest order Raviart-Thomas space, $\mathrm{RT}_0(K)$. Integrating by parts, we have

$$(\boldsymbol{q}_h + \boldsymbol{\nabla}\, u_h^*, \boldsymbol{v})_K = -\langle \widehat{u}_h - u_h^*, \boldsymbol{v}\cdot\boldsymbol{n} \rangle_{\partial K}.$$

Now assume $\boldsymbol{v} \in \boldsymbol{H}(\mathrm{div}, w(e))$. Since $\widehat{u}_h$ is single valued on the faces, summing over all $K \in w(e)$ yields,

$$\sum_{K\in w(e)} (\boldsymbol{q}_h + \boldsymbol{\nabla}\, u_h^*, \boldsymbol{v})_K = -\sum_{F\in\partial K\setminus e} \langle \widehat{u}_h - u_h^*, \boldsymbol{v}\cdot\boldsymbol{n}\rangle_F + \langle\, [\![u_h^*]\!], \boldsymbol{v}\rangle_e.$$

Taking $\boldsymbol{v} \in \mathrm{RT}_0(K)$, such that for each $K \in w(e)$

$$\begin{aligned} \int_e \boldsymbol{v}\cdot\boldsymbol{n} &= \int_e \mathsf{P}_{\mathcal{M}_0}\, [\![u_h^*]\!]\cdot\boldsymbol{n}, &\qquad &\text{for the face } e, \\ \int_F \boldsymbol{v}\cdot\boldsymbol{n} &= 0, &\qquad &\text{for all } F\in\partial K\setminus e, \end{aligned}$$

we obtain

$$\|\, \mathsf{P}_{\mathcal{M}_0}\, [\![u_h^*]\!]\, \|_{0,e}^2 = \sum_{K\in w(e)} (\boldsymbol{q}_h + \boldsymbol{\nabla}\, u_h^*, \boldsymbol{v})_K.$$

The lemma follows from the Cauchy-Schwartz inequality and a standard scaling argument

$$\|\, \boldsymbol{v}\, \|_{0,K} \le C_s h_e^{1/2} \|\, \boldsymbol{v}\cdot\boldsymbol{n}\, \|_{\partial K}.$$

This completes the proof. □

3.3.2 Proof of Reliability and Efficiency of the estimator

We are now ready to prove the reliability of the error estimator.

Theorem 3.3.1 (Reliability of the error estimator)**.** *Under the mesh assumptions* $\mathbf{A_0}, \mathbf{A_1}, \mathbf{A_2}$ *and the boundary condition assumption* $\mathbf{B}$*, we have that*

$$\|\, \boldsymbol{q} - \boldsymbol{q}_h\, \|_{0,\mathcal{T}_h}^2 \le C_2 \eta_h^2.$$

where C_2 *is a constant depending only on the shape-regularity constant* σ*, the maximum polynomial degree* p *and the level of nonconformity* L*.*

Proof. We note that, by Lemma 3.3.2, for any function ϕ in $H^1(\Omega)$, we have

$$\|\, \boldsymbol{q} - \boldsymbol{q}_h\, \|_{0,\mathcal{T}_h}^2 \le\ C_{\sigma,L}(ocs_h^2(f,\mathcal{T}_h) + \eta_\phi^2) - \langle (\boldsymbol{q} - \boldsymbol{q}_h)\cdot\boldsymbol{n}, g - \phi\rangle_\Gamma.$$

We now take $\phi := \tilde{u}_h^* \in W_h^* \cap H^1(\Omega)$, where, by the result of Lemma 3.3.1, the function $\tilde{u}_h^*$ satisfies

$$\tilde{u}_h^* = g \qquad \text{on } \Gamma, \tag{3.3.1a}$$

$$\sum_{K\in\mathcal{T}_h} \| \nabla(u_h^* - \tilde{u}_h^*) \|_{0,K}^2 \le C_j \sum_{e\in\mathcal{E}_h^i} h_e^{-1} \| \, [\![u_h^*]\!] \, \|_{0,e}^2. \tag{3.3.1b}$$

We immediately obtain that

$$\langle (\boldsymbol{q} - \boldsymbol{q}_h) \cdot \boldsymbol{n}, g - \phi \rangle_\Gamma = 0, \tag{3.3.2}$$

by property (3.3.1a), and that

$$\begin{aligned}
\eta_\phi^2 &:= \sum_{K\in\mathcal{T}_h} \| \, \boldsymbol{q}_h + \nabla \tilde{u}_h^* \, \|_{0,K}^2 \\
&\le \sum_{K\in\mathcal{T}_h} \| \, \boldsymbol{q}_h + \nabla u_h^* \, \|_{0,K}^2 + \sum_{K\in\mathcal{T}_h} \| \nabla(u_h^* - \tilde{u}_h^*) \|_{0,K}^2.
\end{aligned}$$

Hence, by property (3.3.1b), we get that

$$\eta_\phi^2 \le \sum_{K\in\mathcal{T}_h} \| \, \boldsymbol{q}_h + \nabla u_h^* \, \|_{0,K}^2 + C_j \sum_{e\in\mathcal{E}_h} h_e^{-1} \| \, [\![u_h^*]\!] \, \|_{0,e}^2. \tag{3.3.3}$$

Moreover, since

$$\begin{aligned}
\sum_{e\in\mathcal{E}_h} h_e^{-1} \| \, [\![u_h^*]\!] \, \|_{0,e}^2 \le\; & 2 \sum_{e\in\mathcal{E}_h} h_e^{-1} \| \, (\mathsf{Id} - \mathsf{P}_{M_0}) \, [\![u_h^*]\!] \, \|_{0,e}^2 \\
&+ 2 \sum_{e\in\mathcal{E}_h} h_e^{-1} \| \, (\mathsf{P}_{\mathcal{M}_0} - \mathsf{P}_{M_0}) \, [\![u_h^*]\!] \, \|_{0,e}^2 \\
&+ 2 \sum_{K\in\mathcal{T}_h} h_e^{-1} \| \, \mathsf{P}_{\mathcal{M}_0} \, [\![u_h^*]\!] \, \|_{0,\partial K}^2,
\end{aligned}$$

after applying Lemma 3.3.3, we get

$$\begin{aligned}
\sum_{e\in\mathcal{E}_h} h_e^{-1} \| \, [\![u_h^*]\!] \, \|_{0,e}^2 \le\; & 2 \sum_{e\in\mathcal{E}_h} h_e^{-1} \| \, (\mathsf{Id} - \mathsf{P}_{M_0}) \, [\![u_h^*]\!] \, \|_{0,e}^2 \\
&+ 2 \sum_{e\in\mathcal{E}_h} h_e^{-1} \| \, (\mathsf{P}_{\mathcal{M}_0} - \mathsf{P}_{M_0}) \, [\![u_h^*]\!] \, \|_{0,e}^2 \\
&+ 2 C_s \| \, \boldsymbol{q}_h + \boldsymbol{\nabla} \, u_h^* \, \|_{0,\mathcal{T}_h}^2.
\end{aligned} \tag{3.3.4}$$

We conclude, from inequalities (3.3.3), (3.3.4) and equation (3.3.2), that

$$\| \boldsymbol{q} - \boldsymbol{q}_h \|^2_{0,\mathcal{T}_h} \le C_2 \eta_h^2.$$

This completes the proof. $\square$

To complete the proof of Theorem 3.2.1, it only remains to prove the following local lower bound for the error $\| \boldsymbol{q} - \boldsymbol{q}_h \|_{0,w(e)}$. To do so, we denote The proof is carried out in two steps. Our first goal is to establish the following lemma.

Lemma 3.3.4. *For any face $e \in \mathcal{F}_h$,*

$$\eta^2_{2,h}(e) + \eta^2_{3,h}(e) \le C(\| \boldsymbol{q} - \boldsymbol{q}_h \|^2_{0,\tilde{w}(e)} + \| \boldsymbol{\nabla} u - \boldsymbol{\nabla} u_h^* \|^2_{0,\tilde{w}(e)}).$$

for some constant $C = C(\sigma, \mathsf{p}, L)$.

Proof. Because of the orthogonality properties of the projections P_{M_0} and $\mathsf{P}_{\mathcal{M}_0}$,

$$\begin{aligned}\eta^2_{2,h}(e) + \eta^2_{3,h}(e) &:= h_e^{-1} \| (\mathsf{Id} - \mathsf{P}_{M_0}) [\![u_h^*]\!] \|^2_{0,e} + h_e^{-1} \| (\mathsf{P}_{M_0} - \mathsf{P}_{\mathcal{M}_0}) [\![u_h^*]\!] \|^2_{0,e} \\ &= h_e^{-1} \| (\mathsf{Id} - \mathsf{P}_{\mathcal{M}_0}) [\![u_h^*]\!] \|^2_{0,e},\end{aligned}$$

and we see that we only need to show that

$$h_e^{-1} \| (\mathsf{Id} - \mathsf{P}_{\mathcal{M}_0}) [\![u_h^*]\!] \|^2_{0,e} \le C(\| \boldsymbol{q} - \boldsymbol{q}_h \|^2_{0,w(e)} + \| \boldsymbol{\nabla} u - \boldsymbol{\nabla} u_h^* \|^2_{0,w(e)}).$$

for some constant $C = C(\sigma, \mathsf{p}, L)$.

To do that, we start from the following equation:

$$(\boldsymbol{q} - \boldsymbol{q}_h, \boldsymbol{v})_K - (u - u_h^*, \nabla \cdot \boldsymbol{v})_K = -(\boldsymbol{q}_h + \boldsymbol{\nabla} u_h^*, \boldsymbol{v})_K + \langle u - u_h^*, \boldsymbol{v} \cdot \boldsymbol{n} \rangle_{\partial K}.$$

which holds for any $\boldsymbol{v} \in \boldsymbol{H}(\mathrm{div}, \Omega)$ such that $\boldsymbol{v} \cdot \boldsymbol{n} \in L^2(\mathcal{E}_h)$. Adding over all $K \in w^*(e)$, we have

$$\begin{aligned}&\sum_{K \in w^*(e)} (\boldsymbol{q} - \boldsymbol{q}_h, \boldsymbol{v})_K - \sum_{K \in w^*(e)} (u - u_h^*, \nabla \cdot \boldsymbol{v})_K \\ &= - \sum_{K \in w^*(e)} (\boldsymbol{q}_h + \boldsymbol{\nabla} u_h^*, \boldsymbol{v})_K + \sum_{K \in w^*(e)} \langle u - u_h^*, \boldsymbol{v} \cdot \boldsymbol{n} \rangle_{\partial K \setminus e} + \langle [\![u_h^*]\!], \boldsymbol{v} \rangle_e.\end{aligned} \tag{3.3.5}$$

where $[\![u_h^*]\!] = (u_h^* - g) \cdot \boldsymbol{n}$ on Γ. For the case of simplex elements, we take the vector valued function $\boldsymbol{v}|_K \in \mathrm{RT}_{\mathsf{p}+2}(K)$ such that

$$\begin{aligned} (\boldsymbol{v}, \boldsymbol{\tau})_K &= 0 && \text{for all } \boldsymbol{\tau} \in \mathcal{P}_{\mathsf{p}+1}(K), \\ \langle \boldsymbol{v} \cdot \boldsymbol{n}, \mu \rangle_{F_e} &= \langle (\mathsf{Id} - \mathsf{P}_{\mathcal{M}_0})\, [\![u_h^*]\!], \mu \rangle_{F_e} && \text{for all } \mu \in \mathcal{P}_{\mathsf{p}+2}(F_e), \\ \langle \boldsymbol{v} \cdot \boldsymbol{n}, \mu \rangle_F &= 0 && \text{for all } \mu \in \mathcal{P}_{\mathsf{p}+2}(F), \quad \forall F \in \partial K \setminus e, \end{aligned}$$

for all elements $K \in v^*(e)$ and $\boldsymbol{v} = \boldsymbol{0}$ on $\tilde{w}(e) \setminus v^*(e)$. For the case of square and cube elements, we take the vector valued function $\boldsymbol{v}|_K \in \mathrm{RT}_{\mathsf{p}+2}(K)$ such that

$$\begin{aligned} (\boldsymbol{v}, \boldsymbol{\tau})_K &= 0 && \text{for all } \boldsymbol{\tau} \in \boldsymbol{\psi}(K), \\ \langle \boldsymbol{v} \cdot \boldsymbol{n}, \mu \rangle_{F_e} &= \langle (\mathsf{Id} - \mathsf{P}_{\mathcal{M}_0})\, [\![u_h^*]\!], \mu \rangle_{F_e} && \text{for all } \mu \in \mathcal{Q}_{\mathsf{p}+2}(F_e), \\ \langle \boldsymbol{v} \cdot \boldsymbol{n}, \mu \rangle_F &= 0 && \text{for all } \mu \in \mathcal{Q}_{\mathsf{p}+2}(F), \quad \forall F \in \partial K \setminus e, \end{aligned}$$

for all elements $K \in v^*(e)$ and $\boldsymbol{v} = \boldsymbol{0}$ on $\tilde{w}(e) \setminus v^*(e)$ where

$$\boldsymbol{\psi}(K) := \begin{cases} \mathcal{P}_{\mathsf{p}-1,\mathsf{p}}(K) \times \mathcal{P}_{\mathsf{p},\mathsf{p}-1}(K) & \text{for square,} \\ \mathcal{P}_{\mathsf{p}-1,\mathsf{p},\mathsf{p}}(K) \times \mathcal{P}_{\mathsf{p},\mathsf{p}-1,\mathsf{p}}(K) \times \mathcal{P}_{\mathsf{p},\mathsf{p},\mathsf{p}-1}(K) & \text{for cube.} \end{cases}$$

It is easy to see that for any $K \in \tilde{w}(e)$,

$$\int_{\partial K} \boldsymbol{v} \cdot \boldsymbol{n} = 0,$$

and that the divergence theorem gives us

$$\int_K \nabla\cdot \boldsymbol{v} = 0.$$

Thus, from the equation (3.3.5), we have that

$$\sum_{K \in \tilde{w}(e)} (\boldsymbol{q} - \boldsymbol{q}_h, \boldsymbol{v})_K - \sum_{K \in \tilde{w}(e)} (u - u_h^* - \mathsf{P}_{W_0}(u - u_h^*), \nabla\cdot \boldsymbol{v})_K = \langle\, [\![u_h^*]\!], \boldsymbol{v} \rangle_e.$$

Applying the Cauchy-Schwartz inequality, we have

$$\begin{aligned} \|\, (\mathsf{Id} - \mathsf{P}_{\mathcal{M}_0})\, [\![u_h^*]\!] \,\|_{0,e}^2 \leq & C_p \sum_{K \in \tilde{w}(e)} (\|\, \boldsymbol{q} - \boldsymbol{q}_h \,\|_{0,K} + h_K^{-1} \,\|\, (\mathsf{Id} - \mathsf{P}_{W_0})(u - u_h^*) \,\|_{0,K}) \\ & \times (\|\, \boldsymbol{v} \,\|_{0,K} + h_K \|\, \nabla\cdot \boldsymbol{v} \,\|_{0,K}) \end{aligned}$$

where P_{W_0} is the L_2-orthogonal projection into the space of piecewise constants. Thus, by the Poincaré inequality, we obtain

$$\|\,(\mathsf{Id}-\mathsf{P}_{\mathcal{M}_0})\,[\![u_h^*]\!]\,\|_{0,e}^2 \le C_p \sum_{K\in\tilde{w}(e)} (\|\,\boldsymbol{q}-\boldsymbol{q}_h\,\|_{0,K} + \|\,\boldsymbol{\nabla}(u-u_h^*)\,\|_{0,K})$$
$$\times\,(\|\,\boldsymbol{v}\,\|_{0,K} + h_K\|\,\nabla\cdot\boldsymbol{v}\,\|_{0,K})$$

Furthermore, a standard scaling argument gives us,

$$\sum_{K\in\tilde{w}(e)} (\|\,\boldsymbol{v}\,\|_{0,K} + h_K\|\,\nabla\cdot\boldsymbol{v}\,\|_{0,K}) \le C_s h_e^{1/2}\|\,\boldsymbol{v}\cdot\boldsymbol{n}\,\|_{0,e},$$

for some constant $C_s = C_s(\sigma,\mathsf{p},L)$. Hence,

$$h_e^{-1/2}\|\,(\mathsf{Id}-\mathsf{P}_{M_0})\,[\![u-u_h^*]\!]\,\|_{0,e} \le C_pC_s \sum_{K\in\tilde{w}(e)} (\|\,\boldsymbol{q}-\boldsymbol{q}_h\,\|_{0,K} + \|\,\boldsymbol{\nabla}(u-u_h^*)\,\|_{0,K}).$$

This completes the proof. $\square$

Our second goal is to obtain the following estimate.

Lemma 3.3.5. *For each element $K\in\mathcal{T}_h$, it holds that*

$$\|\,\boldsymbol{\nabla}(u-u_h^*)\,\|_{0,K} \le C\|\,\boldsymbol{q}-\boldsymbol{q}_h\,\|_{0,K}.$$

for some constant $C = C(\sigma,\mathsf{p})$.

Proof. The inequality follows if we show that

$$\|\,\boldsymbol{q}_h + \boldsymbol{\nabla}\,u_h^*\,\|_{0,K} \le C\|\,\boldsymbol{q}-\boldsymbol{q}_h\,\|_{0,K}.$$

In order to do that, we introduce the semi-norm for the vector variable $\boldsymbol{q}_h$:

$$|\boldsymbol{q}_h|_{curl,K} := \sup_{\substack{\phi\in\boldsymbol{C}_0^\infty(K),\\ \|\,\boldsymbol{\nabla}\times\phi\,\|_{0,K}=1}} (\boldsymbol{q}_h, \boldsymbol{\nabla}\times\phi)_K,$$

where $\boldsymbol{C}_0^\infty(K)$ denotes smooth functions with compact support in K. Now we show that

$$\|\,\boldsymbol{q}_h + \boldsymbol{\nabla}\,u_h^*\,\|_{0,K} \le C|\boldsymbol{q}_h|_{curl,K} \le C\|\,\boldsymbol{q}-\boldsymbol{q}_h\,\|_{0,K}.$$

To prove the first part of the inequality, we begin by constructing, for each element $K \in \mathcal{T}_h$, a reference element $\widehat{K}$ with unit diameter by using the transformation map F given by

$$x = F(\widehat{x}) = h_K \widehat{x} + b.$$

Setting

$$\begin{aligned} u_h^*(x) &:= \widehat{u}_h^*(\widehat{x}), \\ \boldsymbol{q}_h(x) &:= (DF^{-1})\widehat{\boldsymbol{q}}_h(\widehat{x}) = h_K^{-1}\widehat{\boldsymbol{q}}_h(\widehat{x}), \end{aligned}$$

we have

$$\begin{aligned} \boldsymbol{\nabla}\, u_h^* &= h_K^{-1}\widehat{\boldsymbol{\nabla}}\widehat{u}_h^*, \\ \boldsymbol{\nabla}\times \phi(x) &= h_K^{-1}\, \widehat{\boldsymbol{\nabla}}\times \widehat{\phi}(\widehat{x}). \end{aligned}$$

Since

$$\begin{aligned} \int_K |\boldsymbol{q}_h + \boldsymbol{\nabla}\, u_h^*|^2 dx &= h_K^{d-2} \int_{\widehat{K}} |\widehat{\boldsymbol{q}}_h + \widehat{\boldsymbol{\nabla}}\widehat{u}_h^*|^2 d\widehat{x}, \\ \int_K |\, \boldsymbol{\nabla}\times \phi|^2 dx &= h_K^{d-2} \int_{\widehat{K}} |\, \widehat{\boldsymbol{\nabla}}\times \widehat{\phi}|^2 d\widehat{x}, \end{aligned}$$

and

$$\int_K \boldsymbol{q}_h \cdot \boldsymbol{\nabla}\times \phi dx = h_K^{d-2} \int_{\widehat{K}} \widehat{\boldsymbol{q}}_h \cdot \widehat{\boldsymbol{\nabla}}\times \widehat{\phi}\, d\widehat{x},$$

we obtain that

$$\| \, \boldsymbol{q}_h + \boldsymbol{\nabla}\, u_h^* \, \|_{0,K} = h_K^{\frac{d}{2}-1} \| \, \widehat{\boldsymbol{q}}_h + \boldsymbol{\nabla}\, \widehat{u}_h^* \, \|_{0,\widehat{K}}, \tag{3.3.6a}$$

$$|\boldsymbol{q}_h|_{curl,K} = h_K^{\frac{d}{2}-1} |\widehat{\boldsymbol{q}}_h|_{curl,\widehat{K}}. \tag{3.3.6b}$$

Moreover, from the equation defining the post-processing solution (3.2.6)

$$(\boldsymbol{q}_h + \boldsymbol{\nabla}\, u_h^*, \boldsymbol{\nabla}\, w)_K = 0$$

for all $w \in W^*(K)$, we obtain that

$$h_K^{d-2}(\widehat{\boldsymbol{q}}_h + \widehat{\boldsymbol{\nabla}}\widehat{u}_h^*, \widehat{\boldsymbol{\nabla}}\widehat{w})_{\widehat{K}} = 0. \tag{3.3.7}$$

for all $\widehat{w} \in W^*(\widehat{K})$.

Now our task is to show that

$$\| \widehat{\boldsymbol{q}}_h + \widehat{\boldsymbol{\nabla}}\widehat{u}_h^* \|_{0,\widehat{K}} \leq C|\widehat{\boldsymbol{q}}_h|_{curl,\widehat{K}}.$$

Since $\widehat{\boldsymbol{q}}_h$ is in the finite dimensional space $\boldsymbol{V}(\widehat{K})$, we only need to show that $\| \widehat{\boldsymbol{q}}_h + \widehat{\boldsymbol{\nabla}}\widehat{u}_h^* \|_{0,\widehat{K}}$ vanishes when $|\widehat{\boldsymbol{q}}_h|_{curl,\widehat{K}} = 0$. In fact,

$$(\widehat{\boldsymbol{q}}_h, \widehat{\boldsymbol{\nabla}}\times \widehat{\phi})_{\widehat{K}} = (\widehat{\boldsymbol{\nabla}}\times \widehat{\boldsymbol{q}}_h, \widehat{\phi})_{\widehat{K}},$$

for all $\widehat{\phi} \in \boldsymbol{C}_0^\infty(\widehat{K})$. Hence, $(\widehat{\boldsymbol{q}}_h, \widehat{\boldsymbol{\nabla}}\times \widehat{\phi})_{\widehat{K}} = 0$ implies that $\widehat{\boldsymbol{\nabla}}\times \widehat{\boldsymbol{q}}_h = 0$ and $\widehat{\boldsymbol{q}}_h = \widehat{\boldsymbol{\nabla}}\widehat{\psi}$ for some function $\widehat{\psi}$ in the post-processing space $W_h^*(\widehat{K})$. From the equation (3.3.7), taking $\widehat{w} = \widehat{\psi} - \widehat{u}_h^*$, we have

$$\| \widehat{\boldsymbol{q}}_h + \widehat{\boldsymbol{\nabla}}\widehat{u}_h^* \|_{0,\widehat{K}} = 0.$$

Thus, it holds

$$\| \widehat{\boldsymbol{q}}_h + \widehat{\boldsymbol{\nabla}}\widehat{u}_h^* \|_{0,\widehat{K}} \leq C|\widehat{\boldsymbol{q}}_h|_{curl,\widehat{K}} \tag{3.3.8}$$

for some constant C depending on the shape regularity $\sigma(\widehat{K})$ and polynomial degree p.

Considering the family $\widehat{K}(\sigma)$ of all elements $\widehat{K}$ with unit diameter, one vertex in the origin and satisfying the shape regularity condition, we get by compactness that

$$C(\sigma, \mathsf{p}) := \sup_{\widehat{K}\in\widehat{K}(\sigma)} C(\sigma(\widehat{K}), \mathsf{p}) \leq \infty$$

Hence, the first inequality now follows from (3.3.8) and the scaling argument (3.3.6a).

To prove the second part of the inequality, we note that

$$(\boldsymbol{q}, \boldsymbol{\nabla}\times \phi)_K = -(\boldsymbol{\nabla}\, u, \boldsymbol{\nabla}\times \phi)_K = 0,$$

and so

$$\sup_{\substack{\phi\in\boldsymbol{C}_0^\infty(K),\\ \| \boldsymbol{\nabla}\times \phi \|_{0,K}=1}} (\boldsymbol{q}_h, \boldsymbol{\nabla}\times \phi)_K = \sup_{\substack{\phi\in\boldsymbol{C}_0^\infty(K),\\ \| \boldsymbol{\nabla}\times \phi \|_{0,K}=1}} (\boldsymbol{q} - \boldsymbol{q}_h, \boldsymbol{\nabla}\times \phi)_K.$$

Cauchy-Schwartz inequality yields

$$\sup_{\substack{\phi\in\boldsymbol{C}_0^\infty(K),\\ \| \boldsymbol{\nabla}\times \phi \|_{0,K}=1}} (\boldsymbol{q}_h, \boldsymbol{\nabla}\times \phi)_K \leq \| \boldsymbol{q} - \boldsymbol{q}_h \|_{0,K}.$$

This completes the proof.

$\square$

The efficiency of the estimator immediately follows from Lemma 3.3.4 and Lemma 3.3.5.

Theorem 3.3.2 (Local efficiency of the error estimator)**.** *Under the mesh assumptions* $\mathbf{A_0}, \mathbf{A_1}, \mathbf{A_2}$ *and the boundary condition assumption* $\mathbf{B}$*, we have that, for each face* $e \in \mathcal{F}_h$*,*

$$C_1 \eta_h^2(e) \leq \| \boldsymbol{q} - \boldsymbol{q}_h \|_{0,w(e)}^2,$$

where $C_1 = C_1(\sigma, \mathsf{p}, L)$*.*

3.4 A concluding remark

Let us end this chapter by noting that our result also holds for the triangular Brezzi-Douglas-Marini (BDM) elements, their tetrahedral counterparts of Brezzi-Douglas-Durán-Fortin (BDDF) elements, quadrilateral Brezzi-Douglas-Fortin-Marini (BDFM) elements and for the recently uncovered TNT elements for squares and cubes [38].

Chapter 4

A posteriori error analysis for HDG methods

4.1 Introduction

In this chapter, applying a similar idea used in Chapter 3, we present a unified a posteriori error analysis for the HDG methods based on the general framework proposed in [34], see Table 1.2.2.

The chapter is organized as follows. In Section 4.2, we display the above-mentioned conditions and present out main result. In Section 4.3, we apply it to several particular cases and, in Section 4.4, we present its proof. We sketch the extension of our results to nonconforming meshes in Section 4.5. Finally, we end in Section 4.6 by presenting several equivalent error estimators.

4.2 Main results

4.2.1 The error, its estimators and the main assumptions

The conditions on the approximate flux

Our main result provides upper and local lower bounds of the error

$$\mathsf{e}_h^2 := \| \boldsymbol{q} - \tilde{\boldsymbol{q}}_h \|_{\mathcal{T}_h}^2,$$

where $\tilde{\boldsymbol{q}}_h$ is *any* approximation of the flux in the space

$$\tilde{\boldsymbol{V}}_h := \{\boldsymbol{v} \in \boldsymbol{L}^2(\Omega) : \quad \boldsymbol{v}|_K \in \tilde{\boldsymbol{V}}(K) \quad \forall K \in \mathcal{T}_h\},$$

for some auxiliary local space $\tilde{\boldsymbol{V}}(K)$, which satisfies the following two conditions:

$$\begin{aligned}
&\textbf{A1:} -(\tilde{\boldsymbol{q}}_h, \boldsymbol{\nabla}\, w)_{\mathcal{T}_h} + \langle \widehat{\boldsymbol{q}}_h \cdot \boldsymbol{n}, w\rangle_{\partial\mathcal{T}_h} = (\mathsf{P}_W f, w)_{\mathcal{T}_h} \quad \forall w \in W^c_{1,h},\\
&\textbf{A2:} \quad (\tilde{\boldsymbol{q}}_h, \boldsymbol{v})_K + (u_h, \nabla\cdot \boldsymbol{v})_K = \langle \widehat{u}_h, \boldsymbol{v}\cdot\boldsymbol{n}\rangle_{\partial K} \qquad \forall \boldsymbol{v} \in \mathrm{RT}_0(K) \;\; \forall K \in \mathcal{T}_h,
\end{aligned}$$

where, on each element K, $\mathrm{RT}_0(K) := \boldsymbol{\mathcal{P}}_0(K) + \boldsymbol{x}\mathcal{P}_0(K)$ is the lowest index RT space and

$$W^c_{1,h} := \{w \in H^1_0(\Omega) : w|_K \in \mathcal{P}_1(K)\; \forall K \in \mathcal{T}_h\}.$$

We also require that the space of approximate trace satisfies the following condition

$$\textbf{A3:} \quad \langle [\![\widehat{\boldsymbol{q}}_h \cdot \boldsymbol{n}]\!], \mu\rangle_{\mathcal{E}^i_h} = 0 \quad \forall \mu \in \mathsf{M}^c_{1,h}$$

where

$$\mathsf{M}^c_{1,h} := \{\mu \in \mathcal{C}^0(\mathcal{E}_h) : \mu|_e \in \mathcal{P}_1(e)\; \forall e \in \mathcal{E}_h\}.$$

Remark 4.2.1. *The approximation $\tilde{\boldsymbol{q}}_h$, in all our expected case, is an element-wise post-processing of $\boldsymbol{q}_h$, $\widehat{\boldsymbol{q}}_h$ and $\boldsymbol{\nabla}\, u_h$. In fact, if we take $\tilde{\boldsymbol{q}}_h := \boldsymbol{q}_h$, condition* **A1** *is satisfied when $W(K) \supset \mathcal{P}_1(K)$ thanks to the second equation defining the HDG method; condition* **A2** *is satisfied when $\boldsymbol{V}(K) \supset \mathrm{RT}_0(K)$ thanks to the first equation defining the HDG method; and condition* **A3** *is satisfied when $\mathsf{M}(e) \supset \mathcal{P}_1(e)$.*

Local post-processing of the scalar solution

Applying a similar idea used in Chapter 3, we define the local post-processing as follows. We are going to take u_h^* in the finite dimensional space

$$W_h^* = \{w \in L^2(K) : \quad w|_K \in W^*(K) \quad \forall K \in \mathcal{T}_h\}, \tag{4.2.1a}$$

where we assume that the local space $W^*(K)$ satisfies the following properties:

$$\mathcal{P}_0(K) \subset W^*(K), \tag{4.2.1b}$$

$$\{\boldsymbol{v} \in \tilde{\boldsymbol{V}}(K) : \; \boldsymbol{\nabla}\times \boldsymbol{v} = \boldsymbol{0}\} \subset \boldsymbol{\nabla}\, W^*(K), \tag{4.2.1c}$$

for all $K \in \mathcal{T}_h$.

We can now define u_h^* as the element of the space W_h^* determined on the element $K \in \mathcal{T}_h$ by the following equations:

$$(u_h^*, w)_K = (u_h, w)_K \qquad \forall w \in \mathcal{P}_0(K), \tag{4.2.2a}$$

$$(\boldsymbol{\nabla}\, u_h^*, \boldsymbol{\nabla}\, w)_K = -(\tilde{\boldsymbol{q}}_h, \boldsymbol{\nabla}\, w)_K \quad \forall w \in W^*(K). \tag{4.2.2b}$$

It is easy to see that the post-processed solution u_h^* is well defined.

Remark 4.2.2. *Note that the post-processing solution u_h^* is closely associated with the approximation $\tilde{\boldsymbol{q}}_h$. Indeed, when $\boldsymbol{\nabla}\times \tilde{\boldsymbol{q}}_h = \mathbf{0}$ on K, by property* (4.2.1c)*, $\tilde{\boldsymbol{q}}_h$ has to be the gradient of some polynomial in $W^*(K)$ and, by the definition of the post-processing solution u_h^*, we must have that $\tilde{\boldsymbol{q}}_h = -\boldsymbol{\nabla}\, u_h^*$ on K. In this sense, we say that $-\boldsymbol{\nabla}\, u_h^*$ captures the gradient part of $\tilde{\boldsymbol{q}}_h$ locally. This property plays a crucial role in the analysis, as pointed out in Chapter 3.*

Remark 4.2.3. *Note that for the RT methods, and for the choice $W^*(K) := \mathcal{P}_{p+2}(K)$, the post processed solution defined above is different from the one used in [58]. Indeed, in [58], the solution u_h^* is in the space $W^*(K) := \mathcal{P}_{p+1}(K)$ and thus, property* (4.2.1c) *does not hold in this case. Moreover, our post-processed solution u_h^* is related to the auxiliary flux $\tilde{\boldsymbol{q}}_h$ while u_h^* in [58] is related to $\boldsymbol{q}_h$ only.*

Remark 4.2.4. *Note also that for the lowest index RT method, and for the choice $W^*(K) := \mathcal{P}_2(K)$, our post-processed solution u_h^* coincides with the one proposed in [71].*

Data oscillation and error estimator

Using the post-processed solution u_h^* defined above, we construct the following estimators:

$$\eta_{1,h}^2(e) := h_e \| \, [\![\tilde{\boldsymbol{q}}_h]\!] \, \|_e^2 + \sum_{K\in\mathcal{U}_h(e)} h_K^2 \| \, \mathsf{P}_W f - \nabla\cdot \tilde{\boldsymbol{q}}_h \, \|_K^2, \tag{4.2.3a}$$

$$\eta_{2,h}^2(e) := h_e^{-1} \| \, (\mathsf{Id} - \mathsf{P}_{\mathsf{M}_0}) \, [\![u_h^*]\!] \, \|_e^2 + \sum_{K\in\mathcal{U}_h(e)} \| \, \tilde{\boldsymbol{q}}_h + \boldsymbol{\nabla}\, u_h^* \, \|_K^2, \tag{4.2.3b}$$

$$\eta_{3,h}^2(e) := h_e^{-1} \| \, \mathsf{P}_{\mathsf{M}_0} \, [\![u_h^*]\!] \, \|_e^2, \tag{4.2.3c}$$

and introduce the data oscillation term

$$osc_h^2(f, \mathcal{T}_h) := \sum_{K \in \mathcal{T}_h} h_K^2 \| f - \mathsf{P}_W f \|_K^2, \tag{4.2.4}$$

Here, P_W is the $L^2(\Omega)$-orthogonal projection into the space W_h, and $\mathsf{P}_{\mathsf{M}_0}$ the $L^2(\Omega)$-orthogonal projection into the space

$$\mathsf{M}_{0,h} := \{\mu \in L^2(\partial\mathcal{T}_h),\ \mu|_e \in \mathcal{P}_0(e),\ \text{for each face } e \in \mathcal{E}_h\}.$$

Remark 4.2.5. *Let us note that to prove lower bounds for $\eta_{2,h}^2(e)$ and $\eta_{3,h}^2(e)$, we have to proceed in very different ways. This motivates the decomposition of $h_e^{-1} \| [\![u_h^*]\!] \|_e^2$ into the corresponding terms in $\eta_{2,h}^2(e)$ and $\eta_{3,h}^2(e)$.*

4.2.2 The main results

In what follows, we use the notation $'a \preceq b'$ to denote

$$a \leq Cb$$

for some generic constant C depending only on the shape regularity σ and on the maximum dimension of the local spaces $\boldsymbol{V}(K)$, $W(K)$ and $W^*(K)$. We also use the notation $'a \simeq b'$ to denote

$$a \preceq b \preceq a.$$

We are now ready to state our main results.

Theorem 4.2.1 (Reliability of the error estimator)**.** *Suppose that assumption* **B** *on the meshes, assumption* **C** *on the boundary condition, and conditions* **A1** *and* **A3** *are satisfied. Then*

$$\| \boldsymbol{q} - \tilde{\boldsymbol{q}}_h \|_{\mathcal{T}_h}^2 \preceq \eta_h^2 + osc_h^2(f, \mathcal{T}_h),$$

where

$$\eta_h^2 := \sum_{e \in \mathcal{E}_h} \left(\eta_{1,h}^2(e) + \eta_{2,h}^2(e) + \eta_{3,h}^2(e)\right). \tag{4.2.5}$$

Theorem 4.2.2 (Local efficiency of the error estimator). *Suppose that assumption* **B** *on the meshes and assumption* **C** *on the boundary condition are satisfied. Then, for each face* $e \in \mathcal{E}_h$,

$$\eta_{1,h}^2(e) \preceq \sum_{K \in \mathcal{U}_h(e)} \| \boldsymbol{q} - \tilde{\boldsymbol{q}}_h \|_K^2 + osc_h^2(f, \mathcal{U}_h(e)),$$
$$\eta_{2,h}^2(e) \preceq \sum_{K \in \mathcal{U}_h(e)} \| \boldsymbol{q} - \tilde{\boldsymbol{q}}_h \|_K^2.$$

Moreover, if $\tilde{\boldsymbol{q}}_h$ *satisfies condition* **A2**,

$$\eta_{3,h}^2(e) \preceq \eta_{2,h}^2(e) \quad \textit{for all faces } e \in \mathcal{E}_h.$$

Thanks to these results, to derive a posteriori error estimates for any method fitting in our general setting, we *only* need to specify the auxiliary space $\tilde{\boldsymbol{V}}(K)$, $W^*(K)$ the approximate flux $\tilde{\boldsymbol{q}}_h$ and verify conditions **A**.

4.3 Applications

4.3.1 Main Examples

In this section, we apply our main theorems to the methods described in Table 1.2.2; see Table 4.3.1.

Table 4.3.1: The auxiliary flux $\tilde{\boldsymbol{q}}_h$ and the auxiliary local spaces $\tilde{\boldsymbol{V}}(K)$ and $W^*(K)$.

Method	$\tilde{\boldsymbol{q}}_h$	$\tilde{\boldsymbol{V}}(K)$	$W^*(K)$	p
RT-H	$\boldsymbol{q}_h$	$\boldsymbol{\mathcal{P}}_p(K) + \boldsymbol{x}\,\mathcal{P}_p(K)$	$\mathcal{P}_{p+2}(K)$	$p \geq 0$
BDM-H	$\boldsymbol{q}_h$	$\boldsymbol{\mathcal{P}}_p(K)$	$\mathcal{P}_{p+1}(K)$	$p \geq 1$
LDG-H	$\boldsymbol{q}_h^*$	$\boldsymbol{\mathcal{P}}_p(K) + \boldsymbol{x}\,\mathcal{P}_p(K)$	$\mathcal{P}_{p+2}(K)$	$p \geq 2$
LDG-H	$\boldsymbol{q}_h$	$\boldsymbol{\mathcal{P}}_p(K)$	$\mathcal{P}_{p+1}(K)$	$p \geq 1$
IP-H	$\boldsymbol{q}_h$	$\boldsymbol{\mathcal{P}}_p(K)$	$\mathcal{P}_{p+1}(K)$	$p \geq 1$
CG-H	$-\boldsymbol{\nabla}\, u_h$	$\boldsymbol{\mathcal{P}}_{p-1}(K)$	$\mathcal{P}_p(K)$	$p \geq 1$

Next, to establish the reliability and efficiency of the estimator η_h^2 defined in (4.2.5), we only need to verify conditions **A** for all the methods considered in the table above.

4.3.2 Verification of conditions A

RT-H methods

Condition **A2** follows immediately from the equations defining the HDG methods (1.2.2).

For the case $k \geq 1$, conditions **A1** and **A3** hold due to (1.2.2). For the lowest order case, we observe that, since $\tilde{\boldsymbol{q}}_h := \boldsymbol{q}_h$ and $\widehat{\boldsymbol{q}}_h \cdot \boldsymbol{n} := \boldsymbol{q}_h \cdot \boldsymbol{n}$, from (1.2.2), we have

$$\begin{aligned} (\nabla\cdot \boldsymbol{q}_h, w) &= (f_h, w) && \forall w \in \mathcal{P}_0(\mathcal{T}_h),\\ \langle [\![\widehat{\boldsymbol{q}}_h]\!], \mu\rangle_{\mathcal{E}_h^i} &= 0 && \forall \mu \in \mathcal{P}_0(\mathcal{E}_h^i). \end{aligned}$$

Since $\nabla\cdot \boldsymbol{q}_h \in \mathcal{P}_0(\mathcal{T}_h)$, $f_h \in \mathcal{P}_0(\mathcal{T}_h)$ and $[\![\widehat{\boldsymbol{q}}_h]\!] \in \mathcal{P}_0(\mathcal{E}_h^i)$, we obtain $\nabla\cdot \boldsymbol{q}_h = f_h$ and $[\![\widehat{\boldsymbol{q}}_h]\!] = 0$. Thus,

$$\begin{aligned} (\nabla\cdot \boldsymbol{q}_h, w) &= (f_h, w) && \forall w \in W_{1,h}^c,\\ \langle [\![\widehat{\boldsymbol{q}}_h]\!], \mu\rangle_{\mathcal{E}_h^i} &= 0 && \forall \mu \in \mathsf{M}_{1,h}^c. \end{aligned}$$

This verifies conditions **A1** and **A3**.

Remark 4.3.1. *For BDM-H methods, conditions* **A** *can be verified in a similar fashion.*

LDG-H methods

For LDG-H methods, we propose two error estimators.

1. The choice $\tilde{\boldsymbol{q}}_h := \boldsymbol{q}_h^*$. To define $\boldsymbol{q}_h^*$, we follow the idea of [13, 37, 36, 35] and use a slight modification of the RT projection [61]. Let the local space $\boldsymbol{V}(K) = \boldsymbol{\mathcal{P}}_p(K)$. We take $\boldsymbol{q}_h^* \in \tilde{\boldsymbol{V}}(K) = \mathrm{RT}_p(K)$ satisfying

$$(\boldsymbol{q}_h^*, \boldsymbol{v})_K = (\boldsymbol{q}_h, \boldsymbol{v})_K \qquad \forall \boldsymbol{v} \in \boldsymbol{\mathcal{P}}_{p-1}(K), \tag{4.3.1a}$$

$$\langle \boldsymbol{q}_h^* \cdot \boldsymbol{n}, \mu\rangle_e = \langle \widehat{\boldsymbol{q}}_h \cdot \boldsymbol{n}, \mu\rangle_e \quad \forall \mu \in \mathcal{P}_p(e) \text{ for all faces } e \text{ of } K. \tag{4.3.1b}$$

2. The choice $\tilde{\boldsymbol{q}}_h := \boldsymbol{q}_h$. The verification of conditions **A** is similar to that of RT-H methods.

The IP-H method

In view of (1.2.2), the conditions **A** can be directly verified.

The CG-H method

Since $\widehat{u}_h = u_h$, from (1.2.4a), we have $\boldsymbol{q}_h = -\boldsymbol{\nabla}\, u_h$. In view of $W(K) \supset \mathcal{P}_1(K)$ for any $K \in \mathcal{T}_h$ and $\mathsf{M}_h := \mathsf{M}^c_{k,h} \supset \mathsf{M}^c_{1,h}$, conditions **A1** and **A3** are automatically satisfied. Here, we remind the reader that

$$\mathsf{M}^c_{k,h} := \{\mu \in \mathcal{C}^0(\mathcal{E}_h)\ ,\ \mu|_e \in \mathcal{P}_p(e)\}.$$

To verify condition **A2**, we note that $\widehat{u}_h = u_h$ and $\boldsymbol{q}_h = -\boldsymbol{\nabla}\, u_h$. As a consequence, we obtain, by integration by parts, that

$$(\boldsymbol{q}_h, \boldsymbol{v})_K - (u_h, \nabla\cdot \boldsymbol{v})_K = -\langle \widehat{u}_h, \boldsymbol{v}\cdot\boldsymbol{n}\rangle_{\partial K}$$

for any $\boldsymbol{v} \in \mathrm{RT}_0(K)$ on $K \in \mathcal{T}_h$, and we see that condition **A2** is actually verified.

4.4 Proof

In this Section, we provide the proofs of our main results, namely, Theorem 4.2.1 and Theorem 4.2.2.

4.4.1 Proof of the reliability of the estimator, Theorem 4.2.1.

To establish the reliability of the estimator, we follow the approach proposed in Chapter 3.

Preliminaries

We start by gathering two useful auxiliary lemmas.

Lemma 4.4.1. *Suppose that conditions* **A1** *and* **A3** *are satisfied. Then there exists a constant C_σ depending on the shape regularity, such that*

$$\|\, \boldsymbol{q} - \tilde{\boldsymbol{q}}_h \,\|^2_{\mathcal{T}_h} \le C_\sigma(\eta^2_{1,h} + \eta^2_\phi + osc^2_h(f, \mathcal{T}_h)),$$

where

$$\eta^2_{1,h} := \sum_{K\in\mathcal{T}_h} h^2_K \|\, \mathsf{P}_W f - \nabla\cdot \tilde{\boldsymbol{q}}_h \,\|^2_K + \sum_{e\in\mathcal{E}^i_h} h_e \|\, [\![\tilde{\boldsymbol{q}}_h]\!] \,\|^2_e,$$

$$\eta^2_\phi := \inf_{\phi\in H^1(\Omega),\, \phi|_\Gamma = g} \|\, \tilde{\boldsymbol{q}}_h + \boldsymbol{\nabla}\, \phi \,\|^2_{\mathcal{T}_h}.$$

Proof. We have

$$
\begin{aligned}
\|\, \boldsymbol{q} - \tilde{\boldsymbol{q}}_h \,\|_{\mathcal{T}_h}^2 &= \sum_{K \in \mathcal{T}_h} \|\, \boldsymbol{q} - \tilde{\boldsymbol{q}}_h \,\|_K^2 \\
&= \sum_{K \in \mathcal{T}_h} (\boldsymbol{q} - \tilde{\boldsymbol{q}}_h, \boldsymbol{q} + \boldsymbol{\nabla}\, \phi - \tilde{\boldsymbol{q}}_h - \boldsymbol{\nabla}\, \phi)_K, \\
&= \sum_{K \in \mathcal{T}_h} \big((\boldsymbol{q} - \tilde{\boldsymbol{q}}_h, -\boldsymbol{\nabla}\, u + \boldsymbol{\nabla}\, \phi)_K - (\boldsymbol{q} - \tilde{\boldsymbol{q}}_h, \tilde{\boldsymbol{q}}_h + \boldsymbol{\nabla}\, \phi)_K \big) \\
&= \sum_{K \in \mathcal{T}_h} \big((\nabla\cdot (\boldsymbol{q} - \tilde{\boldsymbol{q}}_h), u - \phi)_K - \langle u - \phi, (\boldsymbol{q} - \tilde{\boldsymbol{q}}_h) \cdot \boldsymbol{n} \rangle_{\partial K} \\
&\qquad - (\boldsymbol{q} - \tilde{\boldsymbol{q}}_h, \tilde{\boldsymbol{q}}_h + \boldsymbol{\nabla}\, \phi)_K \big),
\end{aligned}
$$

by integration by parts. Adding and subtracting $\mathsf{P}_W f$ in the first term, we obtain that

$$
\|\, \boldsymbol{q} - \tilde{\boldsymbol{q}}_h \,\|_{\mathcal{T}_h}^2 = \sum_{K \in \mathcal{T}_h} \big(T_{1,K} + T_{2,K} + T_{3,K} + T_{4,h} \big),
$$

where

$$
\begin{aligned}
T_{1,K} &:= (f - \mathsf{P}_W f, u - \phi)_K, \\
T_{2,K} &:= - \langle u - \phi, \boldsymbol{q} \cdot \boldsymbol{n} \rangle_{\partial K}, \\
T_{3,K} &:= (\mathsf{P}_W f - \nabla\cdot \tilde{\boldsymbol{q}}_h, u - \phi)_K + \langle u - \phi, \tilde{\boldsymbol{q}}_h \cdot \boldsymbol{n} \rangle_{\partial K}, \\
T_{4,K} &:= (\boldsymbol{q} - \tilde{\boldsymbol{q}}_h, \tilde{\boldsymbol{q}}_h + \boldsymbol{\nabla}\, \phi)_K.
\end{aligned}
$$

Let us estimate $\sum_{K \in \mathcal{T}_h} T_{1,K}$. By definition of $\mathsf{P}_W f$, we have that, for any constant c, we have that

$$
\begin{aligned}
T_{1,K} &= (f - \mathsf{P}_W f, u - \phi - c)_K \\
&\leq \frac{1}{4\epsilon} h_K^2 \|\, f - \mathsf{P}_W f \,\|_K^2 + \epsilon h_K^{-2} \|\, u - \phi - c \,\|_K^2 \\
&\leq \frac{1}{4\epsilon} h_K^2 \|\, f - \mathsf{P}_W f \,\|_K^2 + C_1\, \epsilon \,\|\, \boldsymbol{\nabla}\, (u - \phi) \,\|_K^2,
\end{aligned}
$$

by the Bramble-Hilbert Lemma, where C_1 depends on the shape regularity constant σ. Thus,

$$
\begin{aligned}
T_{1,K} \;&\leq \frac{1}{4\epsilon} h_K^2 \|\, f - \mathsf{P}_W f \,\|_K^2 + \epsilon C_1 \|\, \boldsymbol{q} + \boldsymbol{\nabla}\, \phi \,\|_K^2 \\
&\leq \frac{1}{4\epsilon} h_K^2 \|\, f - \mathsf{P}_W f \,\|_K^2 + 2\, \epsilon C_1 \|\, \tilde{\boldsymbol{q}}_h + \boldsymbol{\nabla}\, \phi \,\|_K^2 + 2\, \epsilon C_1 \|\, \boldsymbol{q} - \tilde{\boldsymbol{q}}_h \,\|_K^2,
\end{aligned}
$$

and so

$$\sum_{K\in\mathcal{T}_h} T_{1,K} \leq \frac{1}{4\epsilon} osc_h^2(f,\mathcal{T}_h) + 2\,\epsilon C_1\,\eta_\phi^2 + 2\,\epsilon C_1 \,\|\, \boldsymbol{q} - \tilde{\boldsymbol{q}}_h \,\|_{\mathcal{T}_h}^2. \tag{4.4.1}$$

Let us now consider $\sum_{K\in\mathcal{T}_h} T_{2,K}$. Since ϕ is continuous across the edges, we have that

$$\begin{aligned}\sum_{K\in\mathcal{T}_h} T_{2,K} &= -\sum_{K\in\mathcal{T}_h} \langle \boldsymbol{q}\cdot\boldsymbol{n}, u-\phi\rangle_{\partial K}\\ &= -\,\langle \boldsymbol{q}\cdot\boldsymbol{n}, u-\phi\rangle_{\Gamma}\\ &= 0,\end{aligned} \tag{4.4.2}$$

since $u = \phi = g$ on the boundary Γ.

The estimate of $\sum_{K\in\mathcal{T}_h} T_{3,K}$ is the most interesting and is the only one that uses conditions **A1** and **A3**. To obtain it, we begin by noting that, after a simple integration by parts, condition **A1** reads

$$\langle(\widehat{\boldsymbol{q}}_h - \tilde{\boldsymbol{q}}_h)\cdot\boldsymbol{n}, \omega\rangle_{\partial\mathcal{T}_h} = (\mathsf{P}_W f - \nabla\cdot\tilde{\boldsymbol{q}}_h, \omega)_{\mathcal{T}_h} \qquad \forall w \in W_{1,h}^c,$$

and, by condition **A3** and transmission condition (1.2.3b), we see that we have

$$-\langle \tilde{\boldsymbol{q}}_h\cdot\boldsymbol{n}, \omega\rangle_{\partial\mathcal{T}_h} = (\mathsf{P}_W f - \nabla\cdot\tilde{\boldsymbol{q}}_h, \omega)_{\mathcal{T}_h} \qquad \forall w \in W_{1,h}^c.$$

If we now subtract the left-hand side of the above equation with $w := \Pi(u-\phi)$, where Π denotes the Scott-Zhang interpolation [63] into the space $W_{1,h}^c$, from the term $T_{3,K}$, we get that

$$\begin{aligned}T_{3,K} = {}& (\mathsf{P}_W f - \nabla\cdot\tilde{\boldsymbol{q}}_h, (\mathsf{Id}-\Pi)(u-\phi))_K\\ &+ \langle(\mathsf{Id}-\Pi)(u-\phi), \tilde{\boldsymbol{q}}_h\cdot\boldsymbol{n}\rangle_{\partial K\setminus\Gamma}.\end{aligned}$$

Note that since $u = \phi$ on Γ, we also have that $\Pi u = \Pi\phi$ on Γ. Summing over all the elements $K \in \mathcal{T}_h$, we obtain

$$\begin{aligned}
\sum_{K\in\mathcal{T}_h} T_{3,K} = & \sum_{K\in\mathcal{T}_h} (\mathsf{P}_W f - \nabla\cdot\tilde{\boldsymbol{q}}_h, (\mathsf{Id}-\Pi)(u-\phi))_K \\
& + \sum_{K\in\mathcal{T}_h} \langle(\mathsf{Id}-\Pi)(u-\phi),\, [\![\tilde{\boldsymbol{q}}_h]\!]\rangle_{\partial K\setminus\Gamma} \\
\leq & \frac{1}{4\epsilon}\sum_{K\in\mathcal{T}_h} h_K^2 \|\, \mathsf{P}_W f - \nabla\cdot\tilde{\boldsymbol{q}}_h \,\|_K^2 + \frac{1}{4\epsilon}\sum_{e\in\mathcal{E}_h^i} h_e \|\, [\![\tilde{\boldsymbol{q}}_h]\!] \,\|_e^2 \\
& + \epsilon \sum_{K\in\mathcal{T}_h} h_K^{-2} \|\, (\mathsf{Id}-\Pi)(u-\phi) \,\|_K^2 \\
& + \epsilon \sum_{e\in\mathcal{E}_h^i} h_e^{-1} \|\, (\mathsf{Id}-\Pi)(u-\phi) \,\|_e^2,
\end{aligned}$$

by the Cauchy-Schwarz and Young inequalities. Finally, by using the trace inequality and the approximation properties of the Scott-Zhang interpolation operator Π, we readily get that

$$\begin{aligned}
\sum_{K\in\mathcal{T}_h} T_{3,K} \leq & \frac{1}{4\epsilon}\sum_{K\in\mathcal{T}_h} h_K^2 \|\, \mathsf{P}_W f - \nabla\cdot\tilde{\boldsymbol{q}}_h \,\|_K^2 + \frac{1}{4\epsilon}\sum_{e\in\mathcal{E}_h^i} h_e \|\, [\![\tilde{\boldsymbol{q}}_h]\!] \,\|_e^2 \\
& + C_3\,\epsilon\big(\|\, \tilde{\boldsymbol{q}}_h + \boldsymbol{\nabla}\,\phi \,\|_{\mathcal{T}_h}^2 + \|\, \boldsymbol{q} - \tilde{\boldsymbol{q}}_h \,\|_{\mathcal{T}_h}^2\big).
\end{aligned}$$

This implies that

$$\sum_{K\in\mathcal{T}_h} T_{3,K} \leq \frac{1}{4\epsilon}\eta_{1,h}^2 + C_3\epsilon\,\eta_\phi^2 + C_3\,\epsilon\,\|\, \boldsymbol{q} - \tilde{\boldsymbol{q}}_h \,\|_{\mathcal{T}_h}^2. \tag{4.4.3}$$

The estimate of $\sum_{K\in\mathcal{T}_h} T_{4,K}$ follows after a simple application of the Cauchy-Schwarz and Young inequalities,

$$\sum_{K\in\mathcal{T}_h} T_{4,K} \leq \frac{1}{4\epsilon}\sum_{K\in\mathcal{T}_h} \|\, \tilde{\boldsymbol{q}}_h + \boldsymbol{\nabla}\,\phi \,\|_K^2 + \epsilon \sum_{K\in\mathcal{T}_h} \|\, \boldsymbol{q} - \tilde{\boldsymbol{q}}_h \,\|_K^2,$$

and so

$$\sum_{K\in\mathcal{T}_h} T_{4,K} \leq \frac{1}{4\epsilon}\,\eta_\phi^2 + \epsilon\|\, \boldsymbol{q} - \tilde{\boldsymbol{q}}_h \,\|_{\mathcal{T}_h}^2. \tag{4.4.4}$$

Using the estimates obtained in (4.4.1) to (4.4.4), we conclude, after few simple algebraic manipulations, that

$$\begin{aligned}\| \boldsymbol{q} - \tilde{\boldsymbol{q}}_h \|^2_{\mathcal{T}_h} \leq & \frac{1}{4\epsilon} osc^2(f, \mathcal{T}_h) + \frac{1}{4\epsilon}\eta^2_{1,h} + (2\,C_1\epsilon + C_3\epsilon + \frac{1}{4\epsilon})\eta^2_\phi \\ & + \epsilon(1 + 2\,C_1 + C_3)\| \boldsymbol{q} - \tilde{\boldsymbol{q}}_h \|^2_{\mathcal{T}_h}.\end{aligned}$$

The result follows by choosing ϵ small enough. This completes the proof of Lemma 4.4.1.

□

To obtain a computable estimator, we can choose any computable continuous functions ϕ in η_ϕ. On the other hand, ϕ has to be chosen carefully so that η_ϕ gives an accurate estimate on the curl part of the error. In order to choose a proper continuous function ϕ, we are going to make use of the fact that the approximate solution u_h^* can be approximated by a continuous, piecewise polynomial function $\tilde{u}_h^*$ in the post-processing space W_h^*, (4.2.1a). This will allow us to show that the quality of the approximation can be controlled by the size of the interelement jumps of u_h^*. The following result holds for nonconforming meshes with uniform polynomial degree.

Lemma 4.4.2 ([41, 54])**.** *For any $w_h \in W_h^*$ and any multi-index α with $|\alpha| = 0, 1$ the following approximation results holds: Let g be the restriction to Γ of a function in $W_h^* \cap H^1(\Omega)$. Then there exists a function $\tilde{w}_h \in W_h^* \cap H^1(\Omega)$ satisfying $\tilde{w}_h|_\Gamma = g$ and*

$$\sum_{K\in\mathcal{T}_h} \| D^\alpha(w_h - \tilde{w}_h) \|^2_K \leq C_j \sum_{e\in\mathcal{E}_h} h_e^{1-2|\alpha|} \| [\![w_h]\!] \|^2_e + C_j \sum_{e\in\mathcal{E}_h^\partial} h_e^{1-2|\alpha|} \| g - w_h \|^2_e$$

where the constant $C_j = C_j(\sigma, k)$.

Proof of Theorem 4.2.1.

Now we are ready to prove the reliability of estimator, Theorem 4.2.1. The proof is very similar to that of Theorem 3.1 in Chapter 3. However, therein we only considered the case of the RT method, not the wide variety of methods considered here.

We note that, by Lemma 4.4.1, for any function ϕ in $H^1(\Omega)$ with trace $\phi = g$ on the boundary Γ, we have

$$\| \boldsymbol{q} - \tilde{\boldsymbol{q}}_h \|^2_{\mathcal{T}_h} \leq \; C_\sigma(ocs^2_h(f, \mathcal{T}_h) + \eta^2_{1,h} + \eta^2_\phi).$$

We now take $\phi := \tilde{u}_h^* \in W_h^* \cap H^1(\Omega)$, where, by Lemma 4.4.2, the function $\tilde{u}_h^*$ satisfies

$$\tilde{u}_h^*|_\Gamma = g, \tag{4.4.5a}$$

$$\sum_{K\in\mathcal{T}_h} \| \boldsymbol{\nabla}(u_h^* - \tilde{u}_h^*) \|_K^2 \le C_j \sum_{e\in\mathcal{E}_h} h_e^{-1} \| [\![u_h^*]\!] \|_e^2. \tag{4.4.5b}$$

We immediately obtain that

$$\begin{aligned}
\eta_\phi^2 &:= \sum_{K\in\mathcal{T}_h} \| \tilde{\boldsymbol{q}}_h + \boldsymbol{\nabla}\, \tilde{u}_h^* \|_K^2 \\
&\le 2 \sum_{K\in\mathcal{T}_h} \| \tilde{\boldsymbol{q}}_h + \boldsymbol{\nabla}\, u_h^* \|_K^2 + 2 \sum_{K\in\mathcal{T}_h} \| \boldsymbol{\nabla}(u_h^* - \tilde{u}_h^*) \|_K^2 \\
&\le 2 \sum_{K\in\mathcal{T}_h} \| \tilde{\boldsymbol{q}}_h + \boldsymbol{\nabla}\, u_h^* \|_K^2 + 2\, C_j \sum_{e\in\mathcal{E}_h} h_e^{-1} \| [\![u_h^*]\!] \|_e^2,
\end{aligned}$$

by property (4.4.5b). Finally, by the orthogonality property of the projection $\mathsf{P}_{\mathsf{M}_0}$,

$$\begin{aligned}
\eta_\phi^2 &\le 2 \sum_{K\in\mathcal{T}_h} \| \tilde{\boldsymbol{q}}_h + \boldsymbol{\nabla}\, u_h^* \|_K^2 + 2\, C_j \Big(\sum_{e\in\mathcal{E}_h} h_e^{-1} \| (\mathsf{Id} - \mathsf{P}_{\mathsf{M}_0})\, [\![u_h^*]\!] \|_e^2 \\
&\qquad + \sum_{e\in\mathcal{E}_h} h_e^{-1} \| \mathsf{P}_{\mathsf{M}_0}\, [\![u_h^*]\!] \|_e^2 \Big) \\
&\le C \sum_{e\in\mathcal{E}_h} (\eta_{2,h}^2 + \eta_{3,h}^2),
\end{aligned}$$

and the result follows. This completes the proof of Theorem 4.2.1.

4.4.2 Proof of the local efficiency of the estimator, Theorem 4.2.2

To prove the efficiency of the estimator, Theorem 4.2.2, we show that each individual estimator is bounded by the error.

Proof of the efficiency of the estimator $\eta_{1,h}^2(e)$

In order to prove the local efficiency of the first estimator we need to construct proper test functions (associated with any given face or in the element) that will allow us to localize the error analysis.

We construct them as follows. We define the bubble function in the element K as $B_K = \Pi_{i=1}^{d+1} \lambda_i$,where λ_i denotes the linear function defined in K which vanishes on the

i-th face and equal 1 on the i-th node. We also define the bubble function associated to the face e as $B_e = \Pi_{\substack{i=1\\i\neq j}}^{d+1}\lambda_i$,where λ_j vanishes on the face e. The auxiliary result we are going to use is the following.

Lemma 4.4.3. *Given a face e of an element K, and a function $\psi \in \mathcal{P}_p(e)$, there exists a unique function $w \in \mathcal{P}_{p+d}(K)$ satisfying*

$$w = B_e\psi \qquad \text{on } \partial K, \tag{4.4.6a}$$

$$(w, \tilde{w})_K = 0 \qquad \forall\, \tilde{w} \in \mathcal{P}_{p-1}(K), \tag{4.4.6b}$$

$$\|\, w\,\|_K^2 \preceq h_e \|\, \psi\,\|_e^2. \tag{4.4.6c}$$

Proof. We first show that the number of degrees of freedom is equal to the number of equations. Indeed,

$$dim(\mathcal{P}_{p+d}(K)) = dim(\mathcal{P}_{p-1}(K)) + dim(\mathcal{P}^c_{k+d}(\partial K))$$

where $\mathcal{P}^c_{k+d}(\partial K)$ denotes all the polynomials in $\mathcal{P}_{p+d}(\partial K)$ which are continuous on ∂K. Thus, to show the existence of such a function w satisfying (4.4.6), we only need to prove that $w = 0$ when $B_e\psi = 0$. In fact, $B_e\psi = 0$ implies that $w|_{\partial K} = 0$. Hence, w can be written as

$$w = B_K\phi$$

for some $\phi \in \mathcal{P}_{p-1}(K)$. Now, taking the test function $\tilde{w} := \phi$ in the second equation (4.4.6b), we get

$$\int_K B_K\phi^2 = 0.$$

From the equation above, we deduce that $\phi = 0$ and hence that $w = 0$.

Finally, the estimate (4.4.6b) follows from a simple scaling argument. This completes the proof. □

With the auxiliary result just obtained, we are ready to prove the efficiency of the estimator $\eta^2_{1,h}(e)$. We begin by obtaining a first estimate of the term associated with the jumps of $\tilde{\boldsymbol{q}}_h$.

Lemma 4.4.4. *For any face $e \in \mathcal{E}_h$, we have that*

$$h_e\|\, [\![\tilde{\boldsymbol{q}}_h]\!]\,\|_e^2 \preceq \sum_{K\in\mathcal{U}_h(e)} (\|\, \boldsymbol{q} - \tilde{\boldsymbol{q}}_h\,\|_K^2 + h_K^2\|\, f - \nabla\cdot\tilde{\boldsymbol{q}}_h\,\|_K^2).$$

Proof. For the boundary edges, lemma follows immediately because by definition $[\![\tilde{\boldsymbol{q}}_h]\!] = 0$.

For the interior edges, we begin by noting that, for any $w \in H_0^1(\mathcal{U}_h(e))$, we have

$$\begin{aligned}
\langle [\![\tilde{\boldsymbol{q}}_h]\!], w\rangle_e &= \sum_{K\in\mathcal{U}_h(e)} \langle(\boldsymbol{q}-\tilde{\boldsymbol{q}}_h)\cdot\boldsymbol{n}, w\rangle_{\partial K} \\
&= \sum_{K\in\mathcal{U}_h(e)} \big((\boldsymbol{q}-\tilde{\boldsymbol{q}}_h, \boldsymbol{\nabla}\, w)_K + (f-\nabla\cdot\tilde{\boldsymbol{q}}_h, w)_K\big) \\
&\leq \sum_{K\in\mathcal{U}_h(e)} (\|\,\boldsymbol{q}-\tilde{\boldsymbol{q}}_h\,\|_K + h_K\|\, f-\nabla\cdot\tilde{\boldsymbol{q}}_h\,\|_K) \\
&\qquad\qquad \times (\|\,\boldsymbol{\nabla}\, w\,\|_K + h_K^{-1}\|\, w\,\|_K).
\end{aligned}$$

According to Lemma 4.4.3, for each element $K \in \mathcal{U}_h(e)$, there is a test function $w \in \mathcal{P}_{p+d}(K)$ such that

$$w = B_e\,[\![\tilde{\boldsymbol{q}}_h]\!] \quad \text{on } \partial K \quad \text{and} \quad \|w\|_K \preceq h_e^{1/2}\,\|B_e\,[\![\tilde{\boldsymbol{q}}_h]\!]\|_e.$$

Since this function lies in $H_0^1(\mathcal{U}_h(e))$, we can use it in the previous equation to obtain

$$\begin{aligned}
\int_e B_e\,[\![\tilde{\boldsymbol{q}}_h]\!]^2 \preceq &\sum_{K\in\mathcal{U}_h(e)} (\|\,\boldsymbol{q}-\tilde{\boldsymbol{q}}_h\,\|_K + h_K\|\, f-\nabla\cdot\tilde{\boldsymbol{q}}_h\,\|_K) \\
&\qquad\qquad \times h_K^{-1}\, h_e^{1/2}\,\|B_e\,[\![\tilde{\boldsymbol{q}}_h]\!]\|_e,
\end{aligned}$$

by an inverse inequality.

The result now easily follows from the fact that

$$\int_e B_e^2\ [\![\tilde{\boldsymbol{q}}_h]\!]^2 \preceq \int_e [\![\tilde{\boldsymbol{q}}_h]\!]^2 \preceq \int_e B_e\,[\![\tilde{\boldsymbol{q}}_h]\!]^2$$

and since $h_K^{-1}\, h_e^{1/2} \preceq h_e^{-1/2}$ by the shape-regularity assumption on the meshes. This completes the proof. $\square$

We also need the following auxiliary result which we can prove in a similar fashion by using the bubble functions introduced in Lemma 4.4.3.

Lemma 4.4.5. *For any element $K \in \mathcal{T}_h$, we have that*

$$h_K\|\,\mathsf{P}_W f - \nabla\cdot\tilde{\boldsymbol{q}}_h\,\|_K \preceq C(\|\,\boldsymbol{q}-\tilde{\boldsymbol{q}}_h\,\|_K + h_K\|\, f - \mathsf{P}_W f\,\|_K).$$

Proof. We begin by noting that, for any function $w \in H_0^1(K)$, we have

$$(f - \nabla\cdot \tilde{\boldsymbol{q}}_h, w)_K = -(\boldsymbol{q} - \tilde{\boldsymbol{q}}_h, \boldsymbol{\nabla}\, w)_K.$$

Taking $w = B_K(\mathsf{P}_W f - \nabla\cdot \tilde{\boldsymbol{q}}_h)$, we get

$$\begin{aligned}\int_K B_K(\mathsf{P}_W f - \nabla\cdot \tilde{\boldsymbol{q}}_h)^2 &= -(\boldsymbol{q} - \tilde{\boldsymbol{q}}_h, \boldsymbol{\nabla}\, w)_K - (f - \mathsf{P}_W f, w)_K \\ &\le (h_K^{-1} \| \boldsymbol{q} - \tilde{\boldsymbol{q}}_h \|_K + \| f - \mathsf{P}_W f \|_K) \\ &\quad \times (h_K \| \boldsymbol{\nabla}\, w \|_K + \| w \|_K) \\ &\le (h_K^{-1} \| \boldsymbol{q} - \tilde{\boldsymbol{q}}_h \|_K + \| f - \mathsf{P}_W f \|_K) \\ &\quad \times \| B_K(\mathsf{P}_W f - \nabla\cdot \tilde{\boldsymbol{q}}_h) \|_K,\end{aligned}$$

by an inverse inequality and a standard scaling argument.

Finally, the estimate follows by noting that

$$\| \mathsf{P}_W f - \nabla\cdot \tilde{\boldsymbol{q}}_h \|_K \simeq (\int_K B_K(\mathsf{P}_W f - \nabla\cdot \tilde{\boldsymbol{q}}_h)^2)^{1/2} \simeq \| B_K(\mathsf{P}_W f - \nabla\cdot \tilde{\boldsymbol{q}}_h) \|_K.$$

This completes the proof. $\square$

We can now easily see that

$$\begin{aligned}\eta_{1,h}^2(e) &:= h_e \| \, [\![\tilde{\boldsymbol{q}}_h]\!] \, \|_e^2 + \sum_{K\in\mathcal{U}_h(e)} h_K^2 \| \mathsf{P}_W f - \nabla\cdot \tilde{\boldsymbol{q}}_h \|_K^2 \\ &\preceq \sum_{K\in\mathcal{U}_h(e)} \left[\| \boldsymbol{q} - \tilde{\boldsymbol{q}}_h \|_K^2 + h_K^2 \| f - \nabla\cdot \tilde{\boldsymbol{q}}_h \|_K^2 + h_K^2 \| \mathsf{P}_W f - \nabla\cdot \tilde{\boldsymbol{q}}_h \|_K^2 \right],\end{aligned}$$

by Lemma 4.4.4. And, by Lemma 4.4.5,

$$\begin{aligned}\eta_{1,h}^2(e) &\preceq \sum_{K\in\mathcal{U}_h(e)} \left[\| \boldsymbol{q} - \tilde{\boldsymbol{q}}_h \|_K^2 + h_K^2 \| f - \mathsf{P}_W f \|_K^2 \right] \\ &\preceq \sum_{K\in\tilde{w}(e)} \| \boldsymbol{q} - \tilde{\boldsymbol{q}}_h \|_K^2 + osc_h^2(f, \mathcal{U}_h(e)).\end{aligned}$$

This shows the efficiency of the estimator $\eta_{1,h}^2(e)$ as stated in Theorem 4.2.2.

Proof of the efficiency of the estimator $\eta^2_{2,h}(e)$

Lemma 4.4.6. *For any face $e \in \mathcal{E}_h$,*

$$\| (\mathsf{Id} - \mathsf{P}_{\mathsf{M}_0}) [\![u_h^*]\!] \|_e^2 \preceq (\| \boldsymbol{q} - \tilde{\boldsymbol{q}}_h \|^2_{\mathcal{U}_h(e)} + \| \boldsymbol{\nabla} u - \boldsymbol{\nabla} u_h^* \|^2_{\mathcal{U}_h(e)}).$$

Moreover, for each element $K \in \mathcal{T}_h$, we have that

$$\| \tilde{\boldsymbol{q}}_h + \boldsymbol{\nabla} u_h^* \|_K \preceq \| \boldsymbol{q} - \tilde{\boldsymbol{q}}_h \|_K.$$

We refer the reader to Chapter 3 for detailed proofs of the above inequalities. Note that, as a consequence, we have that

$$\begin{aligned}
\eta^2_{2,h}(e) := h_e^{-1} \| (\mathsf{Id} - \mathsf{P}_{\mathsf{M}_0}) [\![u_h^*]\!] \|_e^2 + \sum_{K \in \mathcal{U}_h(e)} \| \tilde{\boldsymbol{q}}_h + \boldsymbol{\nabla} u_h^* \|_K^2 \\
\preceq \| \boldsymbol{q} - \tilde{\boldsymbol{q}}_h \|^2_{\mathcal{U}_h(e)} + \| \boldsymbol{\nabla} u - \boldsymbol{\nabla} u_h^* \|^2_{\mathcal{U}_h(e)} \\
\preceq \| \boldsymbol{q} - \tilde{\boldsymbol{q}}_h \|^2_{\mathcal{U}_h(e)} + \| \tilde{\boldsymbol{q}}_h + \boldsymbol{\nabla} u_h^* \|^2_{\mathcal{U}_h(e)} \\
\preceq \| \boldsymbol{q} - \tilde{\boldsymbol{q}}_h \|^2_{\mathcal{U}_h(e)},
\end{aligned}$$

and this shows the efficiency of the estimator $\eta^2_{2,h}(e)$ as stated in Theorem 4.2.2.

Proof of the efficiency of the estimator $\eta^2_{3,h}(e)$

To prove the efficiency of the last estimator, we are going to use the fact that, thanks to the form of the equations defining the HDG method (1.2.2), the residuals inside the elements are strongly connected with the residuals on their faces.

Lemma 4.4.7. *Suppose that condition* **A2** *is satisfied. Then, for any face $e \in \mathcal{E}_h$, we have*

$$\eta^2_{3,h}(e) := h_e^{-1} \| \mathsf{P}_{\mathsf{M}_0} [\![u_h^*]\!] \|^2_{0,e} \preceq \sum_{K \in \mathcal{U}_h(e)} \| \tilde{\boldsymbol{q}}_h + \boldsymbol{\nabla} u_h^* \|_K \leq \eta^2_{2,h}(e).$$

The proof of this fact is is similar to that of Lemma 3.3 in Chapter 3. For the convenience of the reader, we include a detailed proof.

Proof. Taking into account the first equation defining the post-processing u_h^*, (4.2.2a), condition **A2** can be rewritten as follows:

$$(\tilde{\boldsymbol{q}}_h, \boldsymbol{v})_K - (u_h^*, \nabla \cdot \boldsymbol{v})_K = -\langle \widehat{u}_h, \boldsymbol{v} \cdot \boldsymbol{n} \rangle_{\partial K} \quad \forall\, \boldsymbol{v} \in \mathrm{RT}_0(K).$$

This implies, after a simple integration by parts, that

$$(\tilde{\boldsymbol{q}}_h + \boldsymbol{\nabla}\, u_h^*, \boldsymbol{v})_K = -\langle \widehat{u}_h - u_h^*, \boldsymbol{v} \cdot \boldsymbol{n} \rangle_{\partial K}.$$

Now assume that $\boldsymbol{v} \in \boldsymbol{H}(\mathrm{div}, \mathcal{U}_h(e))$. Since $\widehat{u}_h$ is single valued on the faces, summing over all $K \in \mathcal{U}_h(e)$ yields,

$$\sum_{K \in \mathcal{U}_h(e)} (\tilde{\boldsymbol{q}}_h + \boldsymbol{\nabla}\, u_h^*, \boldsymbol{v})_K = - \sum_{\substack{F \in \partial K \setminus e, \\ K \in \mathcal{U}_h(e)}} \langle \widehat{u}_h - u_h^*, \boldsymbol{v} \cdot \boldsymbol{n} \rangle_F + \langle\, [\![u_h^*]\!], \boldsymbol{v} \rangle_e.$$

Taking $\boldsymbol{v} \in \mathrm{RT}_0(K)$, such that for each $K \in \mathcal{U}_h(e)$

$$\begin{aligned} \int_e \boldsymbol{v} \cdot \boldsymbol{n} &= \int_e \mathsf{P}_{\mathsf{M}_0}\, [\![u_h^*]\!] \cdot \boldsymbol{n}, && \text{for the face } e, \\ \int_F \boldsymbol{v} \cdot \boldsymbol{n} &= 0, && \text{for all } F \in \partial K \setminus e, \end{aligned}$$

we obtain

$$\| \, \mathsf{P}_{\mathsf{M}_0}\, [\![u_h^*]\!] \, \|_e^2 = \sum_{K \in \mathcal{U}_h(e)} (\tilde{\boldsymbol{q}}_h + \boldsymbol{\nabla}\, u_h^*, \boldsymbol{v})_K.$$

The lemma follows from the Cauchy-Schwarz inequality and a standard scaling argument

$$\| \, \boldsymbol{v} \, \|_K \preceq h_e^{1/2} \| \, \boldsymbol{v} \cdot \boldsymbol{n} \, \|_{\partial K}.$$

This completes the proof. $\square$

This completes the proof of Theorem 4.2.2.

4.5 Extensions

Let us end this paper by sketching the extension of the error analysis to nonconforming meshes. To do so, we combine the approaches proposed in [41] for the IP methods and in Chapter 3 for the hybridized mixed methods.

4.5.1 Notation and construction of the meshes

The mesh $\mathcal{T}_h$ is obtained from an initial conforming mesh $\mathcal{T}_h^{(0)}$ via a finite number of refinement steps. Let $\mathcal{T}_h^{(n)}$ be the *conforming* mesh obtained from $\mathcal{T}_h^{(0)}$ via n number of *uniform* refinement steps. We define the level of $K \in \mathcal{T}_h$ as n if $K \in \mathcal{T}_h^{(n)}$ and we denote it as $L(K) = n$. Let $\mathcal{T}_H$ be the largest conforming mesh such that $\mathcal{T}_h$ can be obtained from $\mathcal{T}_H$. We say an element $T \in \mathcal{T}_H$ is the conforming parent of an element $K \in \mathcal{T}_h$ if $K \subset T$. We also define the level of nonconformity as

$$L_n(K) = L(K) - L(T).$$

We denote $\partial\mathcal{T}_h$ as the set of faces of all elements $K \in \mathcal{T}_h$ and

$$\mathcal{F}_h := \{e \in \partial\mathcal{T}_h\ ,\ e \cap \partial K \text{ is a complete face of } K \text{ if } m_{d-1}(e \cap \partial K) > 0\ \}.$$

Fig. 4.5.1 illustrates the faces in $\mathcal{F}_h$ in two space dimensions. For every face $e \in \mathcal{F}_h$, set $n := \min\{L(K)\ : K \in \mathcal{U}_h(e)\,\}$ and $m := \max\{L(K)\ : K \in \mathcal{U}_h(e)\,\}$. We denote

$$\tilde{\mathcal{W}}_h(e) := \{K_1, K_2 \in \mathcal{T}_h^{(n)}\ : e \text{ is a shared face of } K_1 \text{ and } K_2\ \}.$$

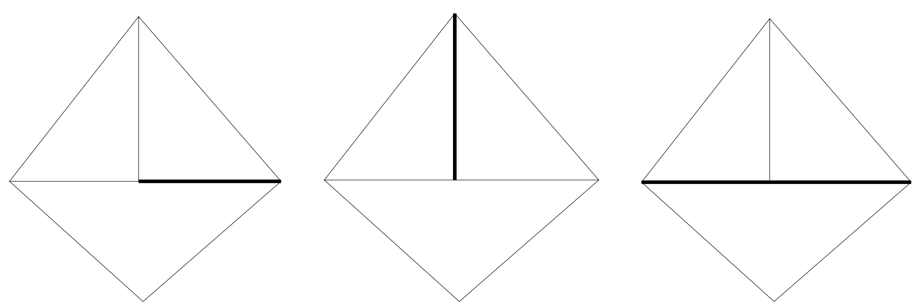

Figure 4.5.1: Example of nonconforming meshes II

4.5.2 Assumption on the meshes

We make the following assumption on the meshes:

D : *The level of nonconformity of* $\mathcal{T}_h$ *remains bounded.*

4.5.3 A posteriori error estimates

Assuming that the HDG methods are well defined [34], our goal is to estimate the error $\| \boldsymbol{q} - \tilde{\boldsymbol{q}}_h \|^2_{\mathcal{T}_h}$ in term of the following estimator

$$\eta_h^2 := \sum_{e \in \mathcal{F}_h} \big(\eta^2_{1,h}(e) + \eta^2_{2,h}(e) + \eta^2_{3,\mathcal{F}_h}(e) + \eta^2_{nc,h}(e)\big),$$

where

$$\begin{aligned}
\eta^2_{1,h}(e) : &= h_e \| \, [\![\tilde{\boldsymbol{q}}_h]\!] \, \|^2_e + \sum_{K \in \mathcal{U}_h(e)} h_K^2 \| \, \mathsf{P}_W f - \nabla \cdot \tilde{\boldsymbol{q}}_h \, \|^2_K, \\
\eta^2_{2,h}(e) : &= h_e^{-1} \| \, (\mathsf{Id} - \mathsf{P}_{\mathsf{M}_0}) \, [\![u_h^*]\!] \, \|^2_e + \sum_{K \in \mathcal{U}_h(e)} \| \, \tilde{\boldsymbol{q}}_h + \boldsymbol{\nabla} \, u_h^* \, \|^2_K, \\
\eta^2_{3,\mathcal{F}_h}(e) : &= h_e^{-1} \| \, \mathsf{P}_{\mathcal{M}_0} \, [\![u_h^*]\!] \, \|^2_e, \\
\eta^2_{nc,h}(e) : &= h_e^{-1} \| \, (\mathsf{P}_{\mathsf{M}_0} - \mathsf{P}_{\mathcal{M}_0}) \, [\![u_h^*]\!] \, \|^2_e.
\end{aligned}$$

Here, $\mathsf{P}_{\mathsf{M}_0}$ is the L^2-orthogonal projection into the space

$$\mathsf{M}_{0,h} := \{\mu \in L^2(\partial \mathcal{T}_h), \, \mu|_e \in \mathcal{P}_0(e), \text{ for each face } e \in \mathcal{E}_h\},$$

and $\mathsf{P}_{\mathcal{M}_0}$ the L^2-orthogonal projection into the space

$$\mathcal{M}_{0,h} := \{\mu \in L^2(\partial \mathcal{T}_h), \, \mu|_e \in \mathcal{P}_0(e), \text{ for each face } e \in \mathcal{F}_h \ \}.$$

Because of the nonconformity of the meshes, $\mathcal{E}_h$ is not necessarily equal to $\mathcal{F}_h$. Note that the estimator $\eta_{nc,h}(e)$ explicitly captures the effects of the nonconformity on the meshes.

Theorem 4.5.1. *Suppose that the assumptions* **B** *and* **D** *on the meshes and the assumption* **C** *on the boundary condition are satisfied. Suppose also that $\tilde{\boldsymbol{q}}_h$ satisfies conditions* **A1** *and* **A3**. *Then*

$$\| \, \boldsymbol{q} - \tilde{\boldsymbol{q}}_h \, \|^2_{\mathcal{T}_h} \preceq \eta_h^2 + osc_h^2(f, \mathcal{T}_h),$$

and for each $e \in \mathcal{F}_h$,

$$\begin{aligned}
\eta^2_{1,h}(e) &\preceq \sum_{K \in \mathcal{U}_h(e)} \| \, \boldsymbol{q} - \tilde{\boldsymbol{q}}_h \, \|^2_K + osc_h^2(f, \mathcal{U}_h(e)), \\
\eta^2_{2,h}(e) + \eta^2_{nc,h}(e) &\preceq \sum_{K \in \tilde{\mathcal{W}}_h(e)} \| \, \boldsymbol{q} - \tilde{\boldsymbol{q}}_h \, \|^2_K.
\end{aligned}$$

Moreover, if $\tilde{\boldsymbol{q}}_h$ satisfies condition **A2***, then for each $e \in \mathcal{F}_h$*

$$\eta^2_{3,\mathcal{F}_h}(e) \preceq \eta^2_{2,h}(e).$$

4.5.4 Sketch of the proof

To establish the reliability and efficiency of the above estimator, we follow the lines in the proof for conforming meshes. Since most of the results established in Section 4 can be trivially extended to the case of nonconforming meshes, here we only emphasize on the main modifications.

To prove the reliability of the estimator, we only need to check that Lemma 4.4.1, Lemma 4.4.2 and the proof of Theorem 4.2.1 hold for nonconforming meshes. The following modifications are required to extend the results in Section 4 to nonconforming meshes:

- Lemma 4.4.2 can be extended to the nonconforming meshes . We refer the reader to [41] and [54] for more details.
- To prove Lemma 4.4.1, we only need to construct an interpolation from $H^1(\Omega)$ to the space of continuous piecewise linear polynomials $W^c_{1,h}$ on the nonconforming meshes $\mathcal{T}_h$ satisfying
  1. $\Pi\psi = 0$ on the boundary Γ if $\psi \in H^1_0(\Omega)$.
  2. $\sum_{K\in\mathcal{T}_h} h_K^{-2} \| \psi - \Pi\psi \|^2_K \preceq \| \boldsymbol{\nabla} \psi \|^2_\Omega$.

To construct such an interpolation, we consider the Scott-Zhang interpolation on $\mathcal{T}_H$, where $\mathcal{T}_H$ is the largest conforming mesh such that $\mathcal{T}_h$ can be obtained from $\mathcal{T}_H$. It is easy to see that such an interpolation preserves the homogeneous boundary condition. Moreover, let $T \in \mathcal{T}_H$ be the conforming parent of $K \in \mathcal{T}_h$. In view of the bounded level of nonconformity (Assumption **C**), we have

$$\sum_{K\subset T} h_K^{-2} \| \psi - \Pi\psi \|^2_K \preceq h_T^{-2} \| \psi - \Pi\psi \|^2_T$$

where the hidden constant depends on the level of nonconformity. Invoking the approximation property of Scott-Zhang interpolation on the conforming mesh $\mathcal{T}_H$, we obtain

$$\sum_{K\in\mathcal{T}_h} h_K^{-2} \| \psi - \Pi\psi \|^2_K \preceq \sum_{T\in\mathcal{T}_H} h_T^{-2} \| \psi - \Pi\psi \|^2_T \preceq \| \boldsymbol{\nabla} \psi \|^2_\Omega.$$

This verifies the approximation property.

With these modifications, it is easy to check that these proofs hold for nonconforming meshes as well.

On the other hand, to prove the efficiency of the estimator, we need to check that Lemma 4.4.4, Lemma 4.4.5, Lemma 4.4.6 and Lemma 4.4.7 hold.

- For the proof of Lemma 4.4.6 and Lemma 4.4.7 on nonconforming meshes, we refer the reader to Chapter 3 .
- Lemma 4.4.5 holds automatically because hanging nodes are not involved.
- We modify the proof of Lemma 4.4.4 as follows.

Proof of Lemma 4.4.4. We consider the two neighbouring elements $K^+, K^- \in \mathcal{U}_h(e)$ for each $e \in \mathcal{E}_h^i$.

If e is the shared face of K^+ and K^-, as illustrated in Fig. 4.5.1 (middle), then the results follows immediately from the conforming case.

Otherwise, e is a face of K^-, but not a face of K^+, as illustrated in Fig. 4.5.1 (left). In this case, we artificially divide K^+ into smaller elements $\{K_i^+\}$ via several refinement steps such that one of these smaller elements, denoted as K_1^+, shares the face e with K^- as shown in Fig. 4.5.2. We set $\mathcal{U}_h^*(e) := \{K^-, K_1^+\}$. From the results of the

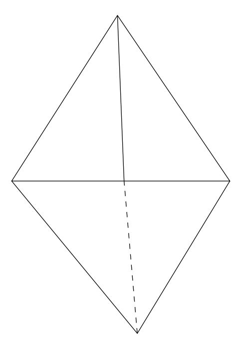

Figure 4.5.2: Example of an artificial refinement.

conforming case and the fact that $\mathcal{U}_h^*(e) \subset \mathcal{U}_h(e)$, we have

$$
\begin{aligned}
h_e \| \, [\![\tilde{\boldsymbol{q}}_h]\!] \, \|_e^2 &\preceq \sum_{K \in \mathcal{W}_h^*(e)} (\| \, \boldsymbol{q} - \tilde{\boldsymbol{q}}_h \, \|_K^2 + h_K^2 \| \, f - \nabla \cdot \tilde{\boldsymbol{q}}_h \, \|_K^2) \\
&\preceq \sum_{K \in \mathcal{U}_h(e)} (\| \, \boldsymbol{q} - \tilde{\boldsymbol{q}}_h \, \|_K^2 + h_K^2 \| \, f - \nabla \cdot \tilde{\boldsymbol{q}}_h \, \|_K^2).
\end{aligned}
$$

This completes the proof. □

It is easy to check that Proposition 4.6.1 holds for nonconforming meshes as well.

4.6 Obtaining other equivalent estimator

In this section, we show how to deduce from our results, well known a posteriori error estimates for mixed methods as well as new a posteriori error estimates for the LDG-H method.

4.6.1 Equivalent Estimators

To do that, we introduce the following estimators:

$$
\eta_{4,h}^2(e) := h_e \| \, [\![\tilde{\boldsymbol{q}}_h]\!]_t \, \|_e^2 + \sum_{K \in \mathcal{U}_h(e)} h_K^2 \| \, \boldsymbol{\nabla} \times \tilde{\boldsymbol{q}}_h \, \|_K^2, \tag{4.6.1a}
$$

$$
\eta_{5,h}^2(e) := h_e \| \, (\boldsymbol{q}_h - \widehat{\boldsymbol{q}}_h) \cdot \boldsymbol{n} \, \|_e^2. \tag{4.6.1b}
$$

The relevant relations between these estimators and the estimators used in our main theorems are contained in the next result.

Proposition 4.6.1 (Relation between the error estimators)**.** *Assume that the assumption* **B** *on the meshes is satisfied. Then, for each face $e \in \mathcal{E}_h$,*

$$
\eta_{2,h}^2(e) \simeq \eta_{4,h}^2(e),
$$

If $\tilde{\boldsymbol{q}}_h = \boldsymbol{q}_h$, then

$$
\eta_{1,h}^2(e) \preceq \sum_{K \in \mathcal{U}_h(e)} \eta_{5,h}^2(\partial K),
$$

and for each $K \in \mathcal{T}_h$,

$$\| \boldsymbol{q}_h + \boldsymbol{\nabla} u_h \|_K^2 \preceq \sum_{e\in\partial K} h_e^{-1} \| \widehat{u}_h - u_h \|_e^2.$$

Proof. The last two inequalities of Proposition 4.6.1 were established in Chapter 2, Lemma 3.3. Here, we only prove the first relation, that is

$$\eta_{2,h}^2(e) \simeq \eta_{4,h}^2(e).$$

The proof is carried out in four steps.

Step One

We begin by showing that

$$\| \tilde{\boldsymbol{q}}_h + \boldsymbol{\nabla} u_h^* \|_K^2 \simeq h_K^2 \| \boldsymbol{\nabla}\times \tilde{\boldsymbol{q}}_h \|_K^2.$$

From the equation defining the scalar post-processing (4.2.2b), we note that $\boldsymbol{\nabla} u_h^*$ is determined entirely by $\boldsymbol{q}_h$. Hence, it is easy to check that $\boldsymbol{q}_h + \boldsymbol{\nabla} u_h^*$ can be viewed as a linear map of $\boldsymbol{q}_h$. Since $\tilde{\boldsymbol{q}}_h$ lies in the finite dimensional space $\boldsymbol{V}(K)$, a standard scaling argument allows us to conclude that we only need to show that $\| \tilde{\boldsymbol{q}}_h + \boldsymbol{\nabla} u_h^* \|_K^2$ vanishes whenever $h_K^2 \| \boldsymbol{\nabla}\times \tilde{\boldsymbol{q}}_h \|_K^2$ equals zero and vice versa.

Assume that $\boldsymbol{\nabla}\times \tilde{\boldsymbol{q}}_h = \boldsymbol{0}$. Then from the definition of u_h^*, (4.2.2), and the inclusion property (4.2.1c), we have $\tilde{\boldsymbol{q}}_h + \boldsymbol{\nabla} u_h^* = \boldsymbol{0}$. On the other hand, if $\tilde{\boldsymbol{q}}_h = -\boldsymbol{\nabla} u_h^*$, then $\boldsymbol{\nabla}\times \tilde{\boldsymbol{q}}_h = \boldsymbol{\nabla}\times \boldsymbol{\nabla} u_h^* = \boldsymbol{0}$.

Step Two

Next, we show that

$$h_e^{-1} \| (\mathsf{Id} - \mathsf{P}_{\mathsf{M}_0}) [\![u_h^*]\!] \|_e^2 \simeq h_e \| [\![\boldsymbol{\nabla} u_h^*]\!]_t \|_e^2.$$

Since $[\![u_h^*]\!]$ lies in a finite dimensional space, by a standard scaling argument, we only need to show that if one term vanishes, then the other term vanishes too.

Recall that, by definition,

$$\begin{aligned}
[\![\boldsymbol{\nabla} u_h^*]\!]_t &:= (\boldsymbol{\nabla} u_h^*)^+ \times \boldsymbol{n}^+ + (\boldsymbol{\nabla} u_h^*)^- \times \boldsymbol{n}^- \\
&= (\boldsymbol{\nabla}_{\boldsymbol{\Gamma}} u_h^*)^+ \times \boldsymbol{n}^+ + (\boldsymbol{\nabla}_{\boldsymbol{\Gamma}} u_h^*)^- \times \boldsymbol{n}^- \\
&= \boldsymbol{\nabla}_{\boldsymbol{\Gamma}}((u_h^*)^+ - (u_h^*)^-) \times \boldsymbol{n}^+,
\end{aligned}$$

where $\boldsymbol{\nabla}_{\boldsymbol{\Gamma}}$ denotes the surface gradient on the face e. Thus, if $[\![\boldsymbol{\nabla}\, u_h^*]\!]_t = \mathbf{0}$ on the face e, then $\boldsymbol{\nabla}_{\boldsymbol{\Gamma}}((u_h^*)^+ - (u_h^*)^-) = \mathbf{0}$ and so $(u_h^*)^+ - (u_h^*)^-$ is constant across the face. This implies that $(\mathsf{Id} - \mathsf{P}_{\mathsf{M}_0})\, [\![u_h^*]\!] = \mathbf{0}$ therein. On the other hand, if $(\mathsf{Id} - \mathsf{P}_{\mathsf{M}_0})\, [\![u_h^*]\!] = \mathbf{0}$, then $(u_h^*)^+ - (u_h^*)^-$ is constant on the face e. Hence we have $[\![\boldsymbol{\nabla}\, u_h^*]\!]_t = \mathbf{0}$.

Step Three

Let us now show that $\eta_{4,h}^2(e) \preceq \eta_{2,h}^2(e)$. Since

$$\begin{aligned}\eta_{4,h}^2(e) &:= h_e \|\, [\![\tilde{\boldsymbol{q}}_h]\!]_t \,\|_e^2 + \sum_{K \in \mathcal{U}_h(e)} h_K^2 \|\, \boldsymbol{\nabla}\times \tilde{\boldsymbol{q}}_h \,\|_K^2 \\ &\preceq h_e \|\, [\![\tilde{\boldsymbol{q}}_h]\!]_t \,\|_e^2 + \sum_{K \in \mathcal{U}_h(e)} \|\, \tilde{\boldsymbol{q}}_h + \boldsymbol{\nabla}\, u_h^* \,\|_K^2,\end{aligned}$$

by Step one, we only need to show that

$$h_e \|\, [\![\tilde{\boldsymbol{q}}_h]\!]_t \,\|_e^2 \preceq h_e^{-1} \|\, (\mathsf{Id} - \mathsf{P}_{\mathsf{M}_0})\, [\![u_h^*]\!] \,\|_e^2 + \sum_{K \in \mathcal{U}_h(e)} \|\, \tilde{\boldsymbol{q}}_h + \boldsymbol{\nabla}\, u_h^* \,\|_K^2 =: \eta_{2,h}^2(e).$$

To do that, we add and subtract $\boldsymbol{\nabla}\, u_h^*$, and apply Cauchy-Schwartz and the triangle inequalities to get

$$\begin{aligned}h_e \|\, [\![\tilde{\boldsymbol{q}}_h]\!]_t \,\|_e^2 &\preceq h_e \|\, [\![\boldsymbol{\nabla}\, u_h^*]\!]_t \,\|_e^2 + h_e \|\, [\![\tilde{\boldsymbol{q}}_h + \boldsymbol{\nabla}\, u_h^*]\!]_t \,\|_e^2 \\ &\preceq h_e^{-1} \|\, (\mathsf{Id} - \mathsf{P}_{\mathsf{M}_0})\, [\![u_h^*]\!] \,\|_e^2 + h_e \|\, [\![\tilde{\boldsymbol{q}}_h + \boldsymbol{\nabla}\, u_h^*]\!]_t \,\|_e^2,\end{aligned}$$

by Step Two. Then, by a standard scaling argument,

$$h_e \|\, [\![\tilde{\boldsymbol{q}}_h]\!]_t \,\|_e^2 \preceq h_e^{-1} \|\, (\mathsf{Id} - \mathsf{P}_{\mathsf{M}_0})\, [\![u_h^*]\!] \,\|_e^2 + \sum_{K \in \mathcal{U}_h(e)} \|\, \tilde{\boldsymbol{q}}_h + \boldsymbol{\nabla}\, u_h^* \,\|_K^2,$$

as wanted.

Step Four

It remains to prove that $\eta_{2,h}^2(e) \preceq \eta_{4,h}^2(e)$. Since

$$\begin{aligned}\eta_{2,h}^2(e) &:= h_e^{-1} \|\, (\mathsf{Id} - \mathsf{P}_{\mathsf{M}_0})\, [\![u_h^*]\!] \,\|_e^2 + \sum_{K \in \mathcal{U}_h(e)} \|\, \tilde{\boldsymbol{q}}_h + \boldsymbol{\nabla}\, u_h^* \,\|_K^2 \\ &\preceq h_e \|\, [\![\boldsymbol{\nabla}\, u_h^*]\!]_t \,\|_e^2 + \sum_{K \in \mathcal{U}_h(e)} h_K^2 \|\, \boldsymbol{\nabla}\times \tilde{\boldsymbol{q}}_h \,\|_K^2.\end{aligned}$$

Adding and subtracting $\tilde{\boldsymbol{q}}_h$ in the first term, we get

$$\begin{aligned} h_e^{-1} \| (\mathsf{Id} - \mathsf{P}_{\mathsf{M}_0}) [\![u_h^*]\!] \|_e^2 &\preceq h_e \| [\![\tilde{\boldsymbol{q}}_h]\!]_t \|_e^2 + h_e \| [\![\tilde{\boldsymbol{q}}_h + \boldsymbol{\nabla} u_h^*]\!]_t \|_e^2 \\ &\preceq h_e \| [\![\tilde{\boldsymbol{q}}_h]\!]_t \|_e^2 + \sum_{K \in \mathcal{U}_h(e)} \| \tilde{\boldsymbol{q}}_h + \boldsymbol{\nabla} u_h^* \|_K^2 \\ &\preceq h_e \| [\![\tilde{\boldsymbol{q}}_h]\!]_t \|_e^2 + \sum_{K \in \mathcal{U}_h(e)} h_K^2 \| \boldsymbol{\nabla} \times \tilde{\boldsymbol{q}}_h \|_K^2, \end{aligned}$$

by Step One. This completes the proof of Proposition 4.6.1.

□

Now we are ready to recover a well-known result for the mixed methods.

4.6.2 The mixed-H methods

Whenever we have that $\widehat{\boldsymbol{q}}_h := \boldsymbol{q}_h$, we say that the method defined by our general formulation is the hybridized version of a mixed method and we refer to it as a mixed-H method. The main examples are the well known RT and BDM methods. For any of these mixed-H methods, we have the following result.

Corollary 4.6.1. *Suppose assumptions* **B** *and* **C** *are satisfied. Suppose also that* $\boldsymbol{V}(K) \supset \mathrm{RT}_0(K)$ *and* $W(K) \supset \mathcal{P}_1(K)$ *for all* $K \in \mathcal{T}_h$, *and that* $\mathsf{M}(e) \supset \mathcal{P}_1(e)$ *for all* $e \in \mathcal{E}_h$. *Then for mixed-H methods, we have that*

$$\| \boldsymbol{q} - \boldsymbol{q}_h \|_{\mathcal{T}_h}^2 \preceq \sum_{e \in \mathcal{E}_h} \eta_{4,h}^2(e) + osc_h^2(f, \mathcal{T}_h).$$

Moreover, for each face $e \in \mathcal{E}_h$,

$$\eta_{4,h}^2(e) \preceq \sum_{K \in \mathcal{U}_h(e)} \| \boldsymbol{q} - \boldsymbol{q}_h \|_K^2,$$

where

$$\eta_{4,h}^2(e) := h_e \| [\![\boldsymbol{q}_h]\!]_t \|_e^2 + \sum_{K \in \mathcal{U}_h(e)} h_K^2 \| \boldsymbol{\nabla} \times \boldsymbol{q}_h \|_K^2.$$

Remark 4.6.1. *The corollary recovers the well known result of [6] by A. Alonso. Note, however, that, while the estimate of [6] was established only for* $d = 2$ *space dimensions, the above corollary shows that the estimate actually holds for* $d = 2, 3$ *space dimensions.*

4.6.3 The LDG-H method

To end, we propose several a posteriori error estimates for the LDG-H method based on different choices for $\tilde{\boldsymbol{q}}_h$. We also obtain an a posteriori estimate for an *energy-like* norm.

The choice $\tilde{\boldsymbol{q}}_h := \boldsymbol{q}_h^*$

Corollary 4.6.2. *Suppose assumptions* **B** *and the boundary condition assumption* **C** *are satisfied. Suppose also that $\mathcal{P}_1(K) \subset W(K)$, $\boldsymbol{\mathcal{P}}_2(K) \subset \boldsymbol{V}(K)$ for all $K \in \mathcal{T}_h$, and that $\mathcal{P}_1(e) \subset \mathsf{M}(e)$ for all $e \in \mathcal{E}_h$. Then for the LDG-H methods, we have that*

$$\| \boldsymbol{q} - \boldsymbol{q}_h^* \|_{\mathcal{T}_h}^2 \preceq \sum_{e \in \mathcal{E}_h} \eta_{4,h}^2(e) + osc_h^2(f, \mathcal{T}_h).$$

Moreover, for each face $e \in \mathcal{E}_h$,

$$\eta_{4,h}^2(e) \preceq \sum_{K \in \mathcal{U}_h(e)} \| \boldsymbol{q} - \boldsymbol{q}_h^* \|_K^2,$$

where

$$\eta_{4,h}^2(e) := h_e \| \, [\![\boldsymbol{q}_h^*]\!]_t \|_e^2 + \sum_{K \in \mathcal{U}_h(e)} h_K^2 \| \, \boldsymbol{\nabla} \times \boldsymbol{q}_h^* \|_K^2.$$

The choice $\tilde{\boldsymbol{q}}_h := \boldsymbol{q}_h$

Corollary 4.6.3 (Estimate of L^2-error)**.** *Suppose assumptions* **B** *and* **C** *are satisfied. Suppose also that $\boldsymbol{V}(K) \supset \mathrm{RT}_0(K)$, $W(K) \supset \mathcal{P}_1(K)$ for all $K \in \mathcal{T}_h$, and that $\mathsf{M}(e) \supset \mathcal{P}_1(e)$ for all $e \in \mathcal{E}_h$. Then for the LDG-H methods, we have that*

$$\| \boldsymbol{q} - \boldsymbol{q}_h \|_{\mathcal{T}_h}^2 \preceq (\sum_{e \in \mathcal{E}_h} \eta_{1,h}^2(e) + \sum_{e \in \mathcal{E}_h} \eta_{4,h}^2(e)) + osc_h^2(f, \mathcal{T}_h).$$

Moreover, for each face $e \in \mathcal{E}_h$,

$$\eta_{1,h}^2(e) + \eta_{4,h}^2(e) \preceq \sum_{K \in \mathcal{U}_h(e)} \| \boldsymbol{q} - \boldsymbol{q}_h \|_K^2 + osc_h^2(f, \mathcal{U}_h(e)),$$

where

$$\eta_{1,h}^2(e) := h_e \| \, [\![\boldsymbol{q}_h]\!] \, \|_e^2 + \sum_{K \in \mathcal{U}_h(e)} h_K^2 \| \, \mathsf{P}_W f - \nabla \cdot \boldsymbol{q}_h \, \|_K^2,$$

$$\eta_{4,h}^2(e) := h_e \| \, [\![\boldsymbol{q}_h]\!]_t \, \|_e^2 + \sum_{K \in \mathcal{U}_h(e)} h_K^2 \| \, \boldsymbol{\nabla} \times \boldsymbol{q}_h \, \|_K^2.$$

To end, we also derive an a posteriori error estimate for the following energy-like norm

$$E_h^2 := \| \, \boldsymbol{q} - \boldsymbol{q}_h \, \|_{\mathcal{T}_h}^2 + \beta \sum_{e \in \mathcal{E}_h} h_e \| \, (\boldsymbol{q}_h - \widehat{\boldsymbol{q}}_h) \cdot \boldsymbol{n} \, \|_e^2,$$

where β is some given parameter.

Corollary 4.6.4 (Estimate of an *energy-like* norm)**.** *Suppose assumptions* **B** *and* **C** *are satisfied. Suppose also that* $\boldsymbol{V}(K) \supset \mathrm{RT}_0(K)$*,* $W(K) \supset \mathcal{P}_1(K)$ *for all* $K \in \mathcal{T}_h$*, and that* $\mathsf{M}(e) \supset \mathcal{P}_1(e)$ *for all* $e \in \mathcal{E}_h$*. Then for the LDG-H methods,*

$$E_h^2 \preceq \Big(\sum_{e \in \mathcal{E}_h} \eta_{4,h}^2(e) + \sum_{e \in \mathcal{E}_h} \eta_{5,h}^2(e) \Big) + osc_h^2(f, \mathcal{T}_h).$$

Moreover, for each face $e \in \mathcal{E}_h$*,*

$$\eta_{4,h}^2(e) + \eta_{5,h}^2(e) \preceq \sum_{K \in \mathcal{U}_h(e)} \| \, \boldsymbol{q} - \boldsymbol{q}_h \, \|_K^2 + \beta h_e \| \, (\boldsymbol{q}_h - \widehat{\boldsymbol{q}}_h) \cdot \boldsymbol{n} \, \|_e^2,$$

where

$$\eta_{4,h}^2(e) := h_e \| \, [\![\boldsymbol{q}_h]\!]_t \, \|_e^2 + \sum_{K \in \mathcal{U}_h(e)} h_K^2 \| \, \boldsymbol{\nabla} \times \boldsymbol{q}_h \, \|_K^2,$$

$$\eta_{5,h}^2(e) := h_e \| \, (\boldsymbol{q}_h - \widehat{\boldsymbol{q}}_h) \cdot \boldsymbol{n} \, \|_e^2.$$

Chapter 5

Convergence and quasi-optimality of AHDG methods

5.1 Introduction

In this chapter, we establish the convergence and optimality of the AHDG methods for the model problem (1.1.1a) with homogeneous boundary condition, that is, $g = 0$ on Γ.

Let us briefly comment on the main difficulties to prove these results. A usual ingredient to establish the convergence of adaptive methods is an orthogonality identity involving the energy norm. Given the structure of the HDG methods, such property does not seem to be readily available. On the other hand, given the similarity of the HDG methods and the mixed methods, we could instead use a quasi-orthogonality property as done by Chen, Holst and Xu [31]. Unfortunately, unlike mixed methods, the approximate flux $\boldsymbol{q}_k$ is not $\boldsymbol{H}(\mathrm{div}, \Omega)$-conforming and extra effort is needed to be able to suitably control the nonconforming part of $\boldsymbol{q}_k$.

The main difficulty to prove the optimality is to establish a "discrete" upper bound for the a posteriori error estimator. While such an estimation was established by Chen, Holst and Xu [31] for the Raviart-Thomas mixed methods in the case bidimensional case, no results are known for the tridimensional case. Our approach to overcome this difficulty is to use an auxiliary estimator proposed in chapter 4. The construction of such an estimator is based on an element-by-element post-processing of the scalar variable which is closely associated with the flux approximation $\boldsymbol{q}_k$. Thanks to the auxiliary estimator, we are able to establish a localized upper bound for the multidimensional case.

The rest of this chapter is organized as follows. In Section 2, we describe the AHDG methods and state and briefly discuss out main results, namely, the contraction of the quasi-error and the quasi-optimality of its rate of convergence. In Section 3, we provide a sketch of the proofs of these results in order to render clear their main steps. We then provide the corresponding detailed proofs in Section 4, for the contraction of the quasi-error, and in Section 5, for the quasi-optimality of its rate of convergence.

5.2 Main Results

5.2.1 Adaptive Procedure

We use the adaptive procedure consisting of the loops of the form

$$\text{SOLVE} \rightarrow \text{ESTIMATE} \rightarrow \text{MARK} \rightarrow \text{REFINE}. \tag{5.2.1}$$

Let $\{\mathcal{T}_k\}_{k\geq 0}$ and $\{\boldsymbol{q}_k\}_{k\geq 0}$ be the meshes and the corresponding flux approximations obtained from the iteration above, respectively. Set $f_k = \mathsf{P}_{W_k} f$, where P_{W_k} is the L^2 projection into the space W_k. Next, we discuss each of these four modules in the following subsection.

The Module SOLVE

Given a mesh $\mathcal{T}_k$, the module SOLVE seeks an approximation $(\boldsymbol{q}_k, u_k, \widehat{u}_k)$ satisfying the discrete HDG formulation (1.2.2):

$$\text{SOLVE}(f_k, \mathcal{T}_k) := (\boldsymbol{q}_k, u_k, \widehat{u}_k).$$

We make the following assumptions on the stabilization function τ_K on each $K \in \mathcal{T}_k$:

A1 The parameter τ_K is a positive constant on ∂K.

A2 If $K \supset T \in \mathcal{T}_{k+1}$, then $\tau_T = \tau_K$.

A3 $\tau_K h_K \leq C_\tau$ for some constant C_τ.

Let us point out that the first assumption is not absolutely necessary, but allows us to simplify the proofs by relating liftings of the residuals on the boundaries of the elements to the residuals in their interior. Indeed, thanks to **A1**, we can show the equivalence

$$h_K \| (\widehat{\boldsymbol{q}}_k - \boldsymbol{q}_k) \cdot \boldsymbol{n} \|_{\partial K}^2 \simeq h_K^2 \| \mathsf{P}_{W_k}^{\perp}(f_k - \nabla\cdot \boldsymbol{q}_k) \|_K^2 + \tau_K^2 h_K^2 \| \mathsf{P}_{\mathbf{V_k}}^{\perp}(\boldsymbol{q}_k + \boldsymbol{\nabla}\, u_k) \|_K^2, \tag{5.2.2}$$

see Lemma 5.6.1. Here, we denote $\mathsf{P}_{\mathbf{V}_k}^{\perp} := (\mathsf{Id} - \mathsf{P}_{\widetilde{\mathbf{V}}_k})$ and $\mathsf{P}_{W_k}^{\perp} := (\mathsf{Id} - \mathsf{P}_{\widetilde{W}_k})$ where $\mathsf{P}_{\widetilde{\mathbf{V}}_k}$ and $\mathsf{P}_{\widetilde{W}_k}$ are the L^2 orthogonal projection onto the space

$$\widetilde{\boldsymbol{V}}_k := \{\boldsymbol{v} \in \boldsymbol{\mathcal{P}}_{p-1}(K) \text{ for all } K \in \mathcal{T}_k\}, \tag{5.2.3a}$$

$$\widetilde{W}_k := \{w \in \mathcal{P}_{p-1}(K) \text{ for all } K \in \mathcal{T}_k\}, \tag{5.2.3b}$$

respectively. Thanks to this equivalence, the residual on the faces can still be evaluated on a refinement of $\mathcal{T}_k$ even though $\widehat{\boldsymbol{q}}_k$ may not be defined on the new faces.

The second assumption states, roughly speaking, that the elements inherit the value of τ from its 'parent'. This assumption is consistent with the a priori bounds obtained in [35, 38] which state that optimal converge for the energy norm are achieved whenever the functions τ and τ^{-1} are positive and uniformly bounded. Note also that if the third assumption is satisfied for the initial mesh $\mathcal{T}_0$, it is automatically satisfied by all the meshes thanks to the second assumption.

The Module ESTIMATE

Given the data f, a mesh $\mathcal{T}_k$ and the approximate solution $(\boldsymbol{q}_k, u_k, \widehat{u}_k) = \text{SOLVE}(f_k, \mathcal{T}_k)$, the module ESTIMATE outputs the error estimator

$$\text{ESTIMATE}(f, \boldsymbol{q}_k, \mathcal{T}_k) := \{\zeta^2(f, \boldsymbol{q}_k, K)\}_{K\in\mathcal{T}_k},$$

defined by

$$\zeta^2(f, \boldsymbol{q}_k, K) := \zeta_{curl}^2(\boldsymbol{q}_k, K) + \zeta_{div}^2(f, \boldsymbol{q}_k, \partial K), \tag{5.2.4a}$$

where

$$\zeta_{curl}^2(\boldsymbol{q}_k, K) := h_K^2 \| \,\boldsymbol{\nabla}\times \boldsymbol{q}_k \|_K^2 + h_K \| \,[\![\boldsymbol{q}_k]\!]_t \|_{\partial K}^2, \tag{5.2.4b}$$

$$\zeta_{div}^2(f, \boldsymbol{q}_k, K) := \tau_K^2 h_K^2 \| (\mathsf{Id} - \mathsf{P}_{\widetilde{\mathbf{V}}_k})\boldsymbol{q}_k \|_K^2 + h_K^2 \| (\mathsf{Id} - \mathsf{P}_{\widetilde{W}_k}) f \|_K^2. \tag{5.2.4c}$$

It is easy to see that the estimator ζ_{curl} gives a measure of how close is $\boldsymbol{q}_k$ to being a gradient. It is less obvious to see that the estimator ζ_{div} measures how close is $\boldsymbol{q}_k$ to $\boldsymbol{H}(\mathrm{div},\Omega)$ and how well f_k captures the source function f. Let us argue why this is the case. By the orthogonality property of the L^2-projection P_{W_k}, we have that

$$h_K^2 \| (\mathsf{Id} - \mathsf{P}_{\widetilde{W}_k}) f \|_K^2 = h_K^2 \| (\mathsf{Id} - \mathsf{P}_{\widetilde{W}_k}) f_k \|_K^2 + h_K^2 \| f - f_k \|_K^2,$$

where $f_k := \mathsf{P}_{W_k} f$. Thanks to the equivalence (5.2.2), we see that

$$\zeta_{div}^2(f, \boldsymbol{q}_k, K) \simeq h_K \| (\widehat{\boldsymbol{q}}_k - \boldsymbol{q}_k) \cdot \boldsymbol{n} \|_{\partial K}^2 + h_K^2 \| f - f_k \|_K^2.$$

Now we see that the first term on the right hand side measures how close is $\boldsymbol{q}_k$ to $\boldsymbol{H}(\mathrm{div},\Omega)$ and that the second term measures how well f_k captures the source function f. Note that the term $h_K^2 \| f - f_k \|_K^2$ is usually called the *oscillation* of f in the element K. In previous work, this term has been treated separately from the error estimator whereas here we completely incorporate in it.

It is interesting to note that if we *formally* set $\widehat{\boldsymbol{q}}_k = \boldsymbol{q}_k$, the estimator (5.2.4a) is nothing but the well known estimator for the mixed methods proposed by Alonso [6]. This is a reflection of how strongly related are the HDG and the mixed methods. Moreover, from the equivalence (5.2.2), we see that the fact that the interelement jumps of $\boldsymbol{q}_k$ are not zero is caused by the fact that $f_k \in W_k$ and $\boldsymbol{q}_k \in \boldsymbol{V}_k$ whereas $\nabla\cdot \boldsymbol{q}_k \in \widetilde{W}_k$ and $\boldsymbol{\nabla} u_k \in \widetilde{\boldsymbol{V}}_k$, as well as by the fact that $\mathsf{P}^{\perp}_{W_k} f_k$ is not equal to zero.

The Module MARK

The module MARK selects a subset $\mathcal{M}_k$ from the mesh $\mathcal{T}_k$ according to the error indicator $\{\zeta^2(f\boldsymbol{q}_k, K)\}_{K\in\mathcal{T}_k}$ and a suitably defined marking strategy. Here, our marking strategy is based on the so-called Dörfler marking [40]. We define it next.

Given the mesh $\mathcal{T}_k$, the indicator $\{\zeta^2(\widehat{\boldsymbol{q}}_k, \boldsymbol{q}_k, K)\}_{K\in\mathcal{T}_k}$, and the parameter $\theta \in (0,1)$, the module MARK selects a **minimal** subset

$$\mathrm{MARK}(\theta, \mathcal{T}_k, \{\zeta^2(f, \boldsymbol{q}_k, K)\}_{K\in\mathcal{T}_k}) := \mathcal{M}_k,$$

satisfying

$$\theta\, \zeta^2(f, \boldsymbol{q}_k, \mathcal{T}_k) \le \zeta^2(f, \boldsymbol{q}_k, \mathcal{M}_k). \tag{5.2.5}$$

The Module REFINE

Given a conforming mesh $\mathcal{T}_k$ and a marked subset $\mathcal{M}_k \subset \mathcal{T}_k$, the module generates a conforming mesh $\mathcal{T}_{k+1} \geq \mathcal{T}_k$,

$$\text{REFINE}(\mathcal{T}_k, \mathcal{M}_k) := \mathcal{T}_{k+1}.$$

In this paper, the module REFINE is based on the newest vertex bisection algorithm [16, 66, 48]. Given a conforming mesh $\mathcal{T}_k$, the algorithm divides a given element $K \in \mathcal{T}_k$ into two children upon joining the midpoint of an edge with the nodes off such an edge. The choice of the refinement edges depends on a labelling associated with the initial mesh $\mathcal{T}_0$ only, see [16] for $d = 2$ and [44, 48, 67] for $d > 2$. A simple but crucial observation is that for each children T of an element K, we always have that

$$h_T \leq r h_K \tag{5.2.6}$$

where $r \in (0, 1)$ is the so-called *diameter reduction factor*.

Next, we list two important properties (**P1** and **P2**) of the newest vertex bisection algorithm.

P1. *The newest vertex bisection preserves the shape regularity property, that is,*

$$h_K/\rho_K \leq \sigma,$$

for any element $K \in \mathcal{T}_{k+1} := \text{REFINE}(\mathcal{T}_k, \mathcal{M}_k)$ *(each element in the marked set* $\mathcal{M}_k$ *is refined at least once), where* σ *denotes the shape regularity constant and* ρ_K *the diameter of the largest ball inside* K*.*

We also note that refining a marked element may create hanging nodes on the faces. Thus, to ensure conformity, additional elements need to be refined once or several times. The newest vertex bisection guarantees that the cumulative number of the added elements is controlled by the number of the marked elements [16, 67, 48]. This property is more precisely stated below.

P2. *For any initial conforming mesh $\mathcal{T}_0$, the newest vertex bisection generates a sequence of meshes $\{\mathcal{T}_k\}_{k\geq 0}$ satisfying*

$$\#\mathcal{T}_k - \#\mathcal{T}_0 \leq \Upsilon_0 \sum_{j=0}^{k-1} \#\mathcal{M}_j,$$

where Υ_0 is a constant depending only on the initial mesh $\mathcal{T}_0$ and dimension d, and where $\#S$ denotes the cardinality of the set S.

Finally, let us introduce some notation. We denote $\mathbb{T}$ as the set of all conforming refinements of an initial mesh $\mathcal{T}_0$ via the bisections. We write $\mathcal{T}_k \leq \mathcal{T}_{k+1}$ to denote that the $\mathcal{T}_{k+1}$ is a conforming refinement of $\mathcal{T}_k$ via bisection. We define the refined set $\mathcal{R}_{\mathcal{T}_k \to \mathcal{T}_{k+1}}$ in $\mathcal{T}_k$ as $\mathcal{T}_k \setminus \mathcal{T}_{k+1}$ and the set of new elements $\mathcal{N}_{\mathcal{T}_k \to \mathcal{T}_{k+1}} = \mathcal{T}_{k+1} \setminus \mathcal{T}_k$. Note that since each marked element is refined at least once, we have $\mathcal{M}_k \subset \mathcal{R}_k$ and note also that each element $T \in \mathcal{N}_{k+1}$ has a corresponding element $K \in \mathcal{R}_k$ such that $T \subset K$. And we say K is the parent of T. To simplify the notation, hereafter, we use $\mathcal{R}_k$ and $\mathcal{N}_{k+1}$ to denote $\mathcal{R}_{\mathcal{T}_k \to \mathcal{T}_{k+1}}$ and $\mathcal{N}_{\mathcal{T}_k \to \mathcal{T}_{k+1}}$ respectively, when it causes no ambiguity.

5.2.2 Convergence and optimality

We are now ready to state and discuss our results on convergence and quasi-optimality of the AHDG method.

The energy error, the error estimator and their modifications

The quasi-error is the sum of an energy-like norm and the error estimator. Here, we define the energy norm as

$$e_k^2 := \| \boldsymbol{q} - \boldsymbol{q}_k \|_\Omega^2 + \gamma\, \zeta_{div}^2(f, \boldsymbol{q}_k, \mathcal{T}_k), \tag{5.2.7}$$

for some constant $\gamma \geq 1$.

The following example provides a motivation of the above definition and illustrates one of the difficulties in establishing our convergence results. Let the domain Ω be a single equilateral triangle in two space dimensions and let the exact solution u be the linear function equal to 1 on two nodes and to -1 on the remaining node, see Fig. 5.2.1. Set $(\boldsymbol{q}_0, u_0, \widehat{u}_0) :=$ SOLVE$(f, \mathcal{T}_0)$ with $p = 0$ and $\tau_K = 1$ on all three edges. A simple

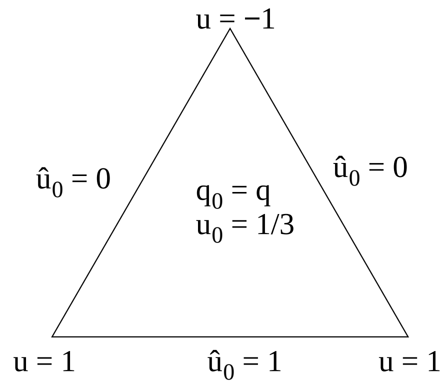

Figure 5.2.1: An example shows unsual phenomena of HDG methods

calculation shows that $\boldsymbol{q}_0 = \boldsymbol{q}$. However, we also have that

$$\zeta_{div}^2(f, \boldsymbol{q}_k, K) \neq 0.$$

Moreover, if $\mathcal{T}_1$ is a refinement of $\mathcal{T}_0$ obtained by bisecting the edge at which $u = 1$, it can be easily checked that $\| \boldsymbol{q} - \boldsymbol{q}_1 \|_\Omega \neq 0$.

This example reveals two unusual phenomena of HDG methods. First, the fact that $\| \boldsymbol{q} - \boldsymbol{q}_k \|_\Omega = 0$ does not imply $\| \boldsymbol{q} - \boldsymbol{q}_{k+1} \|_\Omega^2 = 0$. Second, a lower bound for $\| \boldsymbol{q} - \boldsymbol{q}_{k+1} \|_\Omega^2$ in terms of $\zeta_{div}^2(f, \boldsymbol{q}_k, \mathcal{T}_k)$, which is a key ingredient for the optimal convergence rate, is not available for the HDG methods. These two facts suggest the inclusion of the term ζ_{div} as part of the energy norm above. Our analysis also shows that this energy norm is closely associated with the HDG methods and comes out naturally in the analysis.

Contraction and quasi-optimality for the modified quasi-error

Theorem 5.2.1 (Contraction of the quasi-error)**.** *Assume that the Assumptions* **A1, A2** *are satisfied and that* **A3** *holds for some $C_\tau \in (0, C_\tau^*)$, where C_τ^* depends only on the shape regularity constant σ, the polynomial degree p, the diameter reduction r and the marking parameter θ. Then there exist positive constants β, and $\alpha < 1$ depending on σ, p, r, θ such that*

$$e_k^2 + \beta\, \zeta^2(f, \boldsymbol{q}_k, \mathcal{T}_k) \leq \alpha \{ e_{k+1}^2 + \beta\, \zeta^2(f, \boldsymbol{q}_{k+1}, \mathcal{T}_{k+1}) \}.$$

The actual constant C_τ^* can be easily determined in the proof of this result; see the inequalities (5.3.1a), (5.3.1b), (5.3.3), (5.5.1) and (5.5.7).

To state the quasi-optimality result for the let AHDG method, we need to introduce the approximation class $\mathcal{A}_s$. Let $\mathbb{T}_N \subset \mathbb{T}$ be the set of meshes with at most N more elements than $\mathcal{T}_0$:

$$\mathbb{T}_N := \{\mathcal{T} \in \mathbb{T}\ ,\ \#\mathcal{T} - \#\mathcal{T}_0 \leq N\}.$$

Given a flux $\boldsymbol{q}$, the quality of best approximation in the set $\mathbb{T}_N$ is given by

$$\varepsilon^2(N; f, \boldsymbol{q}) := \inf_{\mathcal{T}_h \in \mathbb{T}_N} e_h^2$$

We define the approximation class $\mathcal{A}_s$ as

$$\mathcal{A}_s := \{(f, \boldsymbol{q})\ ,\ \sup_{N>0} N^s \varepsilon(N; f, \boldsymbol{q}) < \infty\}, \tag{5.2.8}$$

and if $(f, \boldsymbol{q}) \in \mathcal{A}_s$, we define

$$|(f, \boldsymbol{q})|_{\mathcal{A}_s} := \sup N^s \varepsilon(N; f, \boldsymbol{q}). \tag{5.2.9}$$

We are now ready to state our main result.

Theorem 5.2.2 (Quasi-Optimality)**.** *Let the assumptions of Theorem 5.2.1 hold. Let $\boldsymbol{q} \in \boldsymbol{H}(\mathrm{div}, \Omega)$ be the solution of the continuous problem. Let $\{(\mathcal{T}_k, \boldsymbol{q}_k)\}_{k\geq 0}$ be the sequence of meshes and discrete solutions generated by AHDG. If the marking parameter θ lies in $(0, \theta_*)$ for some suitable constant θ_* and if $(f, \boldsymbol{q}) \in \mathcal{A}_s$, then we have that*

$$e_k \preceq (\#\mathcal{T}_k - \#\mathcal{T}_0)^{-s}.$$

5.3 Sketch of the proofs of the main Theorems

In this section, we present the proof of the contraction of the loop of the AHDG method, Theorem 5.2.1, and the proof of quasi-optimality of the method, Theorem 5.2.2. Since the proof is rather long and quite technical, all the auxiliary lemmas are here stated without proof. In this way, the main features of the proofs become more transparent. Detailed proofs of the auxiliary lemmas are presented in the remaining of the paper.

5.3.1 Proof of the contraction property of the AHDG method

Here, we prove Theorem 5.2.1. We proceed in several steps. In what follows, C_i, $i = 1, 2, 3$, denote constants that depend only on the shape-regularity constant of the elements, σ, and on the polynomial degree p. We also set

$$\lambda := 1 - r \quad \text{ and } \Lambda := 1 - r^2,$$

where r is the diameter reduction factor, see (5.2.6).

Hereafter, to simplify the notation, we use

$$\zeta^2_{div,k}(S_k) := \zeta^2_{div}(f, \boldsymbol{q}_k, S_k), \qquad \zeta^2_{curl,k}(S_k) := \zeta^2_{curl}(\boldsymbol{q}_k, S_k),$$

and $\zeta^2_k(S_k) := \zeta^2(f, \boldsymbol{q}_k, S_k)$, for any subset S_k of the triangulation $\mathcal{T}_k$.

Step 1: The quasi-orthogonality property

We begin by trying to relate the L^2- error in the approximation of the flux on a given mesh to the L^2- error in the approximation of the flux on an *arbitrary* refinement. The result is commonly referred to as the quasi-orthogonality property. It only depends on the properties of the HDG method.

Lemma 5.3.1 (Quasi orthogonality)**.** *Let $\mathcal{T}_{k+1}$ and $\mathcal{T}_k$ be any two nested meshes with $\mathcal{T}_k \leq \mathcal{T}_{k+1}$. Assume that* **A1**, **A2** *and* **A3** *are valid. Then, for any positive parameter $\delta_2 \in (0, 1)$, and for any $\epsilon \in (0, 1/4)$, we have that*

$$\begin{aligned}\|\, \boldsymbol{q} - \boldsymbol{q}_{k+1} \,\|^2_\Omega + \gamma\, \zeta^2_{div,k+1}(\mathcal{T}_{k+1}) + \frac{1}{2(1-\epsilon)} \|\, \boldsymbol{q}_{k+1} - \boldsymbol{q}_k \,\|^2_\Omega \\ \leq \frac{1}{1-\epsilon} \|\, \boldsymbol{q} - \boldsymbol{q}_k \,\|^2_\Omega + (1 + \delta_2)\, \gamma\, \zeta^2_{div,k}(\mathcal{T}_k)\end{aligned}$$

provided that the constant C_τ in **A3** *satisfies*

$$C_\tau \leq 1, \tag{5.3.1a}$$

$$C^2_\tau \leq \frac{\epsilon}{2\mathsf{C}_4(1 + \delta_2^{-1}\Lambda^{-1})}. \tag{5.3.1b}$$

Here,

$$\gamma := \frac{\mathsf{C}_4}{\Lambda\epsilon(1-\epsilon)(1+\delta_2)}. \tag{5.3.2a}$$

Let us now describe the basic idea of how to use this result to prove the contraction property. Note that if we formally take $\epsilon = \delta_2 = 0$, the lemma above implies

$$e_{k+1}^2 + \frac{1}{2}\| \boldsymbol{q}_{k+1} - \boldsymbol{q}_k \|_\Omega^2 \leq e_k^2.$$

This suggests that we should prove the inequality

$$\frac{1}{2}\| \boldsymbol{q}_{k+1} - \boldsymbol{q}_k \|_\Omega^2 \geq \big(1-\alpha\big) e_k^2 \quad \text{for some } \alpha \in (0,1),$$

since then we would immediately get that

$$e_{k+1}^2 \leq \alpha \, e_k^2.$$

However, the above lower bound for $\| \boldsymbol{q}_{k+1} - \boldsymbol{q}_k \|_\Omega^2$ may not hold, as was shown for the case of the continuous Galerkin method in [47]. To overcome this difficulty, we follow the approach introduced in [30] and obtain an lower bound for $\frac{1}{2}\| \boldsymbol{q}_{k+1} - \boldsymbol{q}_k \|_\Omega^2$ which also involves the estimators ζ_{k+1} and ζ_k, as we show next.

Step 2: The estimator reduction

Here, we obtain our lower bound for $\| \boldsymbol{q}_{k+1} - \boldsymbol{q}_k \|_\Omega^2$.

Lemma 5.3.2 (Estimator reduction)**.** *Let* **A2** *and* **A3** *be valid. Then there exists a constant* C_3 *such that, for any* $\delta_1 > 0$*, we have*

$$\frac{1}{2(1-\epsilon)}\| \boldsymbol{q}_{k+1} - \boldsymbol{q}_k \|_\Omega^2 \geq \beta \zeta_{k+1}^2(\mathcal{T}_{k+1}) - \beta(1+\delta_1)\{\zeta_k^2(\mathcal{T}_k) - \lambda \zeta_k^2(\mathcal{R}_k)\},$$

where $\beta = \delta_1/(2\mathsf{C}_3(1+\delta_1)(1-\epsilon))$*, provided that the constant* C_τ *in* **A3***, satisfies*

$$C_\tau^2 \leq \frac{1}{2}\mathsf{C}_3. \tag{5.3.3}$$

Note that, if we insert the above upper bound into the quasi-orthogonality inequality of Lemma 5.3.1, we readily get that

$$\begin{aligned} \| \boldsymbol{q} - \boldsymbol{q}_{k+1} \|_\Omega^2 &+ (\gamma+\beta)\zeta_{div,k+1}^2(\mathcal{T}_{k+1}) + \beta \zeta_{curl,k+1}^2(\mathcal{T}_{k+1}) + \Theta_{k+1/2} \\ &\leq \frac{1}{1-\epsilon}\| \boldsymbol{q} - \boldsymbol{q}_k \|_\Omega^2 + \{\gamma(1+\delta_2) + \beta(1+\delta_1)\}\zeta_{div,k}^2(\mathcal{T}_k) \\ &\quad + \beta(1+\delta_1)\zeta_{curl,k+1}^2(\mathcal{T}_k), \end{aligned}$$

where

$$\Theta_{k+1/2} := \beta(1+\delta_1)\ \lambda\ \zeta_k^2(\mathcal{R}_k).$$

We can now see that we need to show that the so-called *error reduction* term $\Theta_{k+1/2}$ contains a fixed amount of each of the three terms on the right hand. In fact, we are going to show that

$$\begin{aligned}T &:= \Theta_{k+1/2} - \{\frac{2\epsilon}{1-\epsilon}\| \boldsymbol{q} - \boldsymbol{q}_k \|_\Omega^2 \\ &\quad + \big(2\gamma\delta_2 + \beta\delta_1(1+\delta_1)\big)\zeta_{div,k}^2(\mathcal{T}_k) + \beta\delta_1(1+\delta_1)\zeta_{curl,k}^2(\mathcal{T}_k)\} \\ &\geq 0\end{aligned}$$

with the parameters ϵ, δ_1, δ_2 and θ properly chosen.

Step 3: The Dörfler property

To do so, we first relate the error reduction term $\Theta_{k+1/2}$ with the term $\zeta_k^2(\mathcal{T}_k)$. This is achieved by using the Dörfler marking strategy, (5.2.5), and the fact that $\mathcal{M}_k \subset \mathcal{R}_k$,

$$\theta\ \zeta^2(\mathcal{T}_k) \leq \zeta^2(\mathcal{M}_k) \leq \zeta^2(\mathcal{R}_k). \tag{5.3.4}$$

Inserting the upper bound of this result in the expression for T, we get

$$\begin{aligned}T &\geq \theta\beta(1+\delta_1)\lambda\zeta_k^2(\mathcal{T}_k) - \frac{2\epsilon}{1-\epsilon}\| \boldsymbol{q} - \boldsymbol{q}_k \|_\Omega^2 \\ &\quad - \big\{2\gamma\delta_2 + \beta\delta_1(1+\delta_1)\big\}\zeta_{div,k}^2(\mathcal{T}_k) + \beta\delta_1(1+\delta_1)\zeta_{curl,k}^2(\mathcal{T}_k) \\ &= T_1 + T_2 + T_3.\end{aligned}$$

where

$$\begin{aligned}T_1 &:= \frac{\lambda\theta}{4}\beta(1+\delta_1)\zeta_k^2(\mathcal{T}_k) - \delta_1\beta(1+\delta_1)\zeta_{curl,k}^2(\mathcal{T}_k), \\ T_2 &:= \frac{\theta\beta\lambda(1+\delta_1)}{4}\zeta_k^2(\mathcal{T}_k) - \frac{2\epsilon}{1-\epsilon}\| \boldsymbol{q} - \boldsymbol{q}_k \|_\Omega^2, \\ T_3 &:= \frac{\theta\beta\lambda(1+\delta_1)}{2}\zeta_k^2(\mathcal{T}_k) - \big\{2\gamma\delta_2 + \beta\delta_1(1+\delta_1)\big\}\zeta_{div,k}^2(\mathcal{T}_k).\end{aligned}$$

0ur next goal is to show that each of these components of T is non-negative. Let us show that we can have $T_1 \geq 0$ by suitably choosing the parameter δ_1. By definition of $\zeta_k(\mathcal{T}_k)$, (5.2.4a), we have that

$$T_1 \geq \big(\frac{\lambda\theta}{4} - \delta_1\big)\ \beta(1+\delta_1)\ \zeta_{curl,k}^2(\mathcal{T}_k) = 0,$$

if we set

$$\delta_1 := \lambda\, \theta/4.$$

Now let us show that we can have $T_3 \geq 0$ by suitably defining the parameter δ_2. By definition of $\zeta_k(\mathcal{T}_k)$, (5.2.4a), we have.

$$\begin{aligned} T_3 &\geq \big\{\frac{\theta\beta\lambda(1+\delta_1)}{2} - 2\gamma\delta_2 - \beta\delta_1(1+\delta_1)\big\}\ \zeta^2_{div,k}(\mathcal{T}_k) \\ &= \big\{(\frac{\theta\,\lambda}{2} - \delta_1)\,\beta(1+\delta_1) - 2\gamma\delta_2\big\}\ \zeta^2_{div,k}(\mathcal{T}_k) \\ &= 2\gamma\big\{(\frac{\theta\,\lambda}{8\,\gamma}\,\beta(1+\delta_1) - \delta_2\big\}\ \zeta^2_{div,k}(\mathcal{T}_k) \\ &\geq 0, \end{aligned}$$

provided we take

$$\delta_2 := \min\{\frac{\lambda^2\theta^2\Lambda\epsilon}{48\mathsf{C}_3\mathsf{C}_4}, 1\} \leq \frac{\theta\beta(1+\delta_1)\lambda}{8\gamma},$$

by the definition of β and γ. It remains to ensure that T_2 is nonnegative.

Step 4: The reliability of the error estimator

To do so, we use the reliability of the error estimator.

Lemma 5.3.3 (Reliability of the error estimator)**.** *There exists a constant $C_1 = C_1(\sigma, p)$ such that*

$$\|\,\boldsymbol{q} - \boldsymbol{q}_k\,\|^2_\Omega \leq C_1\zeta^2_k(\mathcal{T}_k).$$

Thanks to this estimate, we can now write that

$$T_2 \geq\ \big(\frac{\theta\beta\lambda(1+\delta_1)}{4} - \frac{2\epsilon}{1-\epsilon}\,C_1\big)\ \zeta^2_k(\mathcal{T}_k),$$

and we see that $T_2 \geq 0$ if

$$\frac{\theta\beta\lambda(1+\delta_1)}{4C_1} \geq \frac{2\epsilon}{1-\epsilon}.$$

Using the definitions of β, we obtain, after some simple algebraic manipulations that the above inequalities hold if we take

$$\epsilon = \min\left\{\frac{\lambda^2\theta^2}{48\mathsf{C}_3C_1}, \frac{1}{4}\right\}.$$

This completes the proof of the contraction result of Theorem 5.2.1.

5.3.2 Proof of the quasi-optimality of the adaptive HDG methods

The proof of this property can be carried out in a single step as follows.

By the property **P2** for the complexity of the refinement, we have that

$$\#\mathcal{T}_k - \#\mathcal{T}_0 \leq \Upsilon_0 \sum_{i=0}^{k-1} \#\mathcal{M}_i.$$

To continue, we are going to use the following property of the refinement.

Lemma 5.3.4. *Let $(f, \boldsymbol{q}) \in \mathcal{A}_s$ and $\mathcal{M}_k = \mathrm{MARK}(\theta, \mathcal{T}_k, \{\zeta(K)\})$ with $\theta \in (0, \theta_*)$ for some suitable θ_*. Then, the following estimate holds,*

$$\#\mathcal{M}_k \leq (2\mu)^{-\frac{1}{2s}} |(f, \boldsymbol{q})|_{\mathcal{A}_s}^{\frac{1}{s}} e_k^{-\frac{1}{s}},$$

for some constant μ.

Hence, using the above result, we get that

$$\#\mathcal{T}_k - \#\mathcal{T}_0 \leq C_* \sum_{i=1}^{k} e_i^{-\frac{1}{s}},$$

where $C_* = \Upsilon_0 (2\mu)^{-\frac{1}{2s}} |(f, \boldsymbol{q})|_{\mathcal{A}_s}^{\frac{1}{s}}$.

Finally, by the contraction property of the quasi-error, Theorem 5.2.1, we obtain

$$\#\mathcal{T}_k - \#\mathcal{T}_0 \leq C_* \sum_{i=1}^{k} e_k^{-\frac{1}{s}} \alpha^{\frac{i}{s}} \leq \frac{C_*}{1 - \alpha^{\frac{1}{s}}} e_k^{-\frac{1}{s}},$$

and this readily implies that

$$e_k \leq C(\#\mathcal{T}_k - \#\mathcal{T}_0)^{-s}.$$

This completes the proof of the quasi-optimality result of Theorem 5.2.2.

5.4 Completion of the Proof of the quasi-optimality property

In this section, we complete the proof of the contraction of the adaptive HDG method given by Theorem by proving the estimator reduction property, Lemma 5.3.2, and the quasi-orthogonality, Lemma 5.3.1.

5.4.1 Estimator reduction

The estimator reduction property of Lemma 5.3.2 follows immediately from the next lemma after applying condition (5.3.3) on C_τ.

Lemma 5.4.1. *We have*

$$\zeta^2_{div,k+1}(\mathcal{T}_{k+1}) - (1+\delta_1)\{\zeta^2_{div,k}(\mathcal{T}_k) - \Lambda\zeta^2_{div,k}(\mathcal{R}_k)\} \le (1+\delta_1^{-1})C_\tau^2 \, \| \boldsymbol{q}_k - \boldsymbol{q}_{k+1} \|^2_\Omega,$$
$$\zeta^2_{curl,k+1}(\mathcal{T}_{k+1}) - (1+\delta_1)\{\zeta^2_{curl,k}(\mathcal{T}_k) - \lambda\zeta^2_{curl,k}(\mathcal{R}_k)\} \le (1+\delta_1^{-1})\frac{1}{2}\mathsf{C}_3 \, \| \boldsymbol{q}_k - \boldsymbol{q}_{k+1} \|^2_\Omega.$$

Proof. Let us prove the first inequality. Let T be any element in $\mathcal{T}_{k+1}$. Then, by the definition of ζ_{div}, (5.2.4c), we obtain, after a straightforward application of the triangle inequality, that

$$\begin{aligned}|\zeta_{div,k+1}(T) - \zeta_{div,k}(T)| &\le \tau_T h_T \| \mathsf{P}^\perp_{\mathbf{V}_{k+1}}(\boldsymbol{q}_k - \boldsymbol{q}_{k+1}) \|_T \\ &\le \tau_T h_T \| \boldsymbol{q}_k - \boldsymbol{q}_{k+1} \|_T \\ &\le C_\tau \| \boldsymbol{q}_k - \boldsymbol{q}_{k+1} \|_T,\end{aligned}$$

by Assumption **A3**. Using the simple property

$$a^2 \le (1+\delta)b^2 + (1+\delta^{-1})c^2 \quad \forall \delta > 0 \quad \text{provided} \quad |a-b| \le c,$$

with $a := \zeta_{div,k+1}(T)$, $b := \zeta_{div,k}(T)$, and $c := C_\tau \, \| \boldsymbol{q}_k - \boldsymbol{q}_{k+1} \|_T$, we obtain that

$$\zeta^2_{div,k+1}(T) \le (1+\delta)\zeta^2_{div,k}(T) + (1+\delta^{-1})C_\tau^2 \, \| \boldsymbol{q}_k - \boldsymbol{q}_{k+1} \|^2_T.$$

Summing over all the elements $T \in \mathcal{T}_{k+1}$, we get that

$$\zeta^2_{div,k+1}(\mathcal{T}_{k+1}) - (1+\delta_1)\zeta^2_{div,k}(\mathcal{T}_{k+1}) \le (1+\delta_1^{-1})C_\tau^2 \, \| \boldsymbol{q}_k - \boldsymbol{q}_{k+1} \|^2_\Omega.$$

Since

$$\begin{aligned}\zeta^2_{div,k}(\mathcal{T}_{k+1}) &= \zeta^2_{div,k}(\mathcal{T}_{k+1} \cap \mathcal{T}_k) + \zeta^2_{div,k}(\mathcal{N}_{k+1}) \\ &\le \zeta^2_{div,k}(\mathcal{T}_{k+1} \cap \mathcal{T}_k) + r^2\zeta^2_{div,k}(\mathcal{R}_k) \quad \text{by (5.2.6)}, \\ &= \zeta^2_{div,k}(\mathcal{T}_k) - (1-r^2)\zeta^2_{div,k}(\mathcal{R}_k),\end{aligned}$$

we have

$$\zeta^2_{div,k+1}(\mathcal{T}_{k+1}) - (1+\delta_1)\{\zeta^2_{div,k}(\mathcal{T}_k) - \Lambda\zeta^2_{div,k}(\mathcal{R}_k)\} \le (1+\delta_1^{-1})C_\tau^2 \, \| \boldsymbol{q}_k - \boldsymbol{q}_{k+1} \|^2_\Omega.$$

where, by definition, $\Lambda = 1 - r^2$. The first inequality follows after dividing by $(1+\delta_1^{-1})$ on both sides.

Let us now prove the second inequality. Let T be any element in $\mathcal{T}_{k+1}$. Then, by the definition of ζ_{curl}, (5.2.4c), we obtain, after applying the triangle inequality, that

$$|\zeta_{curl,k+1}(T) - \zeta_{curl,k}(T)| \leq \sqrt{\mathsf{C}_3/2}\,\|\,\boldsymbol{q}_k - \boldsymbol{q}_{k+1}\,\|_T,$$

by using standard inverse inequalities. We can now proceed as before to get

$$\frac{\delta_1}{(1+\delta_1)}\zeta^2_{curl}(\boldsymbol{q}_{k+1},\mathcal{T}_{k+1}) - \delta_1\{\zeta^2_{curl}(\boldsymbol{q}_k,\mathcal{T}_k) - \lambda\zeta^2_{curl}(\boldsymbol{q}_k,\mathcal{R}_k)\} \leq \frac{\mathsf{C}_3}{2}\|\,\boldsymbol{q}_k - \boldsymbol{q}_{k+1}\,\|^2_\Omega.$$

This completes the proof of Lemma 5.3.2. □

5.4.2 Proof of the quasi-orthogonality inequality

Now, we provide a proof of the quasi-orthogonality inequality of Lemma 5.3.1. Our approach is based on exploiting the similarity of the HDG methods and the mixed methods. Indeed, using the identity

$$\|\,\boldsymbol{q} - \boldsymbol{q}_{k+1}\,\|^2_\Omega + \|\,\boldsymbol{q}_{k+1} - \boldsymbol{q}_k\,\|^2_\Omega = \|\,\boldsymbol{q} - \boldsymbol{q}_k\,\|^2_\Omega,$$

which holds provided the orthogonality condition $(\boldsymbol{q}-\boldsymbol{q}_{k+1}, \boldsymbol{q}_{k+1}-\boldsymbol{q}_k)_\Omega = 0$ is satisfied, Chen, Holst and Xu [31] established a quasi-orthogonality inequality for mixed methods. Our strategy is to mimic this idea in the framework of HDG methods.

Step 1: A key orthogonality property

However, due to the fact that the approximate flux $\boldsymbol{q}_k$ is not $\boldsymbol{H}(\mathrm{div},\Omega)$-conforming, the above-mentioned orthogonality property does not hold for the HDG methods. In order to overcome this difficulty, we are going to use the following result.

Lemma 5.4.2. *We have*

$$(\boldsymbol{q} - \boldsymbol{q}_{k+1}, \boldsymbol{v})_\Omega = 0 \quad \forall\, \boldsymbol{v} \in \boldsymbol{H}(\mathrm{div},\Omega) \cap \boldsymbol{V}_{k+1} \ \textit{with}\ \nabla\cdot\boldsymbol{v} = 0.$$

Proof. After a simple integration by parts, we get that

$$(\boldsymbol{q},\boldsymbol{v})_{\mathcal{T}_{k+1}} = (u, \nabla\cdot\boldsymbol{v})_{\mathcal{T}_{k+1}} - \langle u, \boldsymbol{v}\cdot\boldsymbol{n}\rangle_{\partial\mathcal{T}_{k+1}} \qquad \forall \boldsymbol{v} \in \boldsymbol{V}_{k+1}.$$

Subtracting the first equation defining the HDG method (1.2.2a) from the equation above, we obtain

$$(\boldsymbol{q} - \boldsymbol{q}_{k+1}, \boldsymbol{v})_{\mathcal{T}_{k+1}} = (u - u_{k+1}, \nabla\cdot \boldsymbol{v})_{\mathcal{T}_{k+1}} - \langle u - \widehat{u}_{k+1}, \boldsymbol{v}\cdot\boldsymbol{n}\rangle_{\partial\mathcal{T}_{k+1}}.$$

Since the trace $u - \widehat{u}_{k+1}$ is single-valued in the interior edges and vanishes on the boundary Γ, we have

$$(\boldsymbol{q} - \boldsymbol{q}_{k+1}, \boldsymbol{v})_{\Omega} = (u - u_{k+1}, \nabla\cdot \boldsymbol{v})_{\mathcal{T}_{k+1}} - \langle u - \widehat{u}_{k+1}, \boldsymbol{v}\cdot\boldsymbol{n}\rangle_{\Gamma} = 0,$$

for all $\boldsymbol{v} \in \boldsymbol{H}(\mathrm{div},\Omega) \cap \boldsymbol{V}_{k+1}$ with $\nabla\cdot \boldsymbol{v} = 0$. This completes the proof. $\square$

Next, to be able to apply this property to derive a quasi-orthogonality, we construct an $\boldsymbol{H}(\mathrm{div},\Omega)$-conforming approximate flux by using a local post-processing.

Step 2: Post-processing

We define a post-processed flux $\boldsymbol{q}_k^*$ by using a slight modification of the Raviart-Thomas projection [61]. We take $\boldsymbol{q}_k^* \in \mathrm{RT}_p(K)$ satisfying

$$(\boldsymbol{q}_k^*, \boldsymbol{v})_K = (\boldsymbol{q}_k, \boldsymbol{v})_K \qquad \forall \boldsymbol{v} \in \boldsymbol{\mathcal{P}}_{p-1}(K), \tag{5.4.1a}$$

$$\langle \boldsymbol{q}_k^* \cdot \boldsymbol{n}, \mu\rangle_e = \langle \widehat{\boldsymbol{q}}_k \cdot \boldsymbol{n}, \mu\rangle_e \quad \forall \mu \in \mathcal{P}_p(e) \text{ for all faces } e \text{ of } K. \tag{5.4.1b}$$

It is worth mentioning two useful properties of the post-processed flux $\boldsymbol{q}_k^*$. First, $\boldsymbol{q}_k^*$ belongs to $\boldsymbol{H}(\mathrm{div},\Omega)$ because the transmission condition (1.2.3b) strongly enforces the single-valueness of the normal component of $\widehat{\boldsymbol{q}}_k$ across the faces. Second, we have $\nabla\cdot \boldsymbol{q}_k^* = f_k$. This follows immediately from the second equations defining the HDG method (1.2.2b),

$$-(\boldsymbol{q}_k^*, \boldsymbol{\nabla} w)_{\mathcal{T}_k} + \langle \boldsymbol{q}_k^* \cdot \boldsymbol{n}, w\rangle_{\partial\mathcal{T}_k} = (f, w)_{\mathcal{T}_k} \quad \forall w \in W_k,$$

after a simple integration by parts.

Step 3: Intermediate solution

In order to build a link between the solution on $\mathcal{T}_k$ with the one on its refinement $\mathcal{T}_{k+1}$, we introduce an intermediate solution

$$(\tilde{\boldsymbol{q}}_{k+1}, \tilde{u}_{k+1}, \widehat{\tilde{u}}_{k+1}) := \mathrm{SOLVE}(f_k, \mathcal{T}_{k+1}),$$

and define $\tilde{\boldsymbol{q}}^*_{k+1}$ to be its corresponding post-processed flux. The intermediate solution $\tilde{\boldsymbol{q}}^*_{k+1}$ relates the approximation $\boldsymbol{q}^*_k$ on the coarse mesh $\mathcal{T}_k$ with $\boldsymbol{q}^*_{k+1}$ on the fine mesh $\mathcal{T}_{k+1}$. Indeed, we observe that

$$\nabla\cdot(\boldsymbol{q}^*_k - \tilde{\boldsymbol{q}}^*_{k+1}) = f_k - f_k = 0. \tag{5.4.2a}$$

This implies that $\boldsymbol{q}^*_k - \tilde{\boldsymbol{q}}^*_{k+1} \in \boldsymbol{\mathcal{P}}_p(T)$ on each element $T \in \mathcal{T}_h$ and hence, that

$$\boldsymbol{q}^*_k - \tilde{\boldsymbol{q}}^*_{k+1} \in \boldsymbol{V}_{k+1} \cap \boldsymbol{H}(\mathrm{div}, \Omega). \tag{5.4.2b}$$

On the other hand, the difference between $\boldsymbol{q}^*_{k+1}$ and $\tilde{\boldsymbol{q}}^*_{k+1}$ is controlled by the oscillation $osc^2(f_{k+1}, \mathcal{R}_k)$, where

$$osc^2(f_{k+1}, S) := \sum_{K\in S} h_K^2 \| f_{k+1} - f_k \|_K^2, \tag{5.4.3}$$

as we see next.

Lemma 5.4.3. *Let Assumptions* **A1***,* **A2***,* **A3** *be valid and the constant C_τ satisfy* (5.3.1a)*. Then there exists a constant $\mathsf{C}_2 = \mathsf{C}_2(\sigma, p)$ such that*

$$\| \boldsymbol{q}^*_{k+1} - \tilde{\boldsymbol{q}}^*_{k+1} \|_\Omega^2 \le \mathsf{C}_2 \; osc^2(f_{k+1}, \mathcal{R}_k).$$

We give a detailed proof of this result in the appendix. This would allow us to maintain the focus on the quasi-orthogonality property. Here, let us just say that the result follows from the stability properties of the HDG methods.

Step 4: Quasi-orthogonality

Next, we use the orthogonality property of Lemma 5.4.2 to obtain the following result.

Lemma 5.4.4. *Under the same assumption of Lemma 5.4.3, it holds that*

$$(1-\epsilon)\| \boldsymbol{q}-\boldsymbol{q}_{k+1} \|_\Omega^2 + \| \boldsymbol{q}_{k+1} - \boldsymbol{q}_k \|_\Omega^2 \le \| \boldsymbol{q} - \boldsymbol{q}_k \|_\Omega^2 + \frac{1}{\epsilon}\| \boldsymbol{q}_{k+1} - \tilde{\boldsymbol{q}}^*_{k+1} - \boldsymbol{q}_k + \boldsymbol{q}^*_k \|_\Omega^2,$$

for any $\epsilon > 0$.

Proof. From the identity

$$\| \boldsymbol{q} - \boldsymbol{q}_{k+1} \|_\Omega^2 + \| \boldsymbol{q}_{k+1} - \boldsymbol{q}_k \|_\Omega^2 = \| \boldsymbol{q} - \boldsymbol{q}_k \|_\Omega^2 - 2\,(\boldsymbol{q} - \boldsymbol{q}_{k+1}, \boldsymbol{q}_{k+1} - \boldsymbol{q}_k)_\Omega$$

we see that we have

$$\begin{aligned}\theta &:= \| \boldsymbol{q} - \boldsymbol{q}_{k+1} \|_\Omega^2 + \| \boldsymbol{q}_{k+1} - \boldsymbol{q}_k \|_\Omega^2 \\ &= \| \boldsymbol{q} - \boldsymbol{q}_k \|_\Omega^2 - 2\,(\boldsymbol{q} - \boldsymbol{q}_{k+1}, \boldsymbol{q}_{k+1} - \boldsymbol{q}_k)_\Omega. \\ &= \| \boldsymbol{q} - \boldsymbol{q}_k \|_\Omega^2 - 2\,(\boldsymbol{q} - \boldsymbol{q}_{k+1}, \boldsymbol{q}_{k+1} - \tilde{\boldsymbol{q}}_{k+1}^* - \boldsymbol{q}_k + \boldsymbol{q}_k^*)_\Omega,\end{aligned}$$

since, by the orthogonality property of Lemma 5.4.2 and property (5.4.2), we have that

$$(\boldsymbol{q} - \boldsymbol{q}_{k+1}, \boldsymbol{q}_k^* - \tilde{\boldsymbol{q}}_{k+1}^*)_\Omega = 0.$$

A simple application of Young's inequality gives

$$\theta \le \| \boldsymbol{q} - \boldsymbol{q}_k \|_\Omega^2 + \epsilon \| \boldsymbol{q} - \boldsymbol{q}_{k+1} \|_\Omega^2 + \frac{1}{\epsilon} \| \boldsymbol{q}_{k+1} - \tilde{\boldsymbol{q}}_{k+1}^* - \boldsymbol{q}_k + \boldsymbol{q}_k^* \|_\Omega^2.$$

and the result immediately follows. This completes the proof. $\square$

Thus, to prove the quasi-orthogonality inequality of Lemma 5.3.1, we only need to suitably estimate the term $T(\Omega) := \| \boldsymbol{q}_{k+1} - \tilde{\boldsymbol{q}}_{k+1}^* - \boldsymbol{q}_k + \boldsymbol{q}_k^* \|_\Omega^2$.

Step 5: Estimation of $T(\Omega)$.

Here we prove the following proposition.

Proposition 5.4.1. *Let the Assumptions* **A1**, **A2** *and* **A3** *be valid and the constant* C_τ *satisfy* (5.3.1b). *Then*

$$T(\Omega) \le \frac{\epsilon}{2} \| \boldsymbol{q}_k - \boldsymbol{q}_{k+1} \|_\Omega^2 + \frac{\mathsf{C}_4}{\Lambda} \{ \zeta_{div,k}^2(\mathcal{T}_k) - (1+\delta_2)^{-1} \zeta_{div,k+1}^2(\mathcal{T}_{k+1}) \}.$$

To prove this lemma, we are going to use the following auxiliary result.

Lemma 5.4.5. *Let Assumptions* **A1** *and* **A2** *be valid. Then,*

$$T(\Omega) \le \mathsf{C}_4 \{ \zeta_{div,k}^2(\mathcal{R}_k) + C_\tau^2 \, \| \boldsymbol{q}_{k+1} - \boldsymbol{q}_k \|_\Omega^2 \}.$$

A detailed proof is provided in the appendix. We are now ready to prove Proposition 5.4.1.

Proof. By Lemma 5.4.5 and by the reduction property of ζ_{div}, that is, by the first inequality of Lemma 5.4.1, we have

$$\Lambda\, \zeta^2_{div,k}(\mathcal{R}_k) \leq \zeta^2_{div,k}(\mathcal{T}_k) - (1+\delta_1)^{-1}\zeta^2_{div,k+1}(\mathcal{T}_{k+1}) + \delta_1^{-1}\, C_\tau^2 \,\|\, \boldsymbol{q}_k - \boldsymbol{q}_{k+1} \,\|^2_\Omega.$$

We immediately obtain

$$\begin{aligned} T(\Omega) \leq\ & \mathsf{C}_4\Lambda^{-1}\{\zeta^2_{div,k}(\mathcal{T}_k) - (1+\delta_1)^{-1}\zeta^2_{div,k+1}(\mathcal{T}_{k+1})\} \\ &+ (1+\delta_1^{-1}\Lambda^{-1})\mathsf{C}_4\, C_\tau^2 \,\|\, \boldsymbol{q}_k - \boldsymbol{q}_{k+1} \,\|^2_\Omega, \end{aligned}$$

and the result follows from the condition on C_τ, (5.3.1b). This completes the proof. □

Step 6: Proof of Lemma 5.3.1

Inserting the estimate of Proposition 5.4.1 into the inequality of Lemma 5.4.4, we readily obtain

$$\begin{aligned} (1-\epsilon)\|\, \boldsymbol{q} - \boldsymbol{q}_{k+1} \,\|^2_\Omega + \frac{1}{2}\|\, \boldsymbol{q}_{k+1} - \boldsymbol{q}_k \,\|^2_\Omega \leq\ & \|\, \boldsymbol{q} - \boldsymbol{q}_k \,\|^2_\Omega \\ &+ \gamma(1-\epsilon)\{(1+\delta_2)\zeta^2_{div,k}(\mathcal{T}_k) - \zeta^2_{div,k+1}(\mathcal{T}_{k+1})\} \end{aligned}$$

by definition of γ, (5.3.2a). The quasi-orthogonality inequality, Lemma 5.3.1, follows immediately from the above inequality after dividing by $(1-\epsilon)$.

5.5 Completion of the Proof of the quasi-optimality property

In this section, we complete the proof of the quasi-optimality of the adaptive HDG method in Theorem 5.2.2 by proving Lemma 5.3.4.

Step One: Global efficiency of the estimator

Lemma 5.5.1 (Efficiency of the error estimator)**.** *There exists a constant* $C_2 = C_2(\sigma, p, \gamma)$ *such that*

$$C_2\zeta^2_k(\mathcal{T}_k) \leq e^2_k.$$

The Lemma follows directly from chapter 4, Corollary 3.3, and the equivalence relation (5.2.2).

Step Two: Localized upper bound

Lemma 5.5.2 (Localized upper bound)**.** *Assume that* **A1***,* **A2** *and* **A3** *holds and that* C_τ *satisfies*

$$C_\tau^2 \leq \frac{1}{4\mathsf{C}_4}. \tag{5.5.1}$$

Then, for any *two nested meshes* $\mathcal{T}_k \leq \mathcal{T}_{k+1}$*, there exists a constant* $C_3 = C_3(\sigma, p, \gamma)$ *such that*

$$3\| \boldsymbol{q}_k - \boldsymbol{q}_{k+1} \|_\Omega^2 + \gamma\zeta_{div,k}^2(\mathcal{R}_k) \leq C_3\zeta_k^2(\mathcal{R}_k).$$

To prove this result, we introduce an auxiliary estimator and the following auxiliary proposition.

Proposition 5.5.1 (Relation between the error estimators)**.** *It holds, for each face* $e \in \mathcal{E}_k$*,*

$$\begin{aligned}\| \boldsymbol{q}_k + \boldsymbol{\nabla}\, u_k^* \|_{K\in\mathcal{U}_k(e)}^2 &+ h_e^{-1}\| \left(\mathsf{Id} - \mathsf{P}_{\mathsf{M}_0}\right) [\![u_k^*]\!] \|_e^2 \\ &\simeq h_K^2\| \;\boldsymbol{\nabla}\times \boldsymbol{q}_k \|_{K\in\mathcal{U}_k(e)}^2 + h_e\| \;[\![\boldsymbol{q}_k]\!]_t \|_e^2.\end{aligned}$$

where u_k^* *is the post-processed scalar variable in the space*

$$W_k^* = \{w \in L^2(\Omega) \;:\; w \in \mathcal{P}_{p+1}(K) \quad \forall K \in \mathcal{T}_k\},$$

satisfying

$$\begin{aligned}(u_k^* - u_k, w)_K &= 0 \quad \forall w \in \mathcal{P}_0(K),\\ (\boldsymbol{\nabla}\, u_k^* + \boldsymbol{q}_k, \boldsymbol{\nabla}\, w)_K &= 0 \quad \forall w \in \mathcal{P}_{p+1}(K),\end{aligned}$$

for all $K \in \mathcal{T}_k$*.*

Now we are ready to prove Lemma 5.5.2.

Proof. Since $\zeta_{div,k}(\mathcal{R}_k) \leq \zeta_k(\mathcal{R}_k)$, by Proposition 5.5.1, we only need to show that

$$\| \boldsymbol{q}_{k+1} - \boldsymbol{q}_k \|_\Omega^2 \preceq \sum_{K\in\mathcal{R}_k} \| \boldsymbol{q}_k + \boldsymbol{\nabla}\, u_k^* \|_K^2 + \sum_{e\in\mathcal{E}_k\setminus\mathcal{E}_{k+1}} h_e^{-1}\| \left(\mathsf{Id} - \mathsf{P}_{\mathsf{M}_0}\right) [\![u_k^*]\!] \|_e^2 + \zeta_{div,k}^2(\mathcal{R}_k).$$

We proceed in several steps.

Step 1. We start by adding and subtracting $\tilde{\boldsymbol{q}}_{k+1}^* - \boldsymbol{q}_k^*$ to get

$$\| \boldsymbol{q}_{k+1} - \boldsymbol{q}_k \|_\Omega^2 = T_1 + T_2,$$

where

$$\begin{aligned} T_1 &= (\boldsymbol{q}_{k+1} - \boldsymbol{q}_k, \boldsymbol{q}_{k+1} - \boldsymbol{q}_k - \tilde{\boldsymbol{q}}_{k+1}^* + \boldsymbol{q}_k^*)_\Omega, \\ T_2 &= (\boldsymbol{q}_{k+1} - \boldsymbol{q}_k, \tilde{\boldsymbol{q}}_{k+1}^* - \boldsymbol{q}_k^*)_\Omega. \end{aligned}$$

We can bound the first term T_1 as follows:

$$\begin{aligned} T_1 &\leq \frac{1}{4} \| \boldsymbol{q}_{k+1} - \boldsymbol{q}_k \|_\Omega^2 + \| \boldsymbol{q}_{k+1} - \boldsymbol{q}_k - \tilde{\boldsymbol{q}}_{k+1}^* + \boldsymbol{q}_k^* \|_\Omega^2 \\ &\leq (\frac{1}{4} + \mathsf{C}_4 \, C_\tau^2) \, \| \boldsymbol{q}_{k+1} - \boldsymbol{q}_k \|_\Omega^2 + \mathsf{C}_4 \zeta_{div,k}^2(\mathcal{R}_k), \end{aligned}$$

by Lemma 5.4.5. Thanks to condition (5.5.1), we immediately obtain

$$T_1 \leq \frac{1}{2} \| \boldsymbol{q}_{k+1} - \boldsymbol{q}_k \|_\Omega^2 + \mathsf{C}_4 \zeta_{div,k}^2(\mathcal{R}_k). \tag{5.5.2}$$

Step 2. Now our goal is to show that

$$\begin{aligned} T_2 \leq \delta \mathsf{C}_5 \| \, (\tilde{\boldsymbol{q}}_{k+1}^* - \boldsymbol{q}_k^*) \, \|_{\mathcal{R}_k}^2 + \delta^{-1} \| \, \boldsymbol{q}_k + \boldsymbol{\nabla} \, u_k^* \, \|_{\mathcal{R}_k}^2 \\ + \delta^{-1} \sum_{e \in \mathcal{E}_k \setminus \mathcal{E}_{k+1}} h_e^{-1} \| \, (\mathsf{Id} - \mathsf{P}_{\mathsf{M}_0}) \, [\![u_k^*]\!] \, \|_e^2, \end{aligned} \tag{5.5.3}$$

for any $\delta > 0$, where C_5 is some constant depending only on the shape regularity constant σ and the polynomial degree p.

By the first equation defining the HDG method, (1.2.2a),

$$(\boldsymbol{q}_{k+1}, \boldsymbol{v})_{\mathcal{T}_{k+1}} = -\langle \widehat{u}_{k+1}, \boldsymbol{v} \cdot \boldsymbol{n} \rangle_{\partial \mathcal{T}_{k+1}} + (u_{k+1}, \nabla \cdot \boldsymbol{v})_{\mathcal{T}_{k+1}} \qquad \forall \boldsymbol{v} \in \boldsymbol{V}_{k+1}.$$

Taking $\boldsymbol{v} := \tilde{\boldsymbol{q}}_{k+1}^* - \boldsymbol{q}_k^*$, we see, by (5.4.2a) and (5.4.2b), that

$$(\boldsymbol{q}_{k+1}, \tilde{\boldsymbol{q}}_{k+1}^* - \boldsymbol{q}_k^*)_{\mathcal{T}_{k+1}} = -\langle \widehat{u}_{k+1}, (\tilde{\boldsymbol{q}}_{k+1}^* - \boldsymbol{q}_k^*) \cdot \boldsymbol{n} \rangle_\Gamma = 0$$

by the boundary condition (1.2.3a). This orthogonality relation implies that

$$T_2 = -(\boldsymbol{q}_k, \tilde{\boldsymbol{q}}_{k+1}^* - \boldsymbol{q}_k^*)_\Omega.$$

Similarly, by the first equation defining the HDG method, (1.2.2a),

$$(\boldsymbol{q}_k, \boldsymbol{v})_{\mathcal{T}_k} = -\langle \widehat{u}_k, \boldsymbol{v}\cdot\boldsymbol{n}\rangle_{\partial\mathcal{T}_k} + (u_k, \nabla\cdot \boldsymbol{v})_{\mathcal{T}_k} \qquad \forall \boldsymbol{v}\in \boldsymbol{V}_k.$$

We claim that the function $\boldsymbol{v} := \Pi_k^{\mathrm{RT}}(\tilde{\boldsymbol{q}}^*_{k+1} - \boldsymbol{q}^*_k)$, where Π_k^{RT} is the Raviart-Thomas projection into the space $\mathrm{RT}_p(\mathcal{T}_k)$, lies in $\boldsymbol{V}_k \cap \boldsymbol{H}(\mathrm{div},\Omega)$. As a consequence, repeating the above argument, we conclude that

$$(\boldsymbol{q}_k, \Pi_k^{\mathrm{RT}}(\tilde{\boldsymbol{q}}^*_{k+1} - \boldsymbol{q}^*_k))_{\mathcal{T}_k} = 0,$$

which readily implies that

$$T_2 = -(\boldsymbol{q}_k, (\mathsf{Id} - \Pi_k^{\mathrm{RT}})(\tilde{\boldsymbol{q}}^*_{k+1} - \boldsymbol{q}^*_k))_\Omega.$$

The claim follows from the fact that $\nabla\cdot \Pi_k^{\mathrm{RT}}(\tilde{\boldsymbol{q}}^*_{k+1} - \boldsymbol{q}^*_k) = \mathsf{P}_{W_k}\, \nabla\cdot(\tilde{\boldsymbol{q}}^*_{k+1} - \boldsymbol{q}^*_k) = 0$, by property (5.4.2a).

Using this new expression for T_2, we easily obtain, after a simple calculation, that

$$\begin{aligned} T_2 = &-(\boldsymbol{q}_k + \boldsymbol{\nabla}\, u^*_k, (\mathsf{Id} - \Pi_k^{\mathrm{RT}})(\tilde{\boldsymbol{q}}^*_{k+1} - \boldsymbol{q}^*_k))_\Omega + (\boldsymbol{\nabla}\, u^*_k, (\mathsf{Id} - \Pi_k^{\mathrm{RT}})(\tilde{\boldsymbol{q}}^*_{k+1} - \boldsymbol{q}^*_k))_\Omega \\ &= T_{21} + T_{22} + T_{23}, \end{aligned}$$

where

$$\begin{aligned} T_{21} &:= -(\boldsymbol{q}_k + \boldsymbol{\nabla}\, u^*_k, (\mathsf{Id} - \Pi_k^{\mathrm{RT}})(\tilde{\boldsymbol{q}}^*_{k+1} - \boldsymbol{q}^*_k))_\Omega \\ T_{22} &:= -(u^*_k, \nabla\cdot(\mathsf{Id} - \Pi_k^{\mathrm{RT}})(\tilde{\boldsymbol{q}}^*_{k+1} - \boldsymbol{q}^*_k))_\Omega \\ T_{23} &:= \sum_{e\in\mathcal{E}_k} \langle [\![u^*_k]\!], (\mathsf{Id} - \Pi_k^{\mathrm{RT}})(\tilde{\boldsymbol{q}}^*_{k+1} - \boldsymbol{q}^*_k)\cdot \boldsymbol{n}\rangle_e. \end{aligned}$$

Next, we estimate the three terms on the right hand side. Let us estimate T_{21}. Since $(\mathsf{Id} - \Pi_k^{\mathrm{RT}})(\tilde{\boldsymbol{q}}^*_{k+1} - \boldsymbol{q}^*_k) = 0$ on the unrefined set $\mathcal{T}_{k+1}\cap\mathcal{T}_k$, we have

$$\begin{aligned} T_{21} = &-(\boldsymbol{q}_k + \boldsymbol{\nabla}\, u^*_k, (\mathsf{Id} - \Pi_k^{\mathrm{RT}})(\tilde{\boldsymbol{q}}^*_{k+1} - \boldsymbol{q}^*_k))_{\mathcal{R}_k} \\ &\le \frac{\delta}{4}\| (\mathsf{Id} - \Pi_k^{\mathrm{RT}})(\tilde{\boldsymbol{q}}^*_{k+1} - \boldsymbol{q}^*_k) \|^2_{\mathcal{R}_k} + \delta^{-1}\| \boldsymbol{q}_k + \boldsymbol{\nabla}\, u^*_k \|^2_{\mathcal{R}_k}, \end{aligned}$$

for any $\delta > 0$.

Let us estimate T_{22}. Thanks to (5.4.2a), we obtain

$$T_{22} = (u^*_k, (\mathsf{Id} - \mathsf{P}_{W_k})\, \nabla\cdot(\tilde{\boldsymbol{q}}^*_{k+1} - \boldsymbol{q}^*_k))_\Omega = 0.$$

Finally, let us now estimate T_{23}. Since $(\mathsf{Id}-\Pi_k^{\mathrm{RT}})(\tilde{\boldsymbol{q}}_{k+1}^*-\boldsymbol{q}_k^*)\cdot\boldsymbol{n}=0$ on the unrefined edges $\mathcal{E}_k\cap\mathcal{E}_{k+1}$, we can write that

$$
\begin{aligned}
T_{23} &= \sum_{e\in\mathcal{E}_k\setminus\mathcal{E}_{k+1}} \langle\, [\![u_k^*]\!], (\mathsf{Id}-\Pi_k^{\mathrm{RT}})(\tilde{\boldsymbol{q}}_{k+1}^*-\boldsymbol{q}_k^*)\cdot\boldsymbol{n}\rangle_e \\
&= \sum_{e\in\mathcal{E}_k\setminus\mathcal{E}_{k+1}} \langle(\mathsf{Id}-\mathsf{P}_{\mathsf{M}_0})\,[\![u_k^*]\!], (\mathsf{Id}-\Pi_k^{\mathrm{RT}})(\tilde{\boldsymbol{q}}_{k+1}^*-\boldsymbol{q}_k^*)\cdot\boldsymbol{n}\rangle_e \quad \text{by definition of } \Pi_k^{\mathrm{RT}}, \\
&\le \frac{\delta}{4}\sum_{e\in\mathcal{E}_k\setminus\mathcal{E}_{k+1}} h_e\|\,(\mathsf{Id}-\Pi_k^{\mathrm{RT}})(\tilde{\boldsymbol{q}}_{k+1}^*-\boldsymbol{q}_k^*)\cdot\boldsymbol{n}\,\|_e^2 \\
&+ \delta^{-1}\sum_{e\in\mathcal{E}_k\setminus\mathcal{E}_{k+1}} h_e^{-1}\|\,(\mathsf{Id}-\mathsf{P}_{\mathsf{M}_0})\,[\![u_k^*]\!]\,\|_e^2.
\end{aligned}
$$

To conclude, we have

$$
\begin{aligned}
T_2 \le \delta^{-1}\|\,\boldsymbol{q}_k+\boldsymbol{\nabla}\,u_k^*\,\|_{\mathcal{R}_k}^2 &+ \delta^{-1}\sum_{e\in\mathcal{E}_k\setminus\mathcal{E}_{k+1}} h_e^{-1}\|\,(\mathsf{Id}-\mathsf{P}_{\mathsf{M}_0})\,[\![u_k^*]\!]\,\|_e^2 \\
&+ \frac{\delta}{4}\sum_{e\in\mathcal{E}_k\setminus\mathcal{E}_{k+1}} h_e\|\,(\mathsf{Id}-\Pi_k^{\mathrm{RT}})(\tilde{\boldsymbol{q}}_{k+1}^*-\boldsymbol{q}_k^*)\cdot\boldsymbol{n}\,\|_e^2 \\
&+ \frac{\delta}{4}\|\,(\mathsf{Id}-\Pi_k^{\mathrm{RT}})(\tilde{\boldsymbol{q}}_{k+1}^*-\boldsymbol{q}_k^*)\,\|_{\mathcal{R}_k}^2.
\end{aligned}
$$

The inequality (5.5.3) follows by using a scaling argument.

Step 3. Next, we show that

$$
\delta\mathsf{C}_5\|\,\tilde{\boldsymbol{q}}_{k+1}^*-\boldsymbol{q}_k^*\,\|_{\mathcal{R}_k}^2 \le \frac{\mathsf{C}_4}{5}\zeta_{div,k}^2(\mathcal{R}_k)+\frac{1}{4}\|\,\boldsymbol{q}_k-\boldsymbol{q}_{k+1}\,\|_\Omega^2, \tag{5.5.4}
$$

with a suitable choice of δ. We have

$$
\begin{aligned}
\|\,\tilde{\boldsymbol{q}}_{k+1}^*-\boldsymbol{q}_k^*\,\|_{\mathcal{R}_k}^2 &\le 2\|\,\boldsymbol{q}_{k+1}-\boldsymbol{q}_k\,\|_{\mathcal{R}_k}^2+2\|\,\tilde{\boldsymbol{q}}_{k+1}^*-\boldsymbol{q}_k^*-\boldsymbol{q}_{k+1}+\boldsymbol{q}_k\,\|_{\mathcal{R}_k}^2 \\
&\le (2+2\mathsf{C}_4C_\tau^2)\|\,\boldsymbol{q}_{k+1}-\boldsymbol{q}_k\,\|_\Omega^2+2\mathsf{C}_4\zeta_{div,k}^2(\mathcal{R}_k) \qquad \text{by Lemma 5.4.5} \\
&\le \frac{5}{2}\|\,\boldsymbol{q}_{k+1}-\boldsymbol{q}_k\,\|_\Omega^2+2\mathsf{C}_4\zeta_{div,k}^2(\mathcal{R}_k)
\end{aligned}
$$

by condition (5.5.1). The inequality (5.5.4) follows by taking $\delta=\frac{1}{10\mathsf{C}_5}$.

Step 4. Combining inequality (5.5.2), (5.5.3) and (5.5.4), we obtain

$$
\begin{aligned}
\|\,\boldsymbol{q}_{k+1}-\boldsymbol{q}_k\,\|_\Omega^2 \le C_3\zeta_{div,k}^2(\mathcal{R}_k)+\frac{3}{4}\|\,\boldsymbol{q}_{k+1}-\boldsymbol{q}_k\,\|_\Omega^2+C_3\|\,\boldsymbol{q}_k+\boldsymbol{\nabla}\,u_k^*\,\|_{\mathcal{R}_k}^2 \\
+\,C_3\sum_{e\in\mathcal{E}_k\setminus\mathcal{E}_{k+1}} h_e^{-1}\|\,(\mathsf{Id}-\mathsf{P}_{\mathsf{M}_0})\,[\![u_k^*]\!]\,\|_e^2.
\end{aligned}
$$

Now the lemma follows after subtracting $\frac{3}{4}\| \boldsymbol{q}_{k+1} - \boldsymbol{q}_k \|_\Omega^2$ to the left side. This completes the proof.

□

Step Three: Optimal Marking

A crucial step to prove Lemma 5.3.4 is to build a connection between the error reduction and the Dörfler marking strategy. Such a connection is stated in the following result.

Lemma 5.5.3. *Given two nested meshes $\mathcal{T}_k \le \mathcal{T}_{k+1}$ such that*

$$e_{k+1}^2 \le \mu\, e_k^2. \tag{5.5.5}$$

where

$$0 < \mu = \frac{1}{2}(1 - \frac{\theta}{\theta_*}) \quad \textit{and} \quad \theta_* = \frac{C_2}{2C_3}. \tag{5.5.6}$$

Assume that the marking parameter $\theta \le \theta_*$ and the constant C_τ in **A3** *satisfy*

$$C_\tau^2 < \frac{1}{2\gamma}. \tag{5.5.7}$$

Then the set $\mathcal{R}_k$ satisfies the marking strategy (5.2.5).

Proof. The proof is carried out in two steps.

Step 1. First, we show that

$$e_k^2 - 2e_{k+1}^2 \le 3\| \boldsymbol{q}_k - \boldsymbol{q}_{k+1} \|_\Omega^2 + \gamma \zeta_{div,k}^2(\mathcal{R}_k). \tag{5.5.8}$$

From the definition of the quasi-energy norm e_k^2,

$$\begin{aligned} e_k^2 - 2e_{k+1}^2 := & \| \boldsymbol{q} - \boldsymbol{q}_k \|_\Omega^2 - 2\| \boldsymbol{q} - \boldsymbol{q}_{k+1} \|_\Omega^2 \\ & + \gamma \sum_{K\in\mathcal{T}_k} h_K^2 \| \mathsf{P}_{W_k}^{\perp} f \|_K^2 - 2\gamma \sum_{K\in\mathcal{T}_{k+1}} h_K^2 \| \mathsf{P}_{W_{k+1}}^{\perp} f \|_K^2 \\ & + \gamma \sum_{K\in\mathcal{T}_k} \tau_K^2 h_K^2 \| \mathsf{P}_{\mathbf{V}_k}^{\perp} \boldsymbol{q}_k \|_K^2 - 2\gamma \sum_{K\in\mathcal{T}_{k+1}} \tau_K^2 h_K^2 \| \mathsf{P}_{\mathbf{V}_{k+1}}^{\perp} \boldsymbol{q}_{k+1} \|_K^2. \end{aligned}$$

By Young's inequality, we have

$$\| \boldsymbol{q} - \boldsymbol{q}_k \|_\Omega^2 - 2\| \boldsymbol{q} - \boldsymbol{q}_{k+1} \|_\Omega^2 \le 2\| \boldsymbol{q}_k - \boldsymbol{q}_{k+1} \|_\Omega^2.$$

Since $\mathsf{P}^{\perp}_{W_k} = \mathsf{P}^{\perp}_{W_{k+1}}$ on the set $\mathcal{T}_k \cap \mathcal{T}_{k+1}$, we note

$$\gamma \sum_{K\in\mathcal{T}_k} h_K^2 \| \mathsf{P}^{\perp}_{W_k} f \|_K^2 - 2\gamma \sum_{K\in\mathcal{T}_{k+1}} h_K^2 \| \mathsf{P}^{\perp}_{W_{k+1}} f \|_K^2 \le \gamma \sum_{K\in\mathcal{R}_k} h_K^2 \| \mathsf{P}^{\perp}_{W_k} f \|_K^2.$$

Similarly, since $\mathsf{P}^{\perp}_{\mathbf{V}_k} = \mathsf{P}^{\perp}_{\mathbf{V}_{k+1}}$ on the set $\mathcal{T}_k \cap \mathcal{T}_{k+1}$,

$$\begin{aligned}
&\gamma \sum_{K\in\mathcal{T}_k} \tau_K^2 h_K^2 \| \mathsf{P}^{\perp}_{\mathbf{V}_k} \boldsymbol{q}_k \|_K^2 - 2\gamma \sum_{K\in\mathcal{T}_{k+1}} \tau_K^2 h_K^2 \| \mathsf{P}^{\perp}_{\mathbf{V}_{k+1}} \boldsymbol{q}_{k+1} \|_K^2 \\
&\quad \le \gamma \sum_{K\in\mathcal{R}_k} \tau_K^2 h_K^2 \| \mathsf{P}^{\perp}_{\mathbf{V}_k} \boldsymbol{q}_k \|_K^2 + 2\gamma \sum_{K\in\mathcal{T}_k\cap\mathcal{T}_{k+1}} \tau_K^2 h_K^2 \| \mathsf{P}^{\perp}_{\mathbf{V}_k} (\boldsymbol{q}_k - \boldsymbol{q}_{k+1}) \|_K^2 \\
&\quad \le \gamma \sum_{K\in\mathcal{R}_k} \tau_K^2 h_K^2 \| \mathsf{P}^{\perp}_{\mathbf{V}_k} \boldsymbol{q}_k \|_K^2 + 2\gamma C_\tau^2 \| \boldsymbol{q}_k - \boldsymbol{q}_{k+1} \|_\Omega^2 \\
&\quad \le \gamma \sum_{K\in\mathcal{R}_k} \tau_K^2 h_K^2 \| \mathsf{P}^{\perp}_{\mathbf{V}_k} \boldsymbol{q}_k \|_K^2 + \| \boldsymbol{q}_k - \boldsymbol{q}_{k+1} \|_\Omega^2,
\end{aligned}$$

by (5.5.7). We conclude that

$$\begin{aligned}
e_k^2 - 2e_{k+1}^2 &\le 3\| \boldsymbol{q}_k - \boldsymbol{q}_{k+1} \|_\Omega^2 + \gamma \sum_{K\in\mathcal{R}_k} h_K^2 (\| \mathsf{P}^{\perp}_{W_k} f \|_K^2 + \tau_K^2 \| \mathsf{P}^{\perp}_{\mathbf{V}_k} \boldsymbol{q}_k \|_K^2) \\
&:= 3\| \boldsymbol{q}_k - \boldsymbol{q}_{k+1} \|_\Omega^2 + \gamma\, \zeta_{div,k}^2(\mathcal{R}_k).
\end{aligned}$$

Step 2. Our goal is to show that

$$\theta \zeta_k^2(\mathcal{T}_k) \le \zeta_k^2(\mathcal{R}_k). \tag{5.5.9}$$

From the efficiency of the estimator, Lemma 5.5.1, we have

$$\begin{aligned}
(1-2\mu) C_2 \zeta_k^2(\mathcal{T}_k) \le (1-2\mu) e_k^2 &\le e_k^2 - 2e_{k+1}^2 && \text{by (5.5.5)}, \\
&\le 3\| \boldsymbol{q}_k - \boldsymbol{q}_{k+1} \|_\Omega^2 + \gamma \zeta_{div,k}^2(\mathcal{R}_k),
\end{aligned}$$

by (5.5.8). By the localized upper bound, Lemma 5.5.2, we obtain

$$(1-2\mu) C_2 \zeta_k^2(\mathcal{T}_k) \le C_3 \zeta_k^2(\mathcal{R}_k).$$

We deduce that

$$\frac{(1-2\mu)C_2}{C_3} \zeta_k^2(\mathcal{T}_k) \le \zeta_k^2(\mathcal{R}_k).$$

Since, by (5.5.6), $\mu \le \frac{1}{2}(1 - \frac{\theta}{\theta_*})$ and $\theta_* := \frac{C_2}{2C_3}$. This completes the proof of (5.5.9).

$\square$

Step Four: Proof of Lemma 5.3.4

Thanks to this lemma, we show that the cardinality of the marked elements is controlled by the error reduction. To do so, let us first introduce the meshes overlay and an important property on the cardinality of the overlay mesh.

Given two meshes $\mathcal{T}_i$ and $\mathcal{T}_k$ in $\mathbb{T}$, we define the overlay $\mathcal{T}_j$ as the smallest conforming mesh in $\mathbb{T}$ such that $\mathcal{T}_i, \mathcal{T}_k \le \mathcal{T}_j$ and we denote $\mathcal{T}_j := \mathcal{T}_i \oplus \mathcal{T}_k$.

Lemma 5.5.4 (Overlay of meshes, [66, 30])**.** *Let $\mathcal{T}_0$ be an initial conforming mesh. Then, given* any *two meshes $\mathcal{T}_i, \mathcal{T}_k \in \mathbb{T}$, the overlay $\mathcal{T}_j := \mathcal{T}_i \oplus \mathcal{T}_k$ satisfies*

$$\#\mathcal{T}_j \le \#\mathcal{T}_i + \#\mathcal{T}_k - \#\mathcal{T}_0.$$

Now we are ready to prove Lemma 5.3.4.

Proof. Set $\psi^2 := \frac{\mu}{2} e_k^2$. According to the definition of the approximation class $\mathcal{A}_s$ (5.2.8), there exists a mesh $\mathcal{T}_i$ such that

$$e_i^2 \le \psi^2, \tag{5.5.10a}$$

$$\#\mathcal{T}_i - \#\mathcal{T}_0 \le \left\{ \frac{|(f, \boldsymbol{q})|_{\mathcal{A}_s}}{\psi} \right\}^{1/s}, \tag{5.5.10b}$$

where $e_i^2 := \| \boldsymbol{q} - \boldsymbol{q}_i \|_\Omega^2 + \gamma \zeta_{div,i}^2(\mathcal{T}_i)$. Let $\mathcal{T}_j := \mathcal{T}_k \oplus \mathcal{T}_i$ be the overlay of $\mathcal{T}_k$ and $\mathcal{T}_i$. Since $\mathcal{T}_j \ge \mathcal{T}_i$, by taking $\epsilon \le 1/4$ and $\delta_2 \le 1$ in Lemma 5.3.1, we obtain

$$e_j^2 \le 2 e_i^2$$

where $e_j^2 := \| \boldsymbol{q} - \boldsymbol{q}_j \|_\Omega^2 + \gamma \zeta_{div,j}^2(\mathcal{T}_j)$. In view of (5.5.10a),

$$e_j^2 \le 2\psi^2 := \mu e_k^2.$$

Hence, by Lemma 5.5.3, the refined set $\mathcal{R}_{\mathcal{T}_k \to \mathcal{T}_j}$ satisfies the marking strategy property (5.2.5). Since the marking procedure ensures the *minimal* cardinality of the marked set, we deduce that

$$\#\mathcal{M}_k \le \#\mathcal{R}_{\mathcal{T}_k \to \mathcal{T}_j} \le \#\mathcal{T}_j - \#\mathcal{T}_k \le \#\mathcal{T}_i - \#\mathcal{T}_0,$$

by Lemma 5.5.4. We conclude from inequality (5.5.10b) that

$$\#\mathcal{M}_k \le (2\mu)^{-\frac{1}{2s}} |f, \boldsymbol{q}|_{\mathcal{A}_s}^{\frac{1}{s}} e_k^{-\frac{1}{s}}.$$

This completes the proof. $\square$

5.6 Proof of Lemma 5.6.2

In this section, we are going to prove Lemma 5.6.2 which is used in Step 5 of the proof of the quasi-orthogonality inequality. It is worth mentioning that the derivation of this lemma depends solely on the property of the HDG methods. Here, we carry out the proof in three steps as follows.

Step One. We introduce a crucial trace residual decomposition. To state the result, let us introduce the following notation. We set

$$(\boldsymbol{q}_{k+1}, u_{k+1}) := \text{LOCAL\_SOLVER}(f_{k+1}, \widehat{u}_{k+1}, \tau_T, T),$$

where $(\boldsymbol{q}_{k+1}, u_{k+1})$ satisfies the equations defining the HDG methods (1.2.2a), (1.2.2b) and (1.2.2) for the element $T \in \mathcal{T}_{k+1}$.

Lemma 5.6.1 (Decomposition of the trace residual)**.** *Let Assumption* **A1** *be valid and set* $(\boldsymbol{q}_{k+1}, u_{k+1}) = \text{LOCAL\_SOLVER}(f_{k+1}, \widehat{u}_{k+1}, \tau_T, T)$. *Then, for each* $T \in \mathcal{T}_{k+1}$*, the trace residual admits a unique orthogonal decomposition*

$$\widehat{u}_{k+1} - u_{k+1} = w_{k+1} + \boldsymbol{v}_{k+1} \cdot \boldsymbol{n} \quad \text{on } \partial T,$$

where

$$w_{k+1} \in W^{\perp}(T) := \{w \in \mathcal{P}_p(T) \; : \; (w, \widetilde{w})_T = 0 \quad \forall \widetilde{w} \in \mathcal{P}_{p-1}(T)\},$$

$$\boldsymbol{v}_{k+1} \in \boldsymbol{V}^{\perp}(T) := \{\boldsymbol{v} \in \boldsymbol{\mathcal{P}}_p(T) \; : \; (\boldsymbol{v}, \widetilde{\boldsymbol{v}})_T = 0 \quad \forall \widetilde{\boldsymbol{v}} \in \boldsymbol{\mathcal{P}}_{p-1}(T)\}.$$

and

$$\langle w_{k+1}, \boldsymbol{v}_{k+1} \cdot \boldsymbol{n} \rangle_{\partial T} = 0.$$

Moreover,

$$\| w_{k+1} \|_{\partial T}^2 \simeq h_T \tau_T^{-2} \| \mathsf{P}_{W_{k+1}}^{\perp} f_{k+1} \|_T^2, \quad \| \boldsymbol{v}_{k+1} \cdot \boldsymbol{n} \|_{\partial T}^2 \simeq h_T \| \mathsf{P}_{\mathbf{V}_{k+1}}^{\perp} \boldsymbol{q}_{k+1} \|_T^2.$$

where the hidden constant depends only on the shape regularity constant σ *and the polynomial degree* p.

Proof. The decomposition

$$\widehat{u}_{k+1} - u_{k+1} = w_{k+1} + \boldsymbol{v}_{k+1} \cdot \boldsymbol{n} \quad \text{on } \partial T,$$

where $w_{k+1} \in W^{\perp}(T)$ and $\boldsymbol{v}_{k+1} \in \boldsymbol{V}^{\perp}(T)$, follows directly from a result established in [38] which states that each function

$$\hat{\mu} \in \mathcal{P}_p(\partial T) := \{\mu \in L^2(\partial T) : \ \mu|_e \in \mathcal{P}_p(e) \text{ for each } e \in \partial T\}$$

has a unique decomposition

$$\hat{\mu} = w + \boldsymbol{v} \cdot \boldsymbol{n} \quad \text{on } \partial T \quad \text{such that } \langle w, \boldsymbol{v} \cdot \boldsymbol{n} \rangle_{\partial T} = 0,$$

for some $w \in W^{\perp}(T)$ and $\boldsymbol{v} \in \boldsymbol{V}^{\perp}(T)$.

Here, we only need to prove that

$$\| w_{k+1} \|_{\partial T}^2 \simeq h_T \tau_T^{-2} \| \mathsf{P}_{W_{k+1}}^{\perp} f_{k+1} \|_T^2, \quad \| \boldsymbol{v}_{k+1} \cdot \boldsymbol{n} \|_{\partial T}^2 \simeq h_T \| \mathsf{P}_{\mathbf{V}_{k+1}}^{\perp} \boldsymbol{q}_{k+1} \|_T^2.$$

After a simple integration by parts, the first two equations defining the HDG method, (1.2.2a) and (1.2.2b), read

$$\begin{aligned} \langle u_{k+1} - \widehat{u}_{k+1}, \boldsymbol{v} \cdot \boldsymbol{n} \rangle_{\partial T} &= (\boldsymbol{q}_{k+1} + \boldsymbol{\nabla}\, u_{k+1}, \boldsymbol{v})_T, \\ \langle (\widehat{\boldsymbol{q}}_{k+1} - \boldsymbol{q}_{k+1}) \cdot \boldsymbol{n}, w \rangle_{\partial T} &= (f_{k+1} - \nabla \cdot \boldsymbol{q}_{k+1}, w)_T. \end{aligned}$$

for all $\boldsymbol{v} \in \boldsymbol{\mathcal{P}}_p(T)$ and $w \in \mathcal{P}_p(T)$. By the definition of the numerical flux, equation (1.2.2),

$$(\widehat{\boldsymbol{q}}_{k+1} - \boldsymbol{q}_{k+1}) \cdot \boldsymbol{n} = \tau_T (u_{k+1} - \widehat{u}_{k+1}).$$

In view of the Assumption **A1** and the orthogonal decomposition of the trace residual, we have

$$\begin{aligned} \langle \boldsymbol{v}_{k+1} \cdot \boldsymbol{n}, \boldsymbol{v} \cdot \boldsymbol{n} \rangle_{\partial T} &= (\boldsymbol{q}_{k+1} + \boldsymbol{\nabla}\, u_{k+1}, \boldsymbol{v})_T \quad \forall \boldsymbol{v} \in \boldsymbol{V}^{\perp}(T), \\ \tau_T \langle w_{k+1}, w \rangle_{\partial T} &= (f_{k+1} - \nabla \cdot \boldsymbol{q}_{k+1}, w)_T \quad \forall w \in W^{\perp}(T). \end{aligned}$$

To show that

$$\| w_{k+1} \|_{\partial T}^2 \preceq h_T \tau_T^{-2} \| \mathsf{P}_{W_{k+1}}^{\perp} f_{k+1} \|_T^2, \quad \| \boldsymbol{v}_{k+1} \cdot \boldsymbol{n} \|_{\partial T}^2 \preceq h_T \| \mathsf{P}_{\mathbf{V}_{k+1}}^{\perp} \boldsymbol{q}_{k+1} \|_T^2,$$

we take $w = w_{k+1}$ and $\boldsymbol{v} = \boldsymbol{v}_{k+1}$, use the Assumption **A1** and obtain

$$\| \boldsymbol{v}_{k+1} \cdot \boldsymbol{n} \|_{\partial T}^2 = (\boldsymbol{q}_{k+1}, \boldsymbol{v}_{k+1})_T, \quad \tau_K \| w_{k+1} \|_{\partial T}^2 = (f_{k+1}, w_{k+1})_T.$$

The estimate follows immediately from the standard inequalities that

$$\| \boldsymbol{v}_{k+1} \|_T \preceq h_T^{1/2} \| \boldsymbol{v}_{k+1} \cdot \boldsymbol{n} \|_{\partial T}, \quad \| w_{k+1} \|_T \preceq h_T^{1/2} \| w_{k+1} \|_{\partial T}.$$

The other direction of the inequalities can be proved in a similar fashion. We take $w = \mathsf{P}^{\perp}_{W_{k+1}} f_{k+1}$ and $\boldsymbol{v} = \mathsf{P}^{\perp}_{\mathbf{V}_{k+1}} \boldsymbol{q}_{k+1}$, and obtain

$$\begin{aligned} \| \mathsf{P}^{\perp}_{\mathbf{V}_{k+1}} \boldsymbol{q}_{k+1} \|_T^2 &= \langle \boldsymbol{v}_{k+1} \cdot \boldsymbol{n}, \mathsf{P}^{\perp}_{\mathbf{V}_{k+1}} \boldsymbol{q}_{k+1} \rangle_{\partial T}, \\ \| \mathsf{P}^{\perp}_{W_{k+1}} f_{k+1} \|_T^2 &= \langle \tau_K w_{k+1}, \mathsf{P}^{\perp}_{W_{k+1}} f_{k+1} \rangle_{\partial T}. \end{aligned}$$

The estimate follows from the inequality that

$$\begin{aligned} \| \mathsf{P}^{\perp}_{\mathbf{V}_{k+1}} \boldsymbol{q}_{k+1} \cdot \boldsymbol{n} \|_{\partial T} &\preceq h_T^{-1/2} \| \mathsf{P}^{\perp}_{\mathbf{V}_{k+1}} \boldsymbol{q}_{k+1} \|_T, \\ \| \mathsf{P}^{\perp}_{W_{k+1}} f_{k+1} \|_{\partial T} &\preceq h_T^{-1/2} \| \mathsf{P}^{\perp}_{W_{k+1}} f_{k+1} \|_T. \end{aligned}$$

This completes the proof of Lemma 5.6.1. □

Step Two. Thanks to this lemma, we can estimate $\| \boldsymbol{q}_{k+1} - \boldsymbol{q}^*_{k+1} \|_T^2$ as follows.

Lemma 5.6.2. *Let Assumption* **A1** *be valid and set*

$$(\boldsymbol{q}_{k+1}, u_{k+1}) := \text{LOCAL\_SOLVER}(f_{k+1}, \widehat{u}_{k+1}, \tau_T, T).$$

Then

$$\| \boldsymbol{q}_{k+1} - \boldsymbol{q}^*_{k+1} \|_T^2 \simeq h_T \| (\widehat{\boldsymbol{q}}_{k+1} - \boldsymbol{q}_{k+1}) \cdot \boldsymbol{n} \|_{\partial T}^2 \leq \mathsf{C}_1 \zeta_{div}^2 (f_{k+1}, \boldsymbol{q}_{k+1}, T).$$

Proof. By a standard scaling argument, we have

$$\begin{aligned} \| \boldsymbol{q}_{k+1} - \boldsymbol{q}^*_{k+1} \|_T^2 &\simeq h_T \| (\boldsymbol{q}_{k+1} - \boldsymbol{q}^*_{k+1}) \cdot \boldsymbol{n} \|_{\partial T}^2 \\ &= h_T \| (\boldsymbol{q}_{k+1} - \widehat{\boldsymbol{q}}_{k+1}) \cdot \boldsymbol{n} \|_{\partial T}^2, \quad \text{by (5.4.1b)}. \end{aligned}$$

By the definition of numerical flux, (1.2.2), we obtain

$$\| \boldsymbol{q}_{k+1} - \boldsymbol{q}^*_{k+1} \|_T^2 = h_T \| \tau_T (u_{k+1} - \widehat{u}_{k+1}) \|_{\partial T}^2.$$

Thanks to Assumption **A1** and the orthogonality decomposition in Lemma 5.6.1

$$\| \boldsymbol{q}_{k+1} - \boldsymbol{q}^*_{k+1} \|_T^2 = \tau_T^2 h_T (\| w_{k+1} \|_{\partial T}^2 + \| \boldsymbol{v}_{k+1} \cdot \boldsymbol{n} \|_{\partial T}^2).$$

By the estimate of $\| w_{k+1} \|_{\partial T}^2$ and $\| \boldsymbol{v}_{k+1} \cdot \boldsymbol{n} \|_{\partial T}^2$ in Lemma 5.6.1, we have

$$\begin{aligned} \| \boldsymbol{q}_{k+1} - \boldsymbol{q}_{k+1}^* \|_T^2 &\simeq h_T^2 \| \mathsf{P}_{W_{k+1}}^{\perp} f_{k+1} \|_T^2 + h_T^2 \tau_T^2 \| \mathsf{P}_{\mathbf{V}_{k+1}}^{\perp} \boldsymbol{q}_{k+1} \|_T^2 \\ &:= \zeta_{div}^2(f_{k+1}, \boldsymbol{q}_{k+1}, T). \end{aligned}$$

This concludes the proof of Lemma 5.6.2 . $\square$

Step Three. Proof of Lemma 5.4.5.

With a simple calculation, we have

$$\begin{aligned} T(\Omega) &\leq 2\| \boldsymbol{q}_{k+1} - \boldsymbol{q}_{k+1}^* - \boldsymbol{q}_k + \boldsymbol{q}_k^* \|_\Omega^2 + 2\| \tilde{\boldsymbol{q}}_{k+1}^* - \boldsymbol{q}_{k+1}^* \|_\Omega^2 \\ &\leq 2\| \boldsymbol{q}_{k+1} - \boldsymbol{q}_{k+1}^* - \boldsymbol{q}_k + \boldsymbol{q}_k^* \|_\Omega^2 + 2\mathsf{C}_2 osc^2(f_{k+1}, \mathcal{R}_k), \end{aligned}$$

by Lemma 5.4.3. Since $osc^2(f_{k+1}, \mathcal{R}_k) \leq \zeta_{div,k}^2(\mathcal{R}_k)$, we only need to show that

$$\| \boldsymbol{q}_{k+1} - \boldsymbol{q}_{k+1}^* - \boldsymbol{q}_k + \boldsymbol{q}_k^* \|_\Omega^2 \preceq \zeta_{div,k}^2(\mathcal{R}_k) + C_\tau^2 \| \boldsymbol{q}_{k+1} - \boldsymbol{q}_k \|_\Omega^2.$$

To do so, we divide the set $\mathcal{T}_k$ into the set of refined elements $\mathcal{R}_k$ and the set of unrefined elements $\mathcal{T}_{k+1} \cap \mathcal{T}_k$.

Step 1. For the unrefined set $\mathcal{T}_{k+1} \cap \mathcal{T}_k$, thanks to Assumption **A2**, we have

$$(\boldsymbol{q}_{k+1} - \boldsymbol{q}_k, u_{k+1} - u_k) = \text{LOCAL\_SOLVER}(0, \widehat{u}_{k+1} - \widehat{u}_k, \tau_T, T)$$

for all $T \in \mathcal{T}_{k+1} \cap \mathcal{T}_k$. By Lemma 5.6.2,

$$\begin{aligned} \| \boldsymbol{q}_{k+1} - \boldsymbol{q}_{k+1}^* - \boldsymbol{q}_k + \boldsymbol{q}_k^* \|_T^2 &\leq \mathsf{C}_1 \zeta_{div}^2(0, \boldsymbol{q}_{k+1} - \boldsymbol{q}_k, T) \\ &:= \mathsf{C}_1 \tau_T^2 h_T^2 \| \mathsf{P}_{\mathbf{V}_{k+1}}^{\perp} (\boldsymbol{q}_{k+1} - \boldsymbol{q}_k) \|_T^2. \end{aligned}$$

Summing over $T \in \mathcal{T}_{k+1} \cap \mathcal{T}_k$, we obtain

$$\begin{aligned} \| \boldsymbol{q}_{k+1} - \boldsymbol{q}_{k+1}^* - \boldsymbol{q}_k + \boldsymbol{q}_k^* \|_{\mathcal{T}_{k+1} \cap \mathcal{T}_k}^2 &\leq \mathsf{C}_1 C_\tau^2 \sum_{T \in \mathcal{T}_{k+1} \cap \mathcal{T}_k} \| \mathsf{P}_{\mathbf{V}_{k+1}}^{\perp} (\boldsymbol{q}_k - \boldsymbol{q}_{k+1}) \|_T^2 \\ &\leq \mathsf{C}_1 C_\tau^2 \| \boldsymbol{q}_k - \boldsymbol{q}_{k+1} \|_\Omega^2. \end{aligned}$$

Step 2. It remains to show that, for the set $\mathcal{R}_k$,

$$\| \boldsymbol{q}_{k+1} - \boldsymbol{q}_{k+1}^* - \boldsymbol{q}_k + \boldsymbol{q}_k^* \|_{\mathcal{R}_k}^2 \preceq \zeta_{div,k}^2(\mathcal{R}_k) + C_\tau^2 \| \boldsymbol{q}_{k+1} - \boldsymbol{q}_k \|_\Omega^2.$$

Since

$$
\begin{aligned}
\| \boldsymbol{q}_{k+1} - \boldsymbol{q}^*_{k+1} - \boldsymbol{q}_k + \boldsymbol{q}^*_k \|^2_{\mathcal{R}_k} &\leq 2\| \boldsymbol{q}_{k+1} - \boldsymbol{q}^*_{k+1} \|^2_{\mathcal{R}_k} + 2\| \boldsymbol{q}_k - \boldsymbol{q}^*_k \|^2_{\mathcal{R}_k} \\
&\leq 2\| \boldsymbol{q}_{k+1} - \boldsymbol{q}^*_{k+1} \|^2_{\mathcal{N}_{k+1}} + 2\| \boldsymbol{q}_k - \boldsymbol{q}^*_k \|^2_{\mathcal{R}_k},
\end{aligned}
$$

we obtain

$$
\| \boldsymbol{q}_{k+1} - \boldsymbol{q}^*_{k+1} - \boldsymbol{q}_k + \boldsymbol{q}^*_k \|^2_{\mathcal{R}_k} \leq 2\mathsf{C}_1 \{ \zeta^2_{div,k}(\mathcal{R}_k) + \zeta^2_{div,k+1}(\mathcal{N}_{k+1}) \}.
$$

by Lemma 5.6.2. Now, we see that it is sufficient to show that

$$
\zeta^2_{div,k+1}(\mathcal{N}_{k+1}) \leq 2\zeta^2_{div,k}(\mathcal{R}_k) + 2 \sum_{T \in \mathcal{N}_{k+1}} \tau^2_T h^2_T \| \boldsymbol{q}_{k+1} - \boldsymbol{q}_k \|^2_T.
$$

To do so, we note that

$$
\begin{aligned}
\zeta^2_{div,k+1}(\mathcal{N}_{k+1}) &:= \sum_{T \in \mathcal{N}_{k+1}} h^2_T \| \mathsf{P}^{\perp}_{W_{k+1}} f \|^2_T + \sum_{T \in \mathcal{N}_{k+1}} \tau^2_T h^2_T \| \mathsf{P}^{\perp}_{\mathbf{V_{k+1}}} \boldsymbol{q}_{k+1} \|^2_T \\
&\leq \sum_{T \in \mathcal{N}_{k+1}} h^2_T \| \mathsf{P}^{\perp}_{W_{k+1}} f \|^2_T + 2 \sum_{T \in \mathcal{N}_{k+1}} \tau^2_T h^2_T \| \mathsf{P}^{\perp}_{\mathbf{V_{k+1}}} \boldsymbol{q}_k \|^2_T \\
&\quad + 2 \sum_{T \in \mathcal{N}_{k+1}} \tau^2_T h^2_T \| \mathsf{P}^{\perp}_{\mathbf{V_{k+1}}} (\boldsymbol{q}_k - \boldsymbol{q}_{k+1}) \|^2_T.
\end{aligned}
$$

Since $\| \mathsf{P}^{\perp}_{\mathbf{V_{k+1}}} \boldsymbol{q}_k \|_T \leq \| \mathsf{P}^{\perp}_{\mathbf{V_k}} \boldsymbol{q}_k \|_T$ and $\| \mathsf{P}^{\perp}_{W_{k+1}} f \|_T \leq \| \mathsf{P}^{\perp}_{W_k} f \|_T$, we obtain

$$
\begin{aligned}
\zeta^2_{div,k+1}(\mathcal{N}_{k+1}) \leq& \sum_{T \in \mathcal{N}_{k+1}} h^2_T \| \mathsf{P}^{\perp}_{W_k} f \|_T + 2 \sum_{T \in \mathcal{N}_{k+1}} \tau^2_T h^2_T \| \mathsf{P}^{\perp}_{\mathbf{V_k}} \boldsymbol{q}_k \|^2_T \\
&+ 2C^2_{\tau} \| \boldsymbol{q}_k - \boldsymbol{q}_{k+1} \|^2_{\Omega} \\
\leq& \sum_{K \in \mathcal{R}_k} h^2_K \| \mathsf{P}^{\perp}_{W_k} f \|^2_K + 2 \sum_{K \in \mathcal{R}_k} \tau^2_K h^2_K \| \mathsf{P}^{\perp}_{\mathbf{V_k}} \boldsymbol{q}_k \|^2_K \\
&+ 2C^2_{\tau} \| \boldsymbol{q}_k - \boldsymbol{q}_{k+1} \|^2_{\Omega},
\end{aligned}
$$

by (5.2.6) that $h_T \leq h_K$ provided that $T \subset K$. This completes the proof.

5.7 Proof of Lemma 5.4.3

In this section, we are going to prove the stability property of the HDG method as we claim in Lemma 5.4.3. Note that the proof is based on the trace residual decomposition which is introduced in the previous section. Let us start by gathering several preliminary results.

Let $(\bar{\boldsymbol{q}}_{k+1}, \bar{u}_{k+1}, \widehat{\bar{u}}_{k+1}) = \text{SOLVE}(f_k - f_{k+1}, \mathcal{T}_{k+1})$ and $\bar{\boldsymbol{q}}^*_{k+1}$ be the corresponding post-processed flux. To show Lemma 5.4.3, we only need to show that

$$\| \bar{\boldsymbol{q}}^*_{k+1} \|^2_{\mathcal{T}_{k+1}} \leq \mathsf{C}_2 osc^2(f_{k+1}, \mathcal{T}_k).$$

To do so, we start by introducing a special vector field $\boldsymbol{\Phi} \in \boldsymbol{L}^2(\Omega)$ and a flux projection $\Pi_{\mathbf{V}_{k+1}}$.

For each element $K \in \mathcal{T}_k$, there exists a vector field $\boldsymbol{\Phi}_K \in H^1(\Omega)$ with compact support in K such that

$$\nabla\cdot \boldsymbol{\Phi}_K = f_{k+1} - f_k \quad \text{in } K,$$

satisfying

$$\| \boldsymbol{\Phi}_K \|_{H^1(\Omega)} \leq C_{reg} \| f_{k+1} - f_k \|_{L^2(K)}.$$

where the constant C_{reg} depends only on the shape regularity of K, see [20, 10, 42]. We construct the vector filed

$$\boldsymbol{\Phi} = \sum_{K \in \mathcal{R}_k} \boldsymbol{\Phi}_K.$$

Since $\boldsymbol{\Phi}_K$ vanishes outside the element K, we have that $\boldsymbol{\Phi}$ satisfies the elliptic regularity

$$\| \boldsymbol{\nabla} \boldsymbol{\Phi} \|_K = \| \boldsymbol{\nabla} \boldsymbol{\Phi}_K \|_K \leq C_{reg} \| f_{k+1} - f_k \|_{L^2(K)} \tag{5.7.1}$$

for each $K \in \mathcal{R}_k$.

We also remind the reader that, for all $T \in \mathcal{T}_{k+1}$, there exists a well-defined projection from $\boldsymbol{H}(\text{div}, T)$ to $\boldsymbol{\mathcal{P}}_k(T)$ such that

$$(\boldsymbol{\Phi} - \Pi_{\boldsymbol{V}_{k+1}} \boldsymbol{\Phi}, \boldsymbol{v})_T = 0 \quad \forall \boldsymbol{v} \in \boldsymbol{\mathcal{P}}_{k-1}(T), \tag{5.7.2}$$

$$\langle (\boldsymbol{\Phi} - \Pi_{\boldsymbol{V}_{k+1}} \boldsymbol{\Phi}) \cdot \boldsymbol{n}, \boldsymbol{v} \cdot \boldsymbol{n} \rangle_{\partial T} = 0 \quad \forall \boldsymbol{v} \in \boldsymbol{\mathcal{P}}^{\perp}_k(T), \tag{5.7.3}$$

see Section 6 in [39] Moreover, the projection so-defined has the approximation property that

$$\| \boldsymbol{\Phi} - \Pi_{\boldsymbol{V}_{k+1}} \boldsymbol{\Phi} \|^2_T \preceq h^2_T \| \boldsymbol{\Phi} \|^2_{H^1(T)}. \tag{5.7.4}$$

Now we are ready to prove the lemma.

Proof of Lemma 5.4.3. We divide the proof into five steps.

Step One. Our first goal is to establish the following energy identity,

$$\|\,\bar{\boldsymbol{q}}_{k+1}\,\|^2_{\mathcal{T}_{k+1}} + \|\,\tau_T^{1/2}(\widehat{\bar{u}}_{k+1} - \bar{u}_{k+1})\,\|^2_{\partial\mathcal{T}_{k+1}} = (f_{k+1} - f_k, \bar{u}_{k+1})_{\mathcal{T}_{k+1}}. \tag{5.7.5}$$

From the following equations defining the HDG method,

$$\begin{aligned}
(\bar{\boldsymbol{q}}_{k+1}, \boldsymbol{v})_{\mathcal{T}_{k+1}} - (\bar{u}_{k+1}, \nabla\cdot \boldsymbol{v})_{\mathcal{T}_{k+1}} &= -\langle \widehat{\bar{u}}_{k+1}, \boldsymbol{v}\cdot\boldsymbol{n}\rangle_{\partial\mathcal{T}_{k+1}} && \forall \boldsymbol{v} \in \boldsymbol{V}_{k+1}\\
-(\bar{\boldsymbol{q}}_{k+1}, \boldsymbol{\nabla}\, w)_{\mathcal{T}_{k+1}} + \langle \widehat{\bar{\boldsymbol{q}}}_{k+1}\cdot\boldsymbol{n}, w\rangle_{\partial\mathcal{T}_{k+1}} &= (f_{k+1} - f_k, w)_{\mathcal{T}_{k+1}} && \forall w \in W_{k+1},
\end{aligned}$$

we take $\boldsymbol{v} = \bar{\boldsymbol{q}}_{k+1}$ and $w = \bar{u}_{k+1}$, add up two equations and obtain, after some algebraic manipulations, that

$$\begin{aligned}
\|\,\bar{\boldsymbol{q}}_{k+1}\,\|^2_{\mathcal{T}_{k+1}} &+ \langle(\widehat{\bar{\boldsymbol{q}}}_{k+1} - \bar{\boldsymbol{q}}_{k+1})\cdot\boldsymbol{n}, \bar{u}_{k+1} - \widehat{\bar{u}}_{k+1}\rangle_{\partial\mathcal{T}_{k+1}}\\
&= (f_{k+1} - f_k, \bar{u}_{k+1})_{\mathcal{T}_{k+1}} - \langle \widehat{\bar{\boldsymbol{q}}}_{k+1}\cdot\boldsymbol{n}, \widehat{\bar{u}}_{k+1}\rangle_{\partial\mathcal{T}_{k+1}}.
\end{aligned}$$

Thanks to the transmission condition (1.2.3b) and the homogeneous boundary condition (1.2.3a), we have

$$\langle \widehat{\bar{\boldsymbol{q}}}_{k+1}\cdot\boldsymbol{n}, \widehat{\bar{u}}_{k+1}\rangle_{\partial\mathcal{T}_{k+1}} = 0.$$

The energy identity (5.7.5) follows from the definition of $\widehat{\bar{\boldsymbol{q}}}_{k+1}$, (1.2.2).

Step Two. Our second goal is to show the following duality identity,

$$\begin{aligned}
(f_{k+1} - f_k, \bar{u}_{k+1}) &= (\bar{\boldsymbol{q}}_{k+1}, (\Pi_{\boldsymbol{V}_{k+1}} - \Pi_k^{\mathrm{RT}})\boldsymbol{\Phi})_{\mathcal{T}_{k+1}}\\
&\quad + \langle \bar{u}_{k+1} - \widehat{\bar{u}}_{k+1}, (\boldsymbol{\Phi} - \Pi_{\boldsymbol{V}_{k+1}}\boldsymbol{\Phi})\cdot\boldsymbol{n}\rangle_{\partial\mathcal{T}_{k+1}}.
\end{aligned} \tag{5.7.6}$$

where Π_k^{RT} denotes the Raviart-Thomas projection into the RT space $\mathrm{RT}_p(\mathcal{T}_k)$.

We start from the equation

$$\begin{aligned}
(f_{k+1} - f_k, \bar{u}_{k+1}) &= (\bar{u}_{k+1}, \nabla\cdot\boldsymbol{\Phi})_{\mathcal{T}_{k+1}}\\
&= \langle \bar{u}_{k+1}, \boldsymbol{\Phi}\cdot\boldsymbol{n}\rangle_{\partial\mathcal{T}_{k+1}} - (\boldsymbol{\nabla}\,\bar{u}_{k+1}, \boldsymbol{\Phi})\\
&= \langle \bar{u}_{k+1}, \boldsymbol{\Phi}\cdot\boldsymbol{n}\rangle_{\partial\mathcal{T}_{k+1}} - (\boldsymbol{\nabla}\,\bar{u}_{k+1}, \Pi_{\boldsymbol{V}_{k+1}}\boldsymbol{\Phi}) \qquad \text{by (5.7.2),}\\
&= (\bar{u}_{k+1}, \nabla\cdot\Pi_{\boldsymbol{V}_{k+1}}\boldsymbol{\Phi})_{\mathcal{T}_{k+1}}\\
&\quad + \langle \bar{u}_{k+1}, (\boldsymbol{\Phi} - \Pi_{\boldsymbol{V}_{k+1}}\boldsymbol{\Phi})\cdot\boldsymbol{n}\rangle_{\partial\mathcal{T}_{k+1}}\\
&= (\bar{\boldsymbol{q}}_{k+1}, \Pi_{\boldsymbol{V}_{k+1}}\boldsymbol{\Phi})_{\mathcal{T}_{k+1}} + \langle \widehat{\bar{u}}_{k+1}, \boldsymbol{\Phi}\cdot\boldsymbol{n}\rangle_{\partial\mathcal{T}_{k+1}}\\
&\quad + \langle \bar{u}_{k+1} - \widehat{\bar{u}}_{k+1}, (\boldsymbol{\Phi} - \Pi_{\boldsymbol{V}_{k+1}}\boldsymbol{\Phi})\cdot\boldsymbol{n}\rangle_{\partial\mathcal{T}_{k+1}},
\end{aligned}$$

by (1.2.2a). Due to the homogeneous boundary condition (1.2.3a), we obtain

$$\begin{aligned}(f_{k+1}-f_k,\bar u_{k+1}) &= (\bar{\boldsymbol q}_{k+1},\Pi_{\boldsymbol V_{k+1}}\boldsymbol\Phi)_{\mathcal T_{k+1}}\\ &\qquad + \langle \bar u_{k+1}-\widehat{\bar u}_{k+1},(\boldsymbol\Phi-\Pi_{\boldsymbol V_{k+1}}\boldsymbol\Phi)\cdot\boldsymbol n\rangle_{\partial\mathcal T_{k+1}}.\end{aligned}$$

To prove the duality identity (5.7.6), it remains to show that

$$(\bar{\boldsymbol q}_{k+1},\Pi_k^{\mathrm{RT}}\boldsymbol\Phi)_{\mathcal T_{k+1}}=0.$$

We note that

$$\nabla\cdot\Pi_k^{\mathrm{RT}}\boldsymbol\Phi=\mathsf P_{W_k}\,\nabla\cdot\boldsymbol\Phi=\mathsf P_{W_k}(f_{k+1}-f_k)=0,$$

which implies that $\Pi_k^{\mathrm{RT}}\boldsymbol\Phi$ belongs to $\boldsymbol V_k$. We also note that $\Pi_k^{\mathrm{RT}}\boldsymbol\Phi$ belongs to $\boldsymbol H(\mathrm{div},\Omega)$. By the first equation defining the HDG method, (1.2.2a), we obtain

$$\begin{aligned}(\bar{\boldsymbol q}_{k+1},\Pi_k^{\mathrm{RT}}\boldsymbol\Phi)_{\mathcal T_{k+1}} &= (\bar u_{k+1},\nabla\cdot\Pi_{\boldsymbol V_k}^{\mathrm{RT}}\boldsymbol\Phi)_{\mathcal T_{k+1}}-\langle\widehat{\bar u}_{k+1},\Pi_k^{\mathrm{RT}}\boldsymbol\Phi\cdot\boldsymbol n\rangle_{\partial\mathcal T_{k+1}}\\ &=0.\end{aligned}$$

This proves the duality identity (5.7.6).

Step Three. According to the trace residual decomposition, Lemma 5.6.1, we have

$$\widehat{\bar u}_{k+1}-\bar u_{k+1}=\bar w_{k+1}+\bar{\boldsymbol v}_{k+1}\cdot\boldsymbol n.$$

Our third goal is to show that, for each $T\in\mathcal T_{k+1}$,

$$(\mathsf P_{\partial T}-\Pi_{\boldsymbol V_{k+1}})\boldsymbol\Phi\cdot\boldsymbol n=\tau_T\bar w_{k+1}\quad\text{ on }\partial T. \tag{5.7.7}$$

We note the function $(\mathsf P_{\partial K}-\Pi_{\boldsymbol V_{k+1}})\boldsymbol\Phi\cdot\boldsymbol n$ defined on the boundary of T belongs to $\mathcal P_p(\partial K)$. By the orthogonal decomposition in Lemma 5.6.1, it can be decomposed as

$$(\mathsf P_{\partial K}-\Pi_{\boldsymbol V_{k+1}})\boldsymbol\Phi\cdot\boldsymbol n=w_{\boldsymbol\Phi}+\boldsymbol v_{\boldsymbol\Phi}\cdot\boldsymbol n$$

where $w_{\boldsymbol\Phi}\in W^\perp(T)$ and $\boldsymbol v_{\boldsymbol\Phi}\in\boldsymbol V^\perp(T)$. Due to the definition of $\Pi_{\mathbf V_{k+1}}$ (5.7.3), we immediately have that $\boldsymbol v_{\boldsymbol\Phi}=0$. Thus, thanks to Assumption **A1**, to prove (5.7.7), we only need to show that

$$\langle(\mathsf P_{\partial T}-\Pi_{\boldsymbol V_{k+1}})\boldsymbol\Phi\cdot\boldsymbol n,w\rangle_{\partial T}=\langle\tau_T\bar w_{k+1},w\rangle_{\partial T}\quad\forall w\in W^\perp(T).$$

After an integration by parts, we obtain, for all $w \in W^{\perp}(T)$,

$$\begin{aligned}
\langle (\mathsf{P}_{\partial T} - \Pi_{\boldsymbol{V}_{k+1}})\boldsymbol{\Phi}\cdot\boldsymbol{n}, w\rangle_{\partial T} &= (\boldsymbol{\Phi} - \Pi_{\boldsymbol{V}_{k+1}}\boldsymbol{\Phi}, \boldsymbol{\nabla}\, w)_T \\
&\quad + (\nabla\cdot(\boldsymbol{\Phi} - \Pi_{\boldsymbol{V}_{k+1}}\boldsymbol{\Phi}), w)_T \\
&= (\nabla\cdot\boldsymbol{\Phi}, w)_T && \text{by (5.7.2)} \\
&= (f_{k+1} - f_k, w)_T
\end{aligned}$$

By the second equation defining the HDG methods (1.2.2b),

$$\begin{aligned}
\langle (\mathsf{P}_{\partial T} - \Pi_{\boldsymbol{V}_{k+1}})\boldsymbol{\Phi}\cdot\boldsymbol{n}, w\rangle_{\partial T} &= -(\bar{\boldsymbol{q}}_{k+1}, \boldsymbol{\nabla}\, w)_T + \langle \widehat{\bar{\boldsymbol{q}}}_{k+1}\cdot\boldsymbol{n}, w\rangle_{\partial T} \\
&= \langle (\widehat{\bar{\boldsymbol{q}}}_{k+1} - \bar{\boldsymbol{q}}_{k+1})\cdot\boldsymbol{n}, w\rangle_{\partial T} + (\nabla\cdot\boldsymbol{q}_{k+1}, w)_T
\end{aligned}$$

By the defintion of the numerical flux (1.2.2),

$$\begin{aligned}
\langle (\mathsf{P}_{\partial T} - \Pi_{\boldsymbol{V}_{k+1}})\boldsymbol{\Phi}\cdot\boldsymbol{n}, w\rangle_{\partial T} &= \langle \tau_T(\bar{u}_{k+1} - \widehat{\bar{u}}_{k+1}), w\rangle_{\partial T} \\
&= \langle \tau_T \bar{w}_{k+1}, w\rangle_{\partial T} + \langle \tau_T \bar{\boldsymbol{v}}_{k+1}\cdot\boldsymbol{n}, w\rangle_{\partial T},
\end{aligned}$$

by the trace residual decomposition in Lemma 5.6.1. By Assumption **A1**, $\langle \tau_T \bar{\boldsymbol{v}}_{k+1}\cdot\boldsymbol{n}, w\rangle_{\partial T} = \tau_T\langle \bar{\boldsymbol{v}}_{k+1}\cdot\boldsymbol{n}, w\rangle_{\partial T} = 0$ for all $w \in \mathcal{P}_p^{\perp}(T)$, the claim (5.7.7) follows.

Step Four. Next, we show

$$\|\,\bar{\boldsymbol{q}}_{k+1}\,\|^2_{\mathcal{T}_{k+1}} \le C^2_{reg} \sum_{K\in\mathcal{T}_k} h_K^2 \|\, f_{k+1} - f_k\,\|^2_K. \tag{5.7.8}$$

Combining the energy identity (5.7.5) and the duality identity (5.7.6), we obtain

$$\begin{aligned}
\|\,\bar{\boldsymbol{q}}_{k+1}\,\|^2_{\Omega} = (\bar{\boldsymbol{q}}_{k+1}, (\Pi_{\boldsymbol{V}_{k+1}} - \Pi_k^{\mathrm{RT}})\boldsymbol{\Phi})_{\mathcal{T}_{k+1}} - \|\,\tau_T^{1/2}(\widehat{\bar{u}}_{k+1} - \bar{u}_{k+1})\,\|^2_{\partial\mathcal{T}_{k+1}} \\
+ \langle \bar{u}_{k+1} - \widehat{\bar{u}}_{k+1}, (\mathsf{P}_{\partial T}\boldsymbol{\Phi} - \Pi_{\boldsymbol{V}_{k+1}}\boldsymbol{\Phi})\cdot\boldsymbol{n}\rangle_{\partial\mathcal{T}_{k+1}}
\end{aligned}$$

In view of the trace residual decomposition, Lemma 5.6.1, and (5.7.7), we have

$$\begin{aligned}
\|\,\bar{\boldsymbol{q}}_{k+1}\,\|^2_{\Omega} &= (\bar{\boldsymbol{q}}_{k+1}, (\Pi_{\boldsymbol{V}_{k+1}} - \Pi_k^{\mathrm{RT}})\boldsymbol{\Phi})_{\mathcal{T}_{k+1}} - \|\,\tau_T^{1/2}\bar{w}_{k+1}\,\|^2_{\partial\mathcal{T}_{k+1}} \\
&\quad - \|\,\tau_T^{1/2}(\bar{\boldsymbol{v}}_{k+1}\cdot\boldsymbol{n})\,\|^2_{\partial\mathcal{T}_{k+1}} + \langle \bar{u}_{k+1} - \widehat{\bar{u}}_{k+1}, \tau_T\bar{w}_{k+1}\rangle_{\partial\mathcal{T}_{k+1}} \\
&= (\bar{\boldsymbol{q}}_{k+1}, (\Pi_{\boldsymbol{V}_{k+1}} - \Pi_k^{\mathrm{RT}})\boldsymbol{\Phi})_{\mathcal{T}_{k+1}} - \|\,\tau_T^{1/2}(\bar{\boldsymbol{v}}_{k+1}\cdot\boldsymbol{n})\,\|^2_{\partial\mathcal{T}_{k+1}} \\
&\le (\bar{\boldsymbol{q}}_{k+1}, (\Pi_{\boldsymbol{V}_{k+1}} - \Pi_k^{\mathrm{RT}})\boldsymbol{\Phi})_{\mathcal{T}_{k+1}}.
\end{aligned}$$

Hence, by the approximation properties of $\Pi_{\boldsymbol{V}_{k+1}}$ and Π_k^{RT}, we obtain

$$\| \bar{\boldsymbol{q}}_{k+1} \|^2_{\mathcal{T}_{k+1}} \leq \| (\Pi_{\boldsymbol{V}_{k+1}} - \Pi_k^{\mathrm{RT}})\boldsymbol{\Phi} \|^2_{\Omega} \preceq \sum_{K\in\mathcal{T}_k} h_K^2 \| \boldsymbol{\nabla} \boldsymbol{\Phi} \|^2_K.$$

By the regularity of the vector field $\boldsymbol{\Phi}$ (5.7.1), we have

$$\| \bar{\boldsymbol{q}}_{k+1} \|^2_{\mathcal{T}_{k+1}} \preceq \sum_{K\in\mathcal{T}_k} h_K^2 \| f_{k+1} - f_k \|^2_K.$$

Step Five. Now we are in the position to prove the lemma. By Young's inequality, we have

$$\| \bar{\boldsymbol{q}}^*_{k+1} \|^2_{\mathcal{T}_{k+1}} \leq 2\| \bar{\boldsymbol{q}}_{k+1} \|^2_{\mathcal{T}_{k+1}} + 2\| \bar{\boldsymbol{q}}^*_{k+1} - \bar{\boldsymbol{q}}_{k+1} \|^2_{\mathcal{T}_{k+1}}$$

By Lemma 5.6.2, we obtain

$$\begin{aligned}
\| \bar{\boldsymbol{q}}^*_{k+1} \|^2_{\mathcal{T}_{k+1}} &\leq 2\| \bar{\boldsymbol{q}}_{k+1} \|^2_{\mathcal{T}_{k+1}} + 2\mathsf{C}_1 \sum_{T\in\mathcal{T}_{k+1}} h_T^2 \tau_T^2 \| \mathsf{P}^{\perp}_{\mathbf{V}_{k+1}} \bar{\boldsymbol{q}}_{k+1} \|^2_T \\
&\quad + 2\mathsf{C}_1 \sum_{T\in\mathcal{T}_{k+1}} h_T^2 \| \mathsf{P}^{\perp}_{W_{k+1}} (f_{k+1} - f_k) \|^2_T \\
&\leq 2(\mathsf{C}_1 C_\tau^2 + 1)\| \bar{\boldsymbol{q}}_{k+1} \|^2_{\Omega} + 2\mathsf{C}_1 osc^2(f_{k+1}, \mathcal{R}_k).
\end{aligned}$$

By the condition on C_τ (5.3.1a) and (5.7.8),

$$\| \bar{\boldsymbol{q}}^*_{k+1} \|^2_{\mathcal{T}_{k+1}} \leq \{2(\mathsf{C}_1 + 1)C_{reg}^2 + 2\mathsf{C}_1\} osc^2(f_{k+1}, \mathcal{R}_k).$$

This completes the proof of Lemma 5.4.3. $\square$

Chapter 6

Conclusion and Discussion

Let us note that the convergence and quasi-optimality of the AHDG methods work not only for simplexes but for other elements like, for example, rectangular and cube elements.

The result could be generalized to second-order elliptic equations in divergence form whose coefficients are piecewise-constant and mixed boundary conditions, that is,

$$\begin{aligned} u &= g \qquad \text{on } \partial\Omega_D, \\ \boldsymbol{q}\cdot\boldsymbol{n} &= \boldsymbol{q}_N \qquad \text{on } \partial\Omega_N, \end{aligned}$$

where g is the restriction to $\partial\Omega$ of a piece-wise polynomial function and $\boldsymbol{q}_N$ restricted on the boundary edges $e \in \mathcal{E}^{\partial}$ is a polynomial in the finite element space $\mathcal{P}_k(e)$.

The convergence and quasi-optimality of the adaptive method for other problems, for example, convection-diffusion equation and Stokes equation, remains an open problem. The study on these topics will constitute the subject of ongoing work.

References

[1] M. Ainsworth. A posteriori error estimation for lowest order Raviart-Thomas mixed finite elements. *SIAM J. Sci. Comput.*, 30, 2007/08.

[2] M. Ainsworth, *A posteriori error estimation for discontinuous Galerkin finite element approximation*, SIAM J. Numer. Anal., 45 (2007), pp. 1777–1798 (electronic).

[3] M. Ainsworth and J. T. Oden A posteriori error estimation in finite element analysis, Pure and Applied Mathematics (New York), (2000).

[4] M. Ainsworth and K. Pinchedez. *hp*-approximation theory for BDFM and RT finite elements on quadrilaterals. *SIAM J. Numer. Anal.*, 40:2047–2068 (electronic) (2003), 2002.

[5] M. Ainsworth and R. Rankin, *Fully computable error bounds for discontinuous Galerkin finite element approximations on meshes with an arbitrary number of levels of hanging nodes*, SIAM J. Numer. Anal., 47 (2010), pp. 4112–4141.

[6] A. Alonso. Error estimators for a mixed method. *Numer. Math.*, 74:385–395, 1996.

[7] D. N. Arnold and F. Brezzi, *Mixed and nonconforming finite element methods: implementation, postprocessing and error estimates*, RAIRO Modél. Math. Anal. Numér. **19** (1985), 7–32.

[8] D. N. Arnold, F. Brezzi, B. Cockburn and L. D. Marini, *Unified analysis of discontinuous Galerkin methods for elliptic problems*, SIAM J. on Numer. Anal. **39** (2002), 1749–1779.

[9] D. N. Arnold, A. Mukherjee, and L. Pouly. Locally adapted tetrahedral meshes using bisection. *SIAM J. Sci. Comput.*, 22(2):431–448, 2000.

[10] D. N. Arnold., L. R. Scott, and M. Vogelius. Regular inversion of the divergence operator with Dirichlet boundary conditions on a polygon. *Ann. Scuola Norm. Sup. Pisa Cl. Sci. (4)*, 15(2):169–192 (1989), 1988.

[11] I. Babuška, and W. C. Rheinboldt. Error estimates for adaptive finite element computations. *SIAM J. Numer. Anal.*, 15(4):736–754, 1978.

[12] I. abuška, and A. Miller. A feedback finite element method with a posteriori error estimation. I. The finite element method and some basic properties of the a posteriori error estimator *Comput. Methods Appl. Mech. Engrg.*, 61(1):1–40, 1987

[13] P. Bastian and B. Rivière, *Superconvergence and $H(\mathrm{div})$ projection for discontinuous Galerkin methods*, Internat. J. Numer. Methods Fluids, 42 (2003), pp. 1043–1057.

[14] R. Becker, P. Hansbo, and M. G. Larson, *Energy norm a posteriori error estimation for discontinuous Galerkin methods*, Comput. Methods Appl. Mech. Engrg., 192 (2003), pp. 723–733.

[15] R. Becker and S. Mao. An optimally convergent adaptive mixed finite element method. *Numer. Math.*, 111(1):35–54, 2008.

[16] P. Binev, W. Dahmen, and R. DeVore. Adaptive finite element methods with convergence rates. *Numer. Math.*, 97:219–268, 2004.

[17] A. Bonito and R. H. Nochetto. Quasi-optimal convergence rate of an adaptive discontinuous Galerkin method. *SIAM J. Numer. Anal.*, 48(2):734–771, 2010.

[18] D. Braess and R. Verfürth. A posteriori error estimators for the Raviart-Thomas element. *SIAM J. Numer. Anal.*, 33:2431–2444, 1996.

[19] J. H. Bramble and J. Xu, *A local post-processing technique for improving the accuracy in mixed finite-element approximations*, SIAM J. Numer. Anal. **26** (1989), no. 6, 1267–1275.

[20] S. C. Brenner and L. R. Scott. *The mathematical theory of finite element methods*, volume 15 of *Texts in Applied Mathematics*. Springer-Verlag, New York, second edition, 2002.

[21] F. Brezzi, B. Cockburn, L. D. Marini and E. Süli, *Stabilization mechanisms in discontinuous Galerkin finite element methods*, Comput. Methods Appl. Mech. Engrg. **195** (2006), 3293–3310.

[22] F. Brezzi, J. Douglas, Jr., R.E. Durán, and M. Fortin. Mixed finite element methods for second order elliptic problems in three variables. *Numer. Math.*, 51:237–250, 1987.

[23] F. Brezzi, J. Douglas, Jr., M. Fortin, and L. D. Marini. Efficient rectangular mixed finite element methods in two and three space variables. *RAIRO Modél. Math. Anal. Numér.*, 21:581–604, 1987.

[24] F. Brezzi, J. Douglas, Jr., and L. D. Marini, *Two families of mixed finite elements for second order elliptic problems*, Numer. Math. **47** (1985), 217–235.

[25] F. Brezzi and M. Fortin, *Mixed and hybrid finite element methods*, Springer Verlag, 1991.

[26] R. Bustinza, G. Gatica, and B. Cockburn, *An a posteriori error estimate for the local discontinuous Galerkin method applied to linear and nonlinear diffusion problems*, J. Sci. Comput., 22/23 (2005), pp. 147–185.

[27] P. Castillo, *An a posteriori error estimate for the local discontinuous Galerkin method*, J. Sci. Comput., 22/23 (2005), pp. 187–204.

[28] C. Carstensen. A posteriori error estimate for the mixed finite element method. *Math. Comp.*, 66:465–476, 1997.

[29] C. Carstensen and T. Gudi and M. Jensen, *A unifying theory of a posteriori error control for discontinuous Galerkin FEM*, Numer. Math., 112 (2009), pp. 363–379.

[30] J. M. Cascon, C. Kreuzer, R. H. Nochetto, and K. G. Siebert. Quasi-optimal convergence rate for an adaptive finite element method. *SIAM J. Numer. Anal.*, 46(5):2524–2550, 2008.

[31] L. Chen, M. Holst, and J. Xu. Convergence and optimality of adaptive mixed finite element methods. *Math. Comp.*, 78(265):35–53, 2009.

[32] S. Cochez-Dhondt and S. Nicaise, *Equilibrated error estimators for discontinuous Galerkin methods*, Numer. Methods Partial Differential Equations, 24 (2008), pp. 1236–1252.

[33] B. Cockburn, B. Dong, and J. Guzmán, *A superconvergent LDG-hybridizable Galerkin method for second-order elliptic problems*, Math. Comp. **77** (2008), 1887–1916.

[34] B. Cockburn, J. Gopalakrishnan, and R. Lazarov, *Unified hybridization of discontinuous Galerkin, mixed and continuous Galerkin methods for second order elliptic problems*, SIAM J. Numer. Anal. 47 (2009), 1319–1365.

[35] B. Cockburn, J. Gopalakrishnan, and F. J. Sayas, *A projection-based error analysis of HDG methods*, Math. Comp., 79 (2010), pp. 1351–1367.

[36] B. Cockburn, J. Guzmán, and H. Wang, *Superconvergent discontinuous Galerkin methods for second-order elliptic problems*, Math. Comp. **78** (2009), 1–24.

[37] B. Cockburn, G. Kanschat, and D. Schötzau, *A locally conservative LDG method for the incompressible Navier-Stokes equations*, Math. Comp., 74 (2005), pp. 1067–1095.

[38] B. Cockburn, W. Qiu and K. Shi. Conditions for superconvergence of HDG methods for second-order elliptic problems. *Math. Comp.*. To appear.

[39] B. Cockburn and F.-J. Sayas, Divergence–conforming HDG methods for Stokes flows. Submitted.

[40] W. Dörfler, *A convergent adaptive algorithm for Poisson's equation*, SIAM J. Numer. Anal. **33** (1996), no. 3, 1106–1124.

[41] O. A. Karakashian and F. Pascal, *Convergence of adaptive discontinuous Galerkin approximations of second order elliptic problems*, SIAM J. Numer. Anal. **45** (2007), 641–665.

[42] R. G. Durán and M. A. Muschietti. An explicit right inverse of the divergence operator which is continuous in weighted norms. *Studia Math.*, 148(3):207–219, 2001.

[43] R. H. W. Hoppe, G. Kanschat, and T. Warburton. Convergence analysis of an adaptive interior penalty discontinuous Galerkin method. *SIAM J. Numer. Anal.*, 47(1):534–550, 2008/09.

[44] I. Kossaczký. A recursive approach to local mesh refinement in two and three dimensions. *J. Comput. Appl. Math.*, 55(3):275–288, 1994.

[45] K. Mekchay and R. H. Nochetto. Convergence of adaptive finite element methods for general second order linear elliptic PDEs. *SIAM J. Numer. Anal.*, 43(5):1803–1827 (electronic), 2005.

[46] P. Morin, R. H. Nochetto, and K. G. Siebert. Convergence of adaptive finite element methods. *SIAM Rev.*, 44(4):631–658 (electronic) (2003), 2002.

[47] P. Morin, R.H. Nochetto, and K.G. Siebert. Data oscillation and convergence of adaptive FEM. *SIAM J. Numer. Anal.*, 38:466–488 (electronic), 2000.

[48] R. H. Nochetto, K. G. Siebert, and A. Veeser. Theory of adaptive finite element methods: an introduction. In *Multiscale, nonlinear and adaptive approximation*, pages 409–542. Springer, Berlin, 2009.

[49] E. Creusé and S. Nicaise *A posteriori error estimator based on gradient recovery by averaging for discontinuous Galerkin methods*, J. Comput. Appl. Math., 234 (2010), pp. 2903–2915

[50] A. Ern, S. Nicaise and M. Vohralík, *An accurate* $\mathbf{H}(\mathrm{div})$ *flux reconstruction for discontinuous Galerkin approximations of elliptic problems*, C. R. Math. Acad. Sci. Paris, 345 (2007), pp. 709–712.

[51] L. Gastaldi and R. Nochetto, *Sharp maximum norm error estimates for general mixed finite element approximations to second order elliptic equations*, RAIRO Modél. Math. Anal. Numér., 23 (1989), pp. 103–128.

[52] P. Houston, D. Schötzau, and T. P. Wihler, *Energy norm a posteriori error estimation of hp-adaptive discontinuous Galerkin methods for elliptic problems*, Math. Models Methods Appl. Sci., 17 (2007), pp. 33–62.

[53] M. Juntunen and R. Stenberg, *On a mixed discontinuous Galerkin method*, Electron. Trans. Numer. Anal., 32 (2008), pp. 17–32.

[54] O. A. Karakashian and F. Pascal, *A posteriori error estimates for a discontinuous Galerkin approximation of a second order elliptic problems*, SIAM J. Numer. Anal. **41** (2003), 2374–2399.

[55] M. G. Larson and A. Målqvist. A posteriori error estimates for mixed finite element approximations of elliptic problems. *Numer. Math.*, 108:487–500, 2008.

[56] R. Lazarov, S. Repin and S. K. Tomar, *Functional a posteriori error estimates for discontinuous Galerkin approximations of elliptic problems*, Numer. Methods Partial Differential Equations, 25 (2009), pp. 952–971.

[57] C. Lovadina and L. Marini, *A-posteriori error estimates for discontinuous Galerkin approximations of second order elliptic problems*, J. Sci. Comput. **40** (2009), 340–359.

[58] C. Lovadina and R. Stenberg. Energy norm a posteriori error estimates for mixed finite element methods. *Math. Comp.*, 75:1659–1674 (electronic), 2006.

[59] J.-C. Nédélec. A new family of mixed finite elements in $\mathbf{R}^3$. *Numer. Math.*, 50:57–81, 1986.

[60] M. E. G. Ong. Hierarchical basis preconditioners in three dimensions. *SIAM J. Sci. Comput.*, 18(2):479–498, 1997.

[61] P. A. Raviart and J. M. Thomas. A mixed finite element method for second order elliptic problems. In I. Galligani and E. Magenes, editors, *Mathematical Aspects*

of Finite Element Method, Lecture Notes in Math. 606, pages 292–315. Springer-Verlag, New York, 1977.

[62] B. Rivière and M. F. Wheeler, *A posteriori error estimates for a discontinuous Galerkin method applied to elliptic problems. Log number: R74*, Comput. Math. Appl., 46 (2003), pp. 141–163. p-FEM2000: p and hp finite element methods—mathematics and engineering practice (St. Louis, MO).

[63] R. Scott and S. Zhang, *Finite element interpolation of nonsmooth functions satisfying boundary conditions*, Math. Comp., 54 (1990), pp. 483–493.

[64] R. Stenberg, *A family of mixed finite elements for the elasticity problem*, Numer. Math., 53 (1988), pp. 513–538.

[65] R. Stenberg, *Postprocessing schemes for some mixed finite elements*, RAIRO Modél. Math. Anal. Numér. **25** (1991), 151–167.

[66] R. Stevenson. Optimality of a standard adaptive finite element method. *Found. Comput. Math.*, 7(2):245–269, 2007.

[67] R. Stevenson. The completion of locally refined simplicial partitions created by bisection. *Math. Comp.*, 77(261):227–241 (electronic), 2008.

[68] S. Zhang. *Multi-level iterative techniques*. ProQuest LLC, Ann Arbor, MI, 1988. Thesis (Ph.D.)–The Pennsylvania State University.

[69] R. Verfürth, *A posteriori error estimation and adaptive mesh-refinement techniques*, J. Comput. Appl. Math. **50** (1994), 67–83.

[70] R. Verfürth, *A review of a posteriori error estimation and adaptive mesh-refinement techniques*, (1996).

[71] M. Vohralík, *A posteriori error estimates for lowest-order mixed finite element discretizations of convection-diffusion-reaction equations*, SIAM J. Numer. Anal., 45 (2007), pp. 1570–1599 (electronic).

[72] S. Funken, D. Praetorius, and P. Wissgott. *Efficient implementation of adaptive P1-FEM in MATLAB*, Preprint, 2008.

[73] R. Sacchi, and A. Veeser. *Locally efficient and reliable a posteriori error estimators for Dirichlet problems*, Math. Models Methods Appl. Sci. **16**, (2006), 319–346.